US00RE48944E

(19) **United States**

(12) **Reissued Patent**

Brindle et al.

(10) **Patent Number: US RE48,944 E**

(45) **Date of Reissued Patent: *Feb. 22, 2022**

(54) **METHOD AND APPARATUS FOR USE IN IMPROVING LINEARITY OF MOSFETS USING AN ACCUMULATED CHARGE SINK**

(71) Applicant: **pSemi Corporation**, San Diego, CA (US)

(72) Inventors: **Christopher N. Brindle**, Poway, CA (US); **Michael A. Stuber**, Carlsbad, CA (US); **Dylan J. Kelly**, San Diego, CA (US); **Clint L. Kemerling**, Escondido, CA (US); **George P. Imthurn**, San Diego, CA (US); **Robert B. Welstand**, San Diego, CA (US); **Mark L. Burgener**, San Diego, CA (US)

(73) Assignee: **pSemi Corporation**, San Diego, CA (US)

(*) Notice: This patent is subject to a terminal disclaimer.

(21) Appl. No.: **16/738,787**

(22) Filed: **Jan. 9, 2020**

Related U.S. Patent Documents

Reissue of:

(64) Patent No.: **10,153,763**
Issued: **Dec. 11, 2018**
Appl. No.: **15/707,970**
Filed: **Sep. 18, 2017**

U.S. Applications:

(60) Continuation of application No. 14/845,154, filed on Sep. 3, 2015, now Pat. No. 9,780,775, which is a (Continued)

(51) **Int. Cl.**
H01L 29/66 (2006.01)
H03K 17/16 (2006.01)
(Continued)

(52) **U.S. Cl.**
CPC ***H03K 17/162*** (2013.01); ***H01L 29/0649*** (2013.01); *H01L 29/1095* (2013.01);
(Continued)

(58) **Field of Classification Search**
CPC H03K 17/162; H03K 17/687; H03K 2217/0018; H01L 29/1095; H01L 29/0649;
(Continued)

(56) **References Cited**

U.S. PATENT DOCUMENTS

3,470,443 A 9/1969 Berry
3,646,361 A 2/1972 Pfiffner
(Continued)

FOREIGN PATENT DOCUMENTS

CN 1256521 6/2000
CN 1256521 A 6/2000
(Continued)

OTHER PUBLICATIONS

US 10,700,199 B1, 06/2020, Brindle (withdrawn)
(Continued)

Primary Examiner — Tuan H Nguyen
(74) *Attorney, Agent, or Firm* — Haynes and Boone, LLP

(57) **ABSTRACT**

A method and apparatus for use in improving the linearity characteristics of MOSFET devices using an accumulated charge sink (ACS) are disclosed. The method and apparatus are adapted to remove, reduce, or otherwise control accumulated charge in SOI MOSFETs, thereby yielding improvements in FET performance characteristics. In one exemplary embodiment, a circuit having at least one SOI MOSFET is configured to operate in an accumulated charge regime. An accumulated charge sink, operatively coupled to the body of the SOI MOSFET, eliminates, removes or otherwise controls accumulated charge when the FET is operated in the accumulated charge regime, thereby reducing the nonlinearity of the parasitic off-state source-to-drain capacitance of the SOI MOSFET. In RF switch circuits implemented with the improved SOI MOSFET devices, harmonic and intermodulation distortion is reduced by
(Continued)

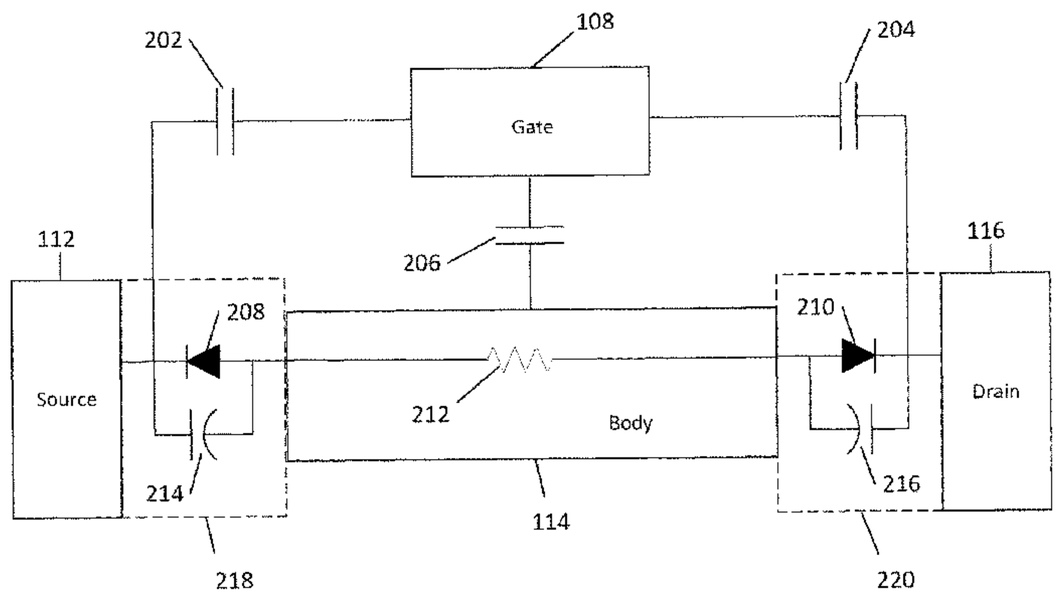

200

removing or otherwise controlling the accumulated charge when the SOI MOSFET operates in an accumulated charge regime.

17 Claims, 22 Drawing Sheets

Related U.S. Application Data

continuation of application No. 13/850,251, filed on Mar. 25, 2013, now Pat. No. 9,130,564, which is a continuation of application No. 13/412,529, filed on Mar. 5, 2012, now Pat. No. 8,405,147, which is a continuation of application No. 13/053,211, filed on Mar. 22, 2011, now Pat. No. 8,129,787, which is a division of application No. 11/484,370, filed on Jul. 10, 2006, now Pat. No. 7,910,993.

(60) Provisional application No. 60/698,523, filed on Jul. 11, 2005.

(51) **Int. Cl.**

H03K 17/687	(2006.01)
H01L 29/786	(2006.01)
H01L 29/06	(2006.01)
H01L 29/10	(2006.01)

(52) **U.S. Cl.**
CPC .. *H01L 29/78609* (2013.01); *H01L 29/78615* (2013.01); *H01L 29/78681* (2013.01); *H01L 29/78684* (2013.01); *H03K 17/687* (2013.01); *H03K 2217/0018* (2013.01)

(58) **Field of Classification Search**
CPC H01L 29/78609; H01L 29/78615; H01L 29/7868; H01L 29/78684
See application file for complete search history.

(56) **References Cited**

U.S. PATENT DOCUMENTS

3,699,359	A	10/1972	Shelby
3,731,112	A	5/1973	Smith
3,878,450	A	4/1975	Greatbatch
3,942,047	A	3/1976	Buchanan
3,943,428	A	3/1976	Whidden
3,955,353	A	5/1976	Astle
3,975,671	A	8/1976	Stoll
3,983,414	A	9/1976	Stafford
3,988,727	A	10/1976	Scott
4,047,091	A	9/1977	Hutchines
4,053,916	A	10/1977	Cricchi et al.
4,061,929	A	12/1977	Asano
4,068,295	A	1/1978	Portmann
4,079,336	A	3/1978	Gross
4,106,086	A	8/1978	Holbrook
4,139,826	A	2/1979	Pradal
4,145,719	A	3/1979	Hand
4,186,436	A	1/1980	Ishiwatari
4,241,316	A	12/1980	Knapp
4,244,000	A	1/1981	Ueda
4,256,977	A	3/1981	Hendrickson
4,316,101	A	2/1982	Minner
4,317,055	A	2/1982	Yoshida
4,321,661	A	3/1982	Sano
4,367,421	A	1/1983	Baker
4,390,798	A	6/1983	Karafuji
4,460,952	A	7/1984	Risinger
RE31,749	E	11/1984	Yamashiro
4,485,433	A	11/1984	Topich
4,621,315	A	11/1986	Vaughn
4,633,106	A	12/1986	Backes
4,638,184	A	1/1987	Kimura
4,679,134	A	7/1987	Bingham
4,703,196	A	10/1987	Arakawa
4,736,169	A	4/1988	Weaver
4,739,191	A	4/1988	Puar
4,746,960	A	5/1988	Valeri
4,748,485	A	5/1988	Vasudev
4,752,699	A	6/1988	Cranford
4,769,784	A	9/1988	Doluca
4,777,577	A	10/1988	Bingham
4,809,056	A	2/1989	Shirato
4,810,911	A	3/1989	Noguchi
4,825,145	A	4/1989	Tanaka
4,839,787	A	6/1989	Kojima
4,847,519	A	7/1989	Wahl
4,849,651	A	7/1989	Estes, Jr.
4,883,976	A	11/1989	Deane
4,890,077	A	12/1989	Sun
4,891,609	A	1/1990	Eilley
4,893,070	A	1/1990	Milberger
4,897,774	A	1/1990	Bingham
4,906,587	A	3/1990	Blake
4,929,855	A	5/1990	Ezzeddine
4,939,485	A	7/1990	Eisenberg
4,984,040	A	1/1991	Yap
4,985,647	A	1/1991	Kawada
4,999,585	A	3/1991	Burt
5,001,528	A	3/1991	Bahraman
5,012,123	A	4/1991	Ayasli et al.
5,023,494	A	6/1991	Tsukii
5,029,282	A	7/1991	Ito
5,032,799	A	7/1991	Milberger
5,038,325	A	8/1991	Douglas
5,041,797	A	8/1991	Belcher
5,061,907	A	10/1991	Rasmussen
5,061,911	A	10/1991	Weidman
5,068,626	A	11/1991	Takagi
5,081,371	A	1/1992	Wong
5,081,706	A	1/1992	Kim
5,095,348	A	3/1992	Houston
5,107,152	A	4/1992	Jain
5,111,375	A	5/1992	Marshall
5,124,762	A	6/1992	Childs
5,125,007	A	6/1992	Yamaguchi
5,126,590	A	6/1992	Chern
5,138,190	A	8/1992	Yamazaki
5,146,178	A	9/1992	Nojima
5,148,393	A	9/1992	Furuyama
5,157,279	A	10/1992	Lee
5,182,529	A	1/1993	Chern
5,193,198	A	3/1993	Yokouchi
5,208,557	A	5/1993	Kersh, III
5,212,456	A	5/1993	Kovalcik
5,272,457	A	12/1993	Heckaman
5,274,343	A	12/1993	Russell
5,283,457	A	2/1994	Matloubian
5,285,367	A	2/1994	Keller
5,306,954	A	4/1994	Chan
5,313,083	A	5/1994	Schindler
5,317,181	A	5/1994	Tyson
5,319,604	A	6/1994	Imondi
5,345,422	A	9/1994	Redwine
5,349,306	A	9/1994	Apel
5,350,957	A	9/1994	Cooper
5,375,256	A	12/1994	Yokoyama
5,375,257	A	12/1994	Lampen
5,392,186	A	2/1995	Alexander
5,392,205	A	2/1995	Zavaleta
5,405,795	A	4/1995	Beyer
5,416,043	A	5/1995	Burgener et al.
5,422,586	A	6/1995	Tedrow
5,422,590	A	6/1995	Coffman
5,442,327	A	8/1995	Longbrake
5,446,418	A	8/1995	Hara
5,448,207	A	9/1995	Kohama
5,455,794	A	10/1995	Javanifard
5,465,061	A	11/1995	Dufour
5,477,184	A	12/1995	Uda
5,488,243	A	1/1996	Tsuruta

(56) **References Cited**

U.S. PATENT DOCUMENTS

5,492,857	A	2/1996	Reedy et al.
5,493,249	A	2/1996	Manning
5,519,360	A	5/1996	Keeth
5,535,160	A	7/1996	Yamaguchi
5,548,239	A	8/1996	Kohama
5,553,012	A	9/1996	Buss
5,553,295	A	9/1996	Pantelakis
5,554,892	A	9/1996	Norimatsu
5,559,368	A	9/1996	Hu
5,572,040	A	11/1996	Reedy et al.
5,576,647	A	11/1996	Sutardja
5,578,853	A	11/1996	Hayashi
5,581,106	A	12/1996	Hayashi
5,587,604	A	12/1996	Machesney et al.
5,589,793	A	12/1996	Kassapian
5,594,371	A	1/1997	Douseki
5,596,205	A	1/1997	Reedy et al.
5,597,739	A	1/1997	Sumi
5,600,169	A	2/1997	Burgener et al.
5,600,588	A	2/1997	Kawashima
5,610,533	A	3/1997	Arimoto
5,629,655	A	5/1997	Dent
5,663,570	A	9/1997	Reedy et al.
5,670,907	A	9/1997	Gorecki
5,672,992	A	9/1997	Nadd
5,677,649	A	10/1997	Martin
5,681,761	A	10/1997	Kim
5,689,144	A	11/1997	Williams
5,694,308	A	12/1997	Cave
5,698,877	A	12/1997	Gonzalez
5,699,018	A	12/1997	Yamamoto
5,717,356	A	2/1998	Kohama
5,729,039	A	3/1998	Beyer
5,731,607	A	3/1998	Kohama
5,734,291	A	3/1998	Tasdighi
5,748,016	A	5/1998	Kurosawa
5,748,053	A	5/1998	Kameyama
5,753,955	A	5/1998	Fechner
5,757,170	A	5/1998	Pinney
5,760,652	A	6/1998	Maemura
5,767,549	A	6/1998	Chen
5,767,721	A	6/1998	Crampton
5,774,411	A	6/1998	Hsieh
5,774,792	A	6/1998	Tanaka
5,777,530	A	7/1998	Nakatuka
5,784,311	A	7/1998	Assaderaghi
5,784,687	A	7/1998	Itoh
5,786,617	A	7/1998	Merrill
5,793,246	A	8/1998	Vest
5,801,577	A	9/1998	Tailliet
5,804,858	A	9/1998	Hsu
5,807,772	A	9/1998	Takemura
5,808,505	A	9/1998	Tsukada
5,812,939	A	9/1998	Kohama
5,814,899	A	9/1998	Okumura
5,818,099	A	10/1998	Burghartz
5,818,278	A	10/1998	Yamamoto
5,818,283	A	10/1998	Tonami
5,818,289	A	10/1998	Chevallier
5,818,766	A	10/1998	Song
5,821,769	A	10/1998	Douseki
5,821,800	A	10/1998	Le
5,825,227	A	10/1998	Kohama
5,861,336	A	1/1999	Reedy et al.
5,864,328	A	1/1999	Kajimoto
5,863,823	A	2/1999	Burgener
5,874,836	A	2/1999	Nowak
5,874,849	A	2/1999	Marotta
5,877,978	A	3/1999	Morishita
5,878,331	A	3/1999	Yamamoto
5,880,620	A	3/1999	Gitlin
5,883,396	A	3/1999	Reedy et al.
5,883,541	A	3/1999	Tahara
5,889,428	A	3/1999	Young
5,892,260	A	4/1999	Okumura
5,892,382	A	4/1999	Ueda
5,892,400	A	4/1999	Van Saders
5,895,957	A	4/1999	Reedy et al.
5,903,178	A	5/1999	Miyatsuji
5,912,560	A	6/1999	Pasternak
5,917,362	A	6/1999	Kohama
5,920,093	A	7/1999	Huang
5,920,233	A	7/1999	Denny
5,926,466	A	7/1999	Ishida
5,930,605	A	7/1999	Mistry
5,930,638	A	7/1999	Reedy et al.
5,945,867	A	8/1999	Uda
5,945,879	A	8/1999	Rodwell
5,953,557	A	9/1999	Kawahara
5,959,335	A	9/1999	Bryant
5,969,560	A	10/1999	Kohama
5,969,571	A	10/1999	Swanson
5,973,363	A	10/1999	Staab et al.
5,973,364	A	10/1999	Kawanaka
5,973,382	A	10/1999	Burgener et al.
5,973,636	A	10/1999	Okubo
5,986,518	A	11/1999	Dougherty
5,990,580	A	11/1999	Weigand
6,020,778	A	2/2000	Shigehara
6,020,781	A	2/2000	Fujioka
6,020,848	A	2/2000	Wallace
6,049,110	A	4/2000	Koh
6,057,555	A	5/2000	Reedy et al.
6,057,723	A	5/2000	Yamaji
6,061,267	A	5/2000	Houston
6,063,686	A	5/2000	Masuda
6,064,253	A	5/2000	Faulkner
6,064,275	A	5/2000	Yamauchi
6,064,872	A	5/2000	Vice
6,066,993	A	5/2000	Yamamoto
6,081,165	A	6/2000	Goldman
6,081,443	A	6/2000	Morishita
6,081,694	A	6/2000	Matsuura
6,084,255	A	7/2000	Ueda
6,087,893	A	7/2000	Oowaki
6,094,088	A	7/2000	Yano
6,100,564	A	8/2000	Bryant
6,104,061	A	8/2000	Forbes
6,107,885	A	8/2000	Miguelez
6,111,778	A	8/2000	MacDonald
6,114,923	A	9/2000	Mizutani
6,118,343	A	9/2000	Winslow
6,122,185	A	9/2000	Utsunomiya
6,130,570	A	10/2000	Pan
6,130,572	A	10/2000	Ghilardelli
6,133,752	A	10/2000	Kawagoe
6,137,367	A	10/2000	Ezzedine
6,160,292	A	12/2000	Flaker et al.
6,169,444	B1	1/2001	Thurber, Jr.
6,172,378	B1	1/2001	Hull
6,173,235	B1	1/2001	Maeda
6,177,826	B1	1/2001	Mashiko
6,188,247	B1	2/2001	Storing
6,188,590	B1	2/2001	Chang
6,191,449	B1	2/2001	Shimo
6,191,653	B1	2/2001	Camp, Jr.
6,195,307	B1	2/2001	Umezawa
6,201,761	B1	3/2001	Wollesen
RE37,124	E	4/2001	Monk
6,215,360	B1	4/2001	Callaway, Jr.
6,218,248	B1	4/2001	Hwang
6,218,890	B1	4/2001	Yamaguchi
6,218,892	B1	4/2001	Soumyanath
6,222,394	B1	4/2001	Allen
6,225,866	B1	5/2001	Kubota
6,239,649	B1	5/2001	Bertin
6,239,657	B1	5/2001	Bauer
6,249,027	B1	6/2001	Burr
6,249,029	B1	6/2001	Bryant
6,249,446	B1	6/2001	Shearon
6,281,737	B1	8/2001	Kuang
6,288,458	B1	9/2001	Berndt
6,297,687	B1	10/2001	Sugimura
6,297,696	B1	10/2001	Abodollahian

(56) **References Cited**

U.S. PATENT DOCUMENTS

6,300,796	B1	10/2001	Troutman
6,304,110	B1	10/2001	Hirano
6,308,047	B1	10/2001	Yamamoto
6,310,508	B1	10/2001	Westerman
6,316,983	B1	11/2001	Kitamura
6,320,225	B1	11/2001	Hargrove
6,337,594	B1	1/2002	Hwang
6,341,087	B1	1/2002	Kunikiyo
6,355,957	B1	3/2002	Maeda
6,356,536	B1	3/2002	Repke
6,365,488	B1	4/2002	Liao
6,380,793	B1	4/2002	Bancal
6,380,796	B2	4/2002	Sakai
6,380,802	B1	4/2002	Pehike
6,387,739	B1	5/2002	Smith, III
6,392,440	B2	5/2002	Nebel
6,392,467	B1	5/2002	Oowaki
6,396,325	B2	5/2002	Goodell
6,396,352	B1	5/2002	Muza
6,400,211	B1	6/2002	Yokomizo
6,407,427	B1	6/2002	Oh
6,407,614	B1	6/2002	Takahashi
6,411,156	B1	6/2002	Borkar
6,411,531	B1	6/2002	Nork
6,414,353	B2	7/2002	Maeda
6,414,863	B1	7/2002	Bayer
6,429,487	B1	8/2002	Kunikiyo
6,429,632	B1	8/2002	Forbes
6,429,723	B1	8/2002	Hastings
6,433,587	B1	8/2002	Assaderaghi
6,433,589	B1	8/2002	Lee
6,449,465	B1	9/2002	Gailus
6,452,232	B1	9/2002	Adan
6,461,902	B1	10/2002	Xu
6,466,082	B1	10/2002	Krishnan
6,469,568	B2	10/2002	Toyoyama
6,486,511	B1	11/2002	Nathanson
6,486,729	B2	11/2002	Imamiya
6,496,074	B1	12/2002	Sowlati
6,498,058	B1	12/2002	Bryant
6,498,370	B1	12/2002	Kim
6,504,212	B1	1/2003	Allen et al.
6,504,213	B1	1/2003	Ebina
6,509,799	B1	1/2003	Franca-Neto
6,512,269	B1	1/2003	Braynt
6,518,645	B2	2/2003	Bae
6,518,829	B2	2/2003	Butler
6,519,191	B1	2/2003	Morishita
6,521,959	B2	2/2003	Kim
6,537,861	B1	3/2003	Kroell
6,559,689	B1	5/2003	Clark
6,563,366	B1	5/2003	Kohama
6,573,533	B1	6/2003	Yamazaki
6,608,785	B2	8/2003	Chuang
6,608,789	B2	8/2003	Sullivan
6,617,933	B2	9/2003	Ito
6,631,505	B2	10/2003	Arai
6,632,724	B2	10/2003	Henley et al.
6,642,578	B1	11/2003	Arnold
6,646,305	B2	11/2003	Assaderaghi
6,653,697	B2	11/2003	Hidaka
6,670,655	B2	12/2003	Lukes
6,677,641	B2	1/2004	Kocon
6,677,803	B1	1/2004	Chiba
6,684,055	B1	1/2004	Blackaby
6,684,065	B2	1/2004	Bult
6,693,326	B2	2/2004	Adan
6,693,498	B1	2/2004	Sasabata
6,698,082	B2	3/2004	Crenshaw
6,698,498	B1	3/2004	Zeigelaar
6,703,863	B2	3/2004	Gion
6,704,550	B1	3/2004	Kohama
6,711,397	B1	3/2004	Petrov
6,714,065	B2	3/2004	Komiya
6,717,458	B1	4/2004	Potanin
6,730,953	B2	5/2004	Brindle
6,762,477	B2	7/2004	Kunikiyo
6,769,110	B2	7/2004	Katoh
6,774,701	B1	8/2004	Heston
6,781,805	B1	8/2004	Urakawa
6,788,130	B2	9/2004	Pauletti
6,790,747	B2	9/2004	Henley et al.
6,801,076	B1	10/2004	Merritt
6,803,680	B2	10/2004	Brindle
6,804,502	B2	10/2004	Burgener et al.
6,804,506	B1	10/2004	Freitag
6,816,000	B2	11/2004	Miyamitsu
6,816,001	B2	11/2004	Khouri
6,816,016	B2	11/2004	Sander
6,819,938	B2	11/2004	Sahota
6,825,730	B1	11/2004	Sun
6,830,963	B1	12/2004	Forbes
6,831,847	B2	12/2004	Perry
6,833,745	B2	12/2004	Hausman
6,835,982	B2	12/2004	Hogyoku
6,836,172	B2	12/2004	Okashita
6,870,241	B2	3/2005	Nakatani
6,871,059	B1	3/2005	Piro
6,879,502	B2	4/2005	Yoshida
6,882,210	B2	4/2005	Asano
6,891,234	B1	5/2005	Connelly
6,897,701	B2	5/2005	Chen
6,898,778	B2	5/2005	Kawanaka
6,901,023	B2	5/2005	Kirsch
6,903,596	B2	6/2005	Geller
6,908,832	B2	6/2005	Farrens et al.
6,917,258	B2	7/2005	Kushitani
6,933,744	B2	8/2005	Das
6,934,520	B2	8/2005	Rozsypal
6,947,720	B2	9/2005	Razavi
6,954,623	B2	10/2005	Chang
6,967,517	B2	11/2005	Mizuno
6,968,020	B1	11/2005	Jayaraman
6,969,668	B1	11/2005	Kang et al.
6,975,271	B2	12/2005	Adachi
6,978,122	B2	12/2005	Kawakyu
6,978,437	B1	12/2005	Rittman et al.
7,023,260	B2	4/2006	Thorp
7,042,245	B2	5/2006	Hidaka
7,045,873	B2	5/2006	Chen
7,056,808	B2	6/2006	Henley et al.
7,057,472	B2	6/2006	Fukamachi
7,058,922	B2	6/2006	Kawanaka
7,068,096	B2	6/2006	Chu
7,082,293	B1	7/2006	Rofougaran
7,088,971	B2	8/2006	Burgener
7,092,677	B1	8/2006	Zhang
7,109,532	B1	9/2006	Lee
7,123,898	B2	10/2006	Burgener
7,129,545	B2	10/2006	Cain
7,132,873	B2	11/2006	Hollmer
7,138,846	B2	11/2006	Suwa
7,161,197	B2	1/2007	Nakatsuka
7,173,471	B2	2/2007	Nakatsuka
7,199,635	B2	4/2007	Nakatsuka
7,202,712	B2	4/2007	Athas
7,202,734	B1	4/2007	Raab
7,212,788	B2	5/2007	Weber
7,248,120	B2	7/2007	Burgener
7,266,014	B2 *	9/2007	Wu G11C 16/0475 365/185.01
7,269,392	B2	9/2007	Nakajima
7,307,490	B2	12/2007	Kizuki
7,345,342	B2	3/2008	Challa
7,345,521	B2	3/2008	Takahashi
7,355,455	B2	4/2008	Hidaka
7,359,677	B2	4/2008	Huang
7,391,282	B2	6/2008	Nakatsuka
7,404,157	B2	7/2008	Tanabe
7,405,982	B1	7/2008	Flaker
7,432,552	B2	10/2008	Park
7,457,594	B2	11/2008	Theobold
7,460,852	B2	12/2008	Burgener
7,515,882	B2	4/2009	Kelcourse

(56) **References Cited**

U.S. PATENT DOCUMENTS

7,546,089	B2	6/2009	Bellantoni	
7,551,036	B2	6/2009	Berroth	
7,561,853	B2	7/2009	Miyazawa	
7,564,103	B2	7/2009	Losehand et al.	
7,616,482	B2	11/2009	Prall	
7,619,462	B2 *	11/2009	Kelly	H04B 1/48 327/427
7,659,152	B2	2/2010	Gonzalez	
7,710,189	B2	5/2010	Toda	
7,719,343	B2	5/2010	Burgener	
7,733,156	B2	6/2010	Brederlow	
7,733,157	B2	6/2010	Brederlow	
7,741,869	B2	6/2010	Hidaka	
7,756,494	B2	7/2010	Fujioka	
7,786,807	B1	8/2010	Li	
7,796,969	B2 *	9/2010	Kelly	H03K 17/693 257/341
7,808,342	B2	10/2010	Prikhokdo	
7,817,966	B2	10/2010	Prikhokdo	
7,860,499	B2	12/2010	Burgener	
7,868,683	B2	1/2011	Iklov	
7,890,891	B2	2/2011	Stuber	
7,910,993	B2 *	3/2011	Brindle	H01L 29/78609 257/347
7,928,759	B2	4/2011	Hidaka	
7,936,213	B2	5/2011	Shin	
7,960,772	B2	6/2011	Englekirk	
7,982,265	B2	7/2011	Challa	
7,984,408	B2	7/2011	Cheng	
8,008,988	B1	8/2011	Yang	
8,081,928	B2 *	12/2011	Kelly	H03K 17/6871 333/101
8,103,226	B2	1/2012	Andrys	
8,111,104	B2	2/2012	Ahadian	
8,129,787	B2	3/2012	Brindle	
8,131,225	B2	3/2012	Botula	
8,131,251	B2	3/2012	Burgener	
8,195,103	B2	6/2012	Waheed	
8,232,627	B2	7/2012	Bryant	
8,253,494	B2	8/2012	Blednov	
8,330,519	B2	12/2012	Lam	
8,350,624	B2	1/2013	Lam	
8,405,147	B2	3/2013	Brindle	
8,427,241	B2	4/2013	Ezzedine	
8,451,044	B2	5/2013	Nisbet et al.	
8,461,903	B1	6/2013	Granger-Jones	
8,487,706	B2	7/2013	Li	
8,525,272	B2	9/2013	Losehand et al.	
8,527,949	B1 *	9/2013	Pleis	G06F 15/7867 717/121
8,529,949	B2 *	9/2013	Ettema	A61K 9/2018 424/464
8,536,636	B2	9/2013	Englekirk	
8,559,907	B2	10/2013	Burgener	
8,583,111	B2	11/2013	Burgener	
8,649,741	B2	2/2014	Iijima	
8,649,754	B2	2/2014	Burgener	
8,669,804	B2	3/2014	Ranta	
8,680,928	B2	3/2014	Jeon	
8,729,948	B2	5/2014	Sugiura	
8,729,949	B2	5/2014	Nisbet et al.	
8,742,502	B2	6/2014	Brindle	
8,779,859	B2	7/2014	Su	
8,954,902	B2	2/2015	Stuber	
9,087,899	B2	7/2015	Brindle	
9,129,836	B2	9/2015	Losehand et al.	
9,130,564	B2	9/2015	Brindle et al.	
9,160,292	B2	10/2015	Olson	
9,177,737	B2	11/2015	Englekirk	
9,178,493	B1	11/2015	Nobbe	
9,184,709	B2	11/2015	Adamski	
9,219,445	B2	12/2015	Nobbe	
9,225,378	B2	12/2015	Burgener et al.	
9,276,526	B2	3/2016	Nobbe	
9,331,738	B2	5/2016	Sharma	
9,369,087	B2	6/2016	Burgener	
9,397,656	B2	7/2016	Dribinsky	
9,419,560	B2	8/2016	Korol	
9,438,223	B2	9/2016	De Jongh	
9,467,124	B2	10/2016	Crandall	
9,608,619	B2	3/2017	Stuber	
9,653,601	B2	5/2017	Brindle	
9,673,155	B2	6/2017	Smith	
9,755,615	B2	9/2017	Ranta	
9,780,775	B2 *	10/2017	Brindle	H03K 17/162
9,780,778	B2	10/2017	Burgener et al.	
9,786,781	B2	10/2017	Brindle et al.	
9,887,695	B2	2/2018	Dribinsky et al.	
9,948,281	B2	4/2018	Ranta	
9,966,988	B2	5/2018	Burgener	
10,074,746	B2	9/2018	Brindle et al.	
10,122,356	B2	11/2018	Kunishi	
10,153,763	B2	12/2018	Brindle	
10,153,767	B2	12/2018	Burgener	
10,622,990	B2	4/2020	Brindle	
10,622,993	B2	4/2020	Burgener	
10,680,600	B2	6/2020	Brindle	
2001/0015461	A1	8/2001	Ebina	
2001/0031518	A1	10/2001	Kim	
2001/0040479	A1	11/2001	Zhang	
2001/0045602	A1	11/2001	Maeda et al.	
2002/0029971	A1	3/2002	Kovacs	
2002/0079971	A1	6/2002	Vathulya	
2002/0093064	A1	7/2002	Inaba	
2002/0115244	A1	8/2002	Park	
2002/0126767	A1	9/2002	Ding	
2002/0195623	A1	12/2002	Horiuchi	
2003/0002452	A1	1/2003	Sahota	
2003/0025159	A1	2/2003	Hogyoku	
2003/0032396	A1	2/2003	Tsuchiya	
2003/0090313	A1	5/2003	Burgener	
2003/0141543	A1	7/2003	Bryant	
2003/0160515	A1	8/2003	Yu	
2003/0181167	A1	9/2003	Iida	
2003/0201494	A1	10/2003	Maeda	
2003/0205760	A1	11/2003	Kawanaka et al.	
2003/0222313	A1	12/2003	Fechner	
2003/0224743	A1	12/2003	Okada	
2003/0227056	A1	12/2003	Wang	
2004/0004251	A1	1/2004	Madurawe	
2004/0021137	A1	2/2004	Fazan	
2004/0061130	A1	4/2004	Morizuka	
2004/0080364	A1	4/2004	Sander	
2004/0121745	A1	6/2004	Meck	
2004/0129975	A1	7/2004	Koh	
2004/0183583	A1	9/2004	Mizuno	
2004/0183588	A1	9/2004	Chandrakasan	
2004/0204013	A1	10/2004	Ma	
2004/0218442	A1	11/2004	Kirsch	
2004/0227565	A1	11/2004	Chen	
2004/0242182	A1	12/2004	Hikada	
2005/0017789	A1	1/2005	Burgener	
2005/0077564	A1	4/2005	Forbes	
2005/0079829	A1	4/2005	Ogawa	
2005/0121699	A1	6/2005	Chen	
2005/0122163	A1	6/2005	Chu	
2005/0127442	A1	6/2005	Veeraraghavan	
2005/0167751	A1	8/2005	Nakajima et al.	
2005/0212595	A1	9/2005	Kusunoki	
2005/0264341	A1	12/2005	Hikita	
2006/0009164	A1	1/2006	Kataoka	
2006/0022526	A1	2/2006	Cartalade	
2006/0077082	A1	4/2006	Shanks	
2006/0118884	A1	6/2006	Losehand et al.	
2006/0160520	A1	7/2006	Miyazawa	
2006/0161520	A1	7/2006	Brewer	
2006/0194558	A1	8/2006	Kelly	
2006/0194567	A1	8/2006	Kelly	
2006/0199563	A1	9/2006	Kelly et al.	
2006/0255852	A1	11/2006	O'Donnell	
2006/0267093	A1 *	11/2006	Tang	H01L 27/108 257/347
2006/0270367	A1	11/2006	Burgener	

(56) **References Cited**

U.S. PATENT DOCUMENTS

2006/0281418	A1	12/2006	Huang	
2007/0018247	A1	1/2007	Brindle et al.	
2007/0023833	A1	2/2007	Okhonin et al.	
2007/0045697	A1	3/2007	Cheng	
2007/0069291	A1	3/2007	Stuber	
2007/0120103	A1	5/2007	Burgener	
2007/0279120	A1	12/2007	Brederlow	
2007/0290744	A1	12/2007	Adachi	
2008/0034335	A1	2/2008	Cheng	
2008/0073719	A1*	3/2008	Fazan	G11C 11/403 257/347
2008/0076371	A1	3/2008	Dribinsky	
2008/0191788	A1	8/2008	Chen	
2008/0303080	A1	12/2008	Bhattacharyya	
2009/0007036	A1	1/2009	Cheng	
2009/0029511	A1*	1/2009	Wu	G11C 11/5628 438/261
2009/0117871	A1	5/2009	Burgener	
2009/0181630	A1	7/2009	Seshita et al.	
2009/0278206	A1	11/2009	Losehand et al.	
2010/0327948	A1	12/2010	Nisbet et al.	
2010/0330938	A1	12/2010	Yin	
2011/0002080	A1	1/2011	Ranta	
2011/0092179	A1	4/2011	Burgener	
2011/0163779	A1	7/2011	Hidaka	
2011/0169550	A1	7/2011	Brindle	
2011/0227637	A1	9/2011	Stuber	
2011/0260780	A1	10/2011	Granger-Jones	
2011/0299437	A1	12/2011	Mikhemar	
2012/0007679	A1	1/2012	Burgener	
2012/0064952	A1	3/2012	Iijima	
2012/0169398	A1	7/2012	Brindle	
2012/0267719	A1*	10/2012	Brindle	H01L 29/78609 257/348
2013/0009725	A1	1/2013	Heaney	
2013/0015717	A1	1/2013	Dykstra	
2013/0260698	A1	10/2013	Nisbet et al.	
2013/0278317	A1	10/2013	Iversen	
2013/0293280	A1	11/2013	Brindle	
2014/0001550	A1	1/2014	Losehand et al.	
2014/0028521	A1	1/2014	Bauder	
2014/0085006	A1	3/2014	Mostov	
2014/0087673	A1	3/2014	Mostov	
2014/0165385	A1	6/2014	Englekirk	
2014/0167834	A1	6/2014	Stuber	
2014/0179249	A1	6/2014	Burgener	
2014/0179374	A1	6/2014	Burgener	
2014/0306767	A1	10/2014	Burgener	
2014/0312422	A1	10/2014	Brindle	
2015/0015321	A1	1/2015	Dribinsky	
2015/0022256	A1	1/2015	Sprinkle	
2015/0236691	A1	8/2015	Cam	
2016/0064561	A1*	3/2016	Brindle	H01L 29/4908 257/348
2016/0191040	A1	6/2016	Brindle et al.	
2016/0191050	A1	6/2016	Englekirk	
2016/0191051	A1	6/2016	Burgener	
2016/0226478	A1	8/2016	Dribinsky	
2016/0329891	A1	11/2016	Bakalski	
2017/0162692	A1	6/2017	Brindle	
2017/0201250	A1	7/2017	Heaney	
2017/0236946	A1	8/2017	Stuber	
2017/0237462	A1	8/2017	Burgener	
2018/0061985	A1	3/2018	Brindle et al.	
2018/0062645	A1	3/2018	Burgener et al.	
2018/0083614	A1	3/2018	Brindle	
2018/0138272	A1	5/2018	Ebihara	
2018/0145678	A1	5/2018	Maxim	
2018/0212599	A1	7/2018	Dribinsky	
2019/0058470	A1	2/2019	Burgener	
2019/0081655	A1	3/2019	Burgener	
2019/0088781	A1	3/2019	Brindle	
2019/0089348	A1	3/2019	Brindle	
2019/0097612	A1	3/2019	Burgener	
2019/0237579	A1	8/2019	Brindle	
2019/0238126	A1	8/2019	Brindle et al.	
2020/0036377	A1	1/2020	Brindle	
2020/0036378	A1	1/2020	Brindle	
2020/0067504	A1	2/2020	Brindle	
2020/0076427	A1	3/2020	Burgener	
2020/0076428	A1	3/2020	Burgener	
2020/0112305	A1	4/2020	Brindle	
2020/0153430	A1	5/2020	Burgener	

FOREIGN PATENT DOCUMENTS

CN	200680025128.7	11/2012
DE	19832565	8/1999
DE	112011103554	9/2013
EP	385641	9/1990
EP	622901	11/1994
EP	782267	7/1997
EP	788185	8/1997
EP	851561	1/1998
EP	913939	5/1999
EP	625831	11/1999
EP	1006584	6/2000
EP	1451890	2/2001
EP	1925030	5/2008
EP	2348532	7/2011
EP	2348533	7/2011
EP	2348534	7/2011
EP	2348535	7/2011
EP	2348536	7/2011
EP	2387094	11/2011
EP	1774620	10/2014
EP	2884586	6/2015
EP	3113280	1/2017
EP	1902474	4/2017
JP	5575348	6/1980
JP	H01254014	10/1989
JP	2161769	6/1990
JP	H0434980	2/1992
JP	H04183008	6/1992
JP	H05299995	11/1993
JP	H06112795	4/1994
JP	H06314985	11/1994
JP	H06334506	12/1994
JP	H07046109	2/1995
JP	H07070245	3/1995
JP	H07106937	4/1995
JP	H08023270	1/1996
JP	H08070245	3/1996
JP	H08148949	6/1996
JP	H08251012	9/1996
JP	H08307305	11/1996
JP	H08330930	12/1996
JP	H098627	1/1997
JP	H9041275	2/1997
JP	H9055682	2/1997
JP	H0992785	4/1997
JP	H09148587	6/1997
JP	H09163721	6/1997
JP	H09181641	7/1997
JP	H09186501	7/1997
JP	H09200021	7/1997
JP	H09200074	7/1997
JP	H09238059	9/1997
JP	H09243738	9/1997
JP	H098621	10/1997
JP	H09270659	10/1997
JP	H09284114	10/1997
JP	H09284170	10/1997
JP	H09298493	10/1997
JP	H09326642	12/1997
JP	H1079467	3/1998
JP	H1093471	4/1998
JP	H10242477	9/1998
JP	H10242826	9/1998
JP	H10242829	9/1998
JP	H10284736	10/1998
JP	10-344247	12/1998
JP	H10335901	12/1998
JP	H1126776	1/1999

(56) **References Cited**

FOREIGN PATENT DOCUMENTS

JP	H11112316	4/1999
JP	H11136111	5/1999
JP	H11163642	6/1999
JP	H11163704	6/1999
JP	H11205188	7/1999
JP	H11274804	10/1999
JP	2000031167	1/2000
JP	2000058842	2/2000
JP	2000101093	4/2000
JP	2000183353	6/2000
JP	19980344247	6/2000
JP	2000188501	7/2000
JP	2000208614	7/2000
JP	2000223713	8/2000
JP	2000243973	9/2000
JP	2000277703	10/2000
JP	2000294786	10/2000
JP	2000311986	11/2000
JP	2001007332	1/2001
JP	2003060451	2/2001
JP	2001094114	4/2001
JP	2001119281	4/2001
JP	2001157487	5/2001
JP	2001156182	6/2001
JP	2001274265	10/2001
JP	2002156602	5/2002
JP	2000358775	6/2002
JP	2002164441	6/2002
JP	2002290104	10/2002
JP	2003101407	4/2003
JP	2003143004	5/2003
JP	2003167615	6/2003
JP	2003189248	7/2003
JP	2003332583	11/2003
JP	2003347553	12/2003
JP	2004147175	5/2004
JP	2004515937	5/2004
JP	2004166470	6/2004
JP	2004199950	7/2004
JP	2004288978	10/2004
JP	2005515657	5/2005
JP	2005203643	7/2005
JP	2005251931	9/2005
JP	200551567	9/2006
JP	2009500868	1/2009
JP	2010506156	2/2010
JP	4659826	3/2011
JP	4892092	3/2012
JP	5215850	3/2013
JP	5591356	9/2014
JP	55678106	2/2015
JP	6006219	10/2016
JP	WO2015015720	3/2017
JP	2014239233	12/2017
KR	19940027615	12/1994
WO	WO86/01037	2/1986
WO	WO9523460	8/1995
WO	WO9806174	2/1998
WO	WO9935695	7/1999
WO	WO0227920	4/2002
WO	WO03032431	4/2003
WO	WO2006038190	4/2006
WO	WO07008934	1/2007
WO	WO07033045	3/2007
WO	WO07035610	3/2007
WO	WO09108391	9/2009
WO	WO12054642	4/2012

OTHER PUBLICATIONS

US 10,700,200 B1, 06/2020, Brindle (withdrawn)

Voldman—"Dynamic Threshold Body- and Gate-coupled SOI ESD Protection Networks", Journal of Electrostatics 44, Mar. 20, 1998, pp. 239-255, Doc 8015.

Matloubian—"Smart Body Contact for SOI MOSFETs" 1989 IEEE SOS/SOI Technology Conference pp. 128-129, Oct. 3-5, 1989, 2 pages, Doc 0425.

Hieda—Floating-Body Effect Free Concave SOI-MOSFETs (COSMOS), ULSI Research Center, Toshiba Corporation, IEEE 1991, pp. 26.2.1-26.2.4, Dec. 8-11, 1991, 4 pages, Doc 0187.

Patel—"A Novel Body Contact for SIMOX Based SOI MOSFETs", Solid-State Electronics vol. 34, No. 10, pp. 1071-1075, Apr. 22, 1991, 6 pages, Doc 3000.

Katzin—"High Speed 100+ W RF Switched Using GaAs MMICs", IEEE Transactions on Microwave Theory and Techniques, Nov. 1992, pp. 1989-1996, 8 pages, Doc 0194.

Armijos—"High Speed DMOS FET Analog Switches and Switch Arrays", Temic Semiconductors Jun. 22, 1994, pp. 1-10, 10 pages, Doc 0202.

LI—"Suppression of Geometric Component of Charge Pumping Current SOI/MOSFETs", Proc. Int. Symp. VLSI Technology, Systems & Applications (IEEE May 31-Jun. 2, 1995), pp. 144-148, 5 pages, Doc 8016.

Chan—"A Novel SOI CBiCMOS Compatible Device Structure for Analog and Mixed-Mode Circuits", Dept. of EECS, University of California at Berkeley, IEEE Nov. 1995, pp. 40-43, 4 pages, Doc 1078.

Kohama—"High Power DPDT Antenna Switch MMIC for Digital Cellular Services", IEEE Journal of Solid-State Circuits, Oct. 1996, pp. 1406-1411, 6 pages, Doc 0244.

Tenbroek—"Electrical Measure of Silicon Film and Oxide Thickness in Partially Depleted SOI Technologies", Solid-State Electronics, vol. 39, No. 7, pp. 1011-1014, Nov. 14, 1995, 4 pages. Doc 8019.

NEC Corporation—"uPG13xG Series L-Band SPDT Switch GaAs MMIC", Document No. P1096EJ1VOANDO (1st Edition), Feb. 1996, 30 pages, Doc 0248.

Kuge—"SOI-DRAM Circuit Technologies for Low Power High Speed Multigiga Scale Memories", Jun. 8-10, 1995, IEEE Journal of Solid-State Circuits, vol. 31, No. 4, Apr. 1996, pp. 586-591, 6 pages, Doc 0259.

Fung—"Frequency Dispersion in Partially Depleted SOI MOSFET Output Resistance", Proceedings 1996 IEEE International SOI Conference, Oct. 1996, pp. 146-147, 2 pages, Doc 0268.

Yamamoto—"A Single-Chip GaAs RF Transceiver for 1.9GHz Digital Mobile Communication Systems", IEEE Dec. 1996, pp. 1964-1973, 10 pages, Doc 0255.

Johnson—"Silicon-On-Sapphire Technology for Microwave Circuit Applications", Dissertation UCSD Jan. 1997, IEEE May 1998, pp. 1-184, 214 pages, Doc 0288.

Koh—"1Giga Bit SOI DRAM with Fully Bulk Compatible Process and Body-Contacted SOI MOSFET Structure", IEEE Dec. 10, 1997, pages, Doc 8021.

Maeda—"A Highly Reliable .35 μm Field Body-Tied SOI Gate Array for Substrate-Bias-Effect Free Operation", 1997 Symposium on VLSI Technology Digest of Technical Papers, Jun. 10-12, 1997, 2 pages, Doc 8020.

Koh—"Body-Contacted SOI MOSFET Structure with Fully Bulk CMOS Compatible Layout and Process", IEEE Electron Device Letters, vol. 18, No. 3, Mar. 1997, pp. 102-104, 3 pages, Doc 0305.

Huang—"Device Physics, Performance Simulations and Measured Results of SOI MOS and DTMOS Transistors and Integrated Circuits", Beijing Microelectronics Technology Institute, Oct. 23, 1998 IEEE, pp. 712-715, 4 pages, Doc 0333.

Hirota—"0.5V 320MHz 8b Multiplexer/Demultiplier Chips Based on a Gate Array with Regular-Structured DRMOS/SOI", Feb. 5-7, 1998, 1998 IEEE International Solid-State Circuits Conference. Digest of Technical Papers, ISSCC. First Edition, pp. 12.2-1-12.2-11, 11 pages, Doc 0351.

Chuang—"SOI for Digital CMOS VLSI Design: Design Considerations and Advances", Proceedings of the IEEE vol. 86, No. 4, Apr. 1, 1998 pp. 689-720, 32 pages, Doc 1079.

Duyet—"Suppression of Geometric Component of Charge Pumping Current in Thin Film Silicon on insulator Metal-Oxide-Semiconductor Field-Effect Transistors", Japanese Journal of Applied Physics, Jul. 15, 1998, vol. 37, pp. L855-858, 4 pages, Doc 0729.

(56) **References Cited**

OTHER PUBLICATIONS

Gil—"A High Speed and Low Power SOI Inverter using Active Body-Bias", Proceedings International Symposium on Low Power Electronics and Design, Sep. 1998, pp. 59-63, 5 pages, Doc 0359.
Tseng—"AC Floating-Body Effects an Submicron Fully Depleted (FD) SOI nMOSFETs and the Impact on Analog Applications", IEEE Electron Devices, vol. 19, No. 9, Sep. 1998, pp. 351-353, 3 pages, Doc 0362.
Duyet—"Effects of Body Reverse Pulse Bias on Geometric Component of Charge Pumping Current in FD SOI MOSFETs", Proceedings IEEE Intl SOI Conference, Oct. 5-8, 1998, pp. 79-80, 2 pages, Doc 0364.
Chung—"A New SOI MOSFET Structure with Junction Type Body Contact", International Electron Device Meeting (IEDM) Technical Digest, Dec. 5-8, 1999, pp. 59-62, 4 pages, Doc 0379.
Devlin—"The Design of Integrated Switches and Phase Shifters", Nov. 24, 1999, 15 pages, Doc 0381.
Lim—"Partial SOI LDMOSFETs for High-Side Switching", Dept. of Engineering, University of Cambridge, Oct. 5-9, 1999 IEEE, pp. 149-152, 4 pages, Doc 0393.
Maeda—"Substrate Bias Effect and Source Drain Breakdown Characteristics in Body Tied Short Channel SOI MOSFETs", IEEE Transactions on Electron Devices, vol. 46, No. 1, Jan. 1999, pp. 151-158, 8 pages, Doc 0397.
Rodgers—"Silicon UTSi CMOS RFIC for CDMA Wireless Communications System", IEEE MTT-S Digest, Jun. 14-15, 1999, pp. 485-488, 4 pages, Doc 0406.
Yamamoto—"A 2.2-V Operation, 2.4-GHz Single-Chip GaAs MMIC Transceiver for Wireless Applications", IEEE Journal of Solid-State Circuits, vol. 34, No. 4, Apr. 1999, pp. 502-512, 11 pages, Doc 0417.
Chen—"Low Power, Multi-Gigabit DRAM Cell Design Issues Using SOI Technologies", http://bwrc.eecs.berkeley.edu/people/grad_students/chenff/reports, May 14, 1999, 6 pages, Doc 0418.
Allen—"Characterization and Modeling of Silicon-on-Insulator Field Effect Transistors", Department of Electrical Engineering and Computer Science, MIT May 20, 1999, 80 pages, Doc 0419.
Tseng—"AC Floating-Body Effects and the Resultant Analog Circuit Issues in Submicron Floating Body and Body-Grounded SOI MOSFETs", IEEE Transactions on Electron Devices, vol. 46, No. 8, Aug. 1999, 8 pages, Doc 0420.
Fung—"Controlling Floating-Body Effects for 0.13 μm and 0.10 μm SOI CMOS", IDEM 00-231-234, Dec. 10-13, 2000, IEEE, 4 pages, Doc 8017.
Imam—"A Simple Method to Determine the Floating-Body Voltage of SOI CMOS Devices", IEEE Electron Device Letters, vol. 21, No. 1, Jan. 2000, pp. 21-23, 3 pages, Doc 0441.
Kanda—"A Si RF Switch MMIC for the Cellular Frequency Band Using SOI-CMOS Technology", The Institute of Electronics, Information and Communication Engineers, vol. 100, No. 152, Jun. 2000, pp. 79-83, 5 pages, Doc 0443.
Shahidi—"Issues in SOI CMOS Technology and Design", IEEE 2000 Custom Integrated Circuits Conference, Publication/Presentation dated May 21, 2000, 78 pages, Doc 8014.
Horiuchi—"A Dynamic-Threshold SOI Device with a J-FET Embedded Source Structure and a Merged Body-Bias-Control Transistor—Part II: Circuit Simulation", IEEE Transactions on Electron Devices, vol. 47, No. 8, Aug. 2000, pp. 1593-1598, 6 pages, Doc 0457.
Horiuchi—"A Dynamic-Threshold SOI Device with a J-FET Embedded Source Structure and a Merged Body-Bias-Control Transistor—Part I: A J-Fet Embedded Source Structure Properties", IEEE Transactions on Electron Devices, vol. 47, No. 8, Aug. 2000, pp. 1587-1592, 6 pages, Doc 0456.
Scheinberg—"A Computer Simulation Model for Simulating Distortion in FET Resistors", IEEE Transactions on Computer-Aided Design of Integrated Circuits and Systems, vol. 19, No. 9, Sep. 2000, pp. 981-989, 9 pages, Doc 0461.
Cristoloveanu—"The Four-Gate Transistor", Institute of Microelectronics, Electromagnetism and Photonics, ESSDERC Sep. 24-26, 2002, pp. 323-326, 4 pages, Doc 0478.
Reedy—"Utsi CMOS: A Complete RF SOI Solution", Peregrine Semiconductor Nov. 2000, pp. 1-6, 6 pages, Doc 0508.
Yamamoto—"A 2.4GHz Band 1.8V Operation Single Chip SI-CMOS T/R MMIC Front End with a Low Insertion Loss Switch", IEEE Journal of Solid-State Circuits, vol. 36, No. 8, Aug. 2001, pp. 1186-1197, 12 pages, Doc 0527.
Adan—"OFF-State Leakage Current Mechanisms in BulkSi and SOI MOSFETs and Their Impact on CMOS ULSIs Standby Current", IEEE Transactions on Electron Devices, vol. 48, No. 9, Sep. 2001, pp. 2050-2057, 8 pages, Doc 0528.
Goldman—"0.15 μm SOI DRAM Technology Incorporating Sub-Volt Dynamic Threshold Devices for Embedded Mixed-Signal & RF Circuits", Oct. 1-4, 2001 IEEE SOI Conference, pp. 97-98, 2 pages, Doc 0531.
Fung—"Present Status and Future Direction of BSIM SOIL Model for High-Performance/Low-Power/RF Application", IBM Microelectronics, Semiconductor Research and Development Center, April 2002, 4 pages, Doc 0554.
Adan—"Linearity and Low-Noise Performance of SOI MOSFETs for RF Applications", IEEE Transactions on Electron Devices, May 2002 vol. 49, No. 5, pp. 881-888, 8 pages, Doc 0555.
Akarvardar—"Multi-Bias Dependence of Threshold Voltage, Subthreshold Swing, and Mobility in G4-FETs", Institute of Microelectronics, Electromagnetism, and Photonics, IEEE Oct. 2003, pp. 127-130, 4 pages, Doc 1075.
Dufrene—"The G4-FET: Low Voltage to High Voltage Operation and Performance", Dept. of Electrical and Computer Engineering, The University of Tennessee, IEEE Jan. 2003, pp. 55-56, 2 pages, Doc 0565.
Marks—"SOI for Frequency Synthesis in RF Integrated Circuits", Thesis submitted to North Carolina State University, May 2003, 155 pages, Doc 0574.
Zhu Ming—"A New Structure of Silicon-on-Insulator Metal-Oxide Semiconductor Field Effect Transistor to Suppress the Floating Body Effect", Nov. 4, 2002, Chin. Phys. Lett., vol. 20, No. 5 (2003) pp. 767-769, 3 pages, Doc 0575.
Fung—"On the Body-Source Built-In Potential Lowering of SOI MOSFETS", IEEE Electron Device Letters, vol. 24, No. 2, Feb. 2003, pages, Doc 8018.
Tinella—"Study of the Potential of CMOS-SOI Technologies Partially Abandoned for Radiofrequency Applications", Thesis for obtaining the standard of Doctor of INPG, National Polytechnic of Grenoble, Sep. 25, 2003, 187 pages, Doc 0594.
De Houck—"Design of EEPROM Memory Cells in Fully Depleted 'CMOS SOI Technology'", Universite Catholique de Louvain Faculty of Applied Science, Laboratory of Electronics and Microelectronics, Academic Year 2003-2004, Jan. 2003, 94 pages, Doc 0599.
Streetman—"Solid State Electronic Devices", Microelectronics Research Center, Dept. of Electrical and Computer Engineering, The University of Texas at Austin, Chapter 6, Jan. 2004 by Pearson Education Inc., 4 pages, Doc 0602.
Zhu—"Simulation of Suppression of Floating-Body Effect in Partially Depleted SOI MOSFET Using a Sil-xGex Dual Source Structure", Materials Science and Engineering B 114-115 Dec. 15, 2004, pp. 264-268, 5 pages, Doc 0604.
Chen—"G4-FET Based Voltage Reference", Masters Theses, University of Tennessee, Knoxville, Trace: Tennessee Research and Creative Exchange, May 2004, 57 pages, Doc 0607.
Ippoushi—"SOI Structure Avoids Increases in Chip Area and Parasitic Capacitance Enables Operational Control of Transistor Threshold Voltage", Renesas Edge, vol. 2004.5, Jul. 2004, p. 15, 1 page, Doc 0610.
Akarvardar—"Threshold Voltage Model of the SOI 4-Gate Transistor", 2004 IEEE International SOI Conference, October 4-7, 2004, pp. 89-90, 2 pages, Doc 0613.
Dufrene—"Investigation of the Four-Gate Action in G4-FETs", IEEE Transactions on Electron Devices, vol. 51, No. 11, Dec. 2004, pp. 1931-1935, 5 pages, Doc 0617.
Cathelin—"Antenna Switch Devices in RF Modules for Mobile Applications", ST Microelectronics, Front-End Technology Manufacturing, Crolles, France, Mar. 2005, 42 pages, Doc 0623.
Analog Devices—"LC2MOS High Speed, Quad SPST Switch", Rev. B, 8 pages, Apr. 1988, Doc 1076.

(56) **References Cited**

OTHER PUBLICATIONS

Analog Devices—"LC2MOS Quad SPST Switch", Rev. B, 6 pages, Jul. 1992, Doc 1077.
Le TMOS en technologie SOI, 3.7.2.2 Pompage de charges, pp. 110-111, 2 pages, Doc 1081.
Linear Systems—"High-Speed DMOS FET Analog Switches and Switch Arrays", 11 pages, Doc 1082.
Orndorff—"CMOS/SOS/LSI Switching Regulator Control Device", IEEE International Solid-State Circuits Conference, ISSCC 78, Feb. 1978, pp. 234-235, 282, 3 pages, Doc 0151.
Nelson Pass—Pass Labs, "Cascode Amp Design", Audio Electronics, pp. 1-4, Mar. 1978, 4 pages, Doc 0153.
Kwok—"An X-Band SOS Resistive Gate Insulator Semiconductor (RIS) Switch", IEEE Transactions on Electron Device, Feb. 1980, pp. 442-448, 7 pages, Doc 0154.
Ayasli—"An X-Band 10 W Monolithic Transmit-Receive GaAs FET Switch", Raytheon Research Division, May 31-Jun. 1, 1983 IEEE, pp. 42-46, 5 pages, Doc 0155.
Ayasli—"Microwave Switching with GaAs FETs", Microwave Journal, Nov. 1982, pp. 719-723, 10 pages, Doc 0156.
Pucel—"A Multi-Chip GaAs Monolithic Transmit/Receive Module for X-Band", Research Division. Raytheon Company, Jun. 15-17, 1982 IEEE MTT-S Digest, pp. 489-492, 4 pages, Doc 0157.
Sedra—"Microelectronic Circuits", University of Toronto, Oxford University Press, Fourth Edition, 1982, 1987, 1991, 1998, pp. 374-375, 4 pages, Doc 0158.
Ayasli—"A Monolithic Single-Chip X-Band Four-Bit Phase Shifter", IEEE Transactions on Microwave Theory and Techniques, vol. MTT-30, No. 12, Dec. 1982, pp. 2201-2206, 6 pages, Doc 0159.
Heller—"Cascode Voltage Switch Logic: A Different CMOS Logic Family", IEEE International Solid-State Circuits Conference, Feb. 22-24, 1984, pp. 16-17, 2 pages, Doc 0160.
Gopinath—"GaAs FET RF Switches", IEEE Transactions on Electron Devices, Jul. 1985, pp. 1272-1278, 7 pages, Doc 0161.
Yamao—"GaAs Broadband Monolithic Switches", 1986, pp. 63-71, 10 pages, Doc 0162.
Barker—"Communications Electronics-Systems, Circuits and Devices", Jan. 1, 1987 Prentice-Hall, 347 pages, Doc 0163 (A-D).
Harjani—"A Prototype Framework for Knowledge Based Analog Circuit Synthesis", IEEE Design Automation Conference, Jun. 28-Jul. 1, 1987, pp. 42-49, 8 pages, Doc 0164.
Colinge—"An SOI Voltage-Controlled Bipolar-MOS Device", IEEE Transactions on Electron Devices, vol. ED-34, Apr. 1987, pp. 845-849, 5 pages, Doc 0165.
Schindler—"DC-40 GHz and 20-40GHz MMIC SPDT Switches", IEEE Transactions of Electron Devices, vol. ED-34, No. 12, Dec. 1987, pp. 2595-2602, 8 pages, Doc 0167.
Colinge—"Fully Depleted SOI CMOS for Analog Applications", IEEE Transactions on Electron Devices, 1998, pp. 1010-1016, 7 pages, Doc 0168.
Nakayama—"A 1.9 GHz Single-Chip RF Front End GaAs MMIC with Low-Distortion Cascode FET Mixer for Personal Handy-Phone System Terminals", Radio Frequency Integrated Circuits Symposium, 1988, pp. 205-208, 4 pages, Doc 0169.
Peregrine Semiconductor Corporation—"An Ultra-Thin Silicon Technology that Provides Integration Solutions on Standard CMOS", 1988, 4 pages, Doc 0170.
Shifrin—"High Power Control Components Using a New Monolithic FET Structure", IEEE Microwave and Millimeter-Wave Monolithic Circuits Symposium, 1988, pp. 51-56, 6 pages, Doc 0171.
Schindler—"DC-20 GHz N X M Passive Switches", IEEE Transactions on Microwave Theory and Techniques, vol. 36, No. 12, Dec. 1988, pp. 1604-1613, 10 pages, Doc 0172.
Eisenberg—"High Isolation 1-20 GHz MMIC Switches with On-Chip Drivers", IEEE Microwave and Millimeter Wave Monolithic Circuits Symposium, 1989, pp. 41-45, 5 pages, Doc 0173.
Houng—"60-70 dB Isolation 2-19 GHz Switches", Raytheon Electromagnetic Systems Division, 1989 IEEE, GaAs IC Symposium, pp. 173-176, 4 pages, Doc 0174.
Schindler—"A 2-18 GHz Non-Blocking Active 2×2 Switch", Raytheon Company, 1989 IEEE, GaAs IC Symposium, pp. 181-183, 3 page, Doc 0175.
Slobodnik—"Millimeter Wave GaAs Switch FET Modeling", Microwave Journal, 1989, 7 pages, Doc 0176.
Chen—"Dual-Gate GaAs FET: A Versatile Circuit Component for MMICs", Microwave Journal, Jun. 1989, pp. 125-135, 7 pages, Doc 0177.
Shifrin—"Monolithic FET Structure for High Power Control Component Applications", IEEE Transactions on Microwave Theory and Techniques, vol. 37, No. 12, Dec. 1989, pp. 2134-2142, 8 pages, Doc 0178.
Schindler—"A High Power 2-18 GHz T/R Switch", 1988 IEEE, IEEE 1990 Microwave and Millimeter-Wave Circuits Symposium, pp. 119-122, 4 pages, Doc 0180.
Schindler—"A Single Chip 2-20 GHz T/R Module" 1988 IEEE, IEEE 1990 Microwave and Millimeter-Wave Monolithic Circuits Symposium, pp. 99-102, 4 pages, Doc 0182.
Valeri—"A Composite High Voltage Device Using Low Voltage SOI MOSFETs", IEEE, 1990, pp. 169-170, 2 pages, Doc 0183.
Yun—"High Power-GaAs MMIC Switches with Planar Semi-Insulated Gate FETs (SIGFETs)", International Symposium on Power Semiconductor Devices & Ics, 1990, pp. 55-58, 4 pages, Doc 0184.
Wang—"Threshold Voltage Instability at Low Temperatures in Partially Depleted Thin Film SOI MOSFETs", IEEE SOS/SOI Technology Conference, Jun. 1991, pp. 91-92, 2 pages, Doc 0185.
Bernkopf—" A High Power K/Ka-Band Monolithic T/R Switch", 1991 IEEE, IEEE 1991 Microwave and Millimeter-Wave Monolithic Circuits Symposium, pp. 15-18, 4 pages, Doc 0186.
McGrath—"Multi Gate FET Power Switches", Applied Microwave 1991, pp. 77-88, 7 pages, Doc 0188.
McGrath—"Novel High Performance SPDT Power Switches Using Multi-Gate FETs", 1991 IEEE, 1991 IEEE MTT-S Digest, pp. 839-842, 4 pages, Doc 0189.
Valeri—"A Silicon-on-Insulator Circuit for High Temperature, High-Voltage Applications", IEEE, 1991, pp. 60-61, 2 pages, Doc 0191.
Giffard: "Dynamic Effects in SOI MOSFETs", IEEE SOS/SOI Technology Conference, Oct. 1991, pp. 160-161, 2 pages, Doc 0192.
Baker—"Stacking Power MOSFETs for Use in High Speed Instrumentation", American Institute of Physics, 1992, pp. 5799-5801, 3 pages, Doc 0193
Eron—"Small and Large Signal Analysis of MESETs as Switches", Microwave Journal, 1995, 7 pages, Doc 0216.
Kusunoki—"SPDT Switch MMIC Using E/D Mode GaAs JFETs for Personal Communications", IEEE GaAs IC Symposium, 1992, pp. 135-138, 4 pages, Doc 0195.
Shifrin—"A New Power Amplifier Topology with Series Biasing and Power Combining of Transistors", IEEE 1992 Microwave and Millimeter-Wave Monolithic Circuits Symposium, 1992, pp. 39-41, 3 pages, Doc 0196.
Van Der Pujie—"Telecommunication Circuit Design", Wiley 1992, 187 pages, Doc 0197 (A-B).
Baker—"Series Operation of Power MOSFETs for High Speed Voltage Switching Applications", American Institute of Physics, 1993, pp. 1655-1656, 2 pages, Doc 0198.
Devlin—"A 2.4 GHz Single Chip Transceiver", Microwave and Millimeter-Wave Monolithic Circuits Symposium 1993, pp. 23-26, 4 pages, Doc 0199.
Uda—"High Performance GaAs Switch IC's Fabricated Using MESFETs with Two Kinds of Pinch Off Voltages", IEEE GaAs IC Symposium, 1993, pp. 247-250, 4 pages, Doc 0200.
Apel—"A GaAs MMIC Transceiver for 2.45 GHz Wireless Commercial Products", Microwave and Millimeter-Wave Monolithic Circuits Symposium, 1994, pp. 15-18, 4 pages, Doc 0201.
Assaderaghi—"A Dynamic Threshold Voltage Mosfet (DTMOS) for Ultra-low Voltage Operation", 1994, IEEE p. 33.1.1-33.1.4, 4 pages, Doc 0203.
Baker—"Designing Nanosecond High Voltage Pulse Generators Using Power MOSFETs", Electronic Letters, 1994, pp. 1634-1635, 2 pages, Doc 0204.

(56) **References Cited**

OTHER PUBLICATIONS

Caverly—"Distortion in GaAs MESFET Switch Circuits", 1994, 5 pages, Doc 0205.
Miyatsuji—"A GaAs High Power RF Single Pole Double Throw Switch IC for Digital Mobile Communication System", IEEE International Solid-State Circuits Conference, 1994, pp. 34-35, 2 pages, Doc 0206.
Puechberty—"A GaAs Power Chip Set for 3V Cellular Communications", 1994, 4 pages, Doc 0207.
Szedon—"Advanced Silicon Technology for Microwave Circuits." Naval Research Laboratory, 1994, pp. 1-110, 122 pages, Doc 0208.
Uda—"High-Performance GaAs Switch IC's Fabricated Using MESFETs with Two Kinds of Pinch-off Voltages and a Symmetrical Pattern Configuration", IEEE Journal of Solid-State Circuits, vol. 29, No. 10, Oct. 1994, pp. 1262-1269, 8 pages, Doc 0209.
Assaderaghi—"Dynamic Threshold Voltage MOSFET (DTMOS) for Ultra Low Voltage Operation", International Electron Devices Meeting, Dec. 1994, pp. 809-812, 4 pages, Doc 0212.
Abidi—"Low Power Radio Frequency IC's for Portable Communications", IEEE 1995, pp. 544-569, 26 pages, Doc 0213.
Couch—"Modern Communication System", Prentice-Hall, 1995, 316 pages, Doc 0214 (A-D).
De La Houssaye—"Microwave Performance of Optically Fabricated T-Gate Thin Film Silicon on Sapphire Based MOSFETs", IEEE Electron Device Letters, 1995, pp. 289-292, 4 pages, Doc 0215.
Gautier—"Body Charge Related Transient Effects in Floating Body SOI NMOSFETs", IEDM Tech. Digest 1995, pp. 623-626, 4 pages, Doc 0217.
Hittite Microwave—"Miniature Dual Control SP4T Switches for Low Cost Multiplexing", Hittite Microwave, 1995, 5 pages, Doc 0218.
Ionescu—"A Physical Analysis of Drain Current Transients at Low Drain Voltage in Thin Film SOI MOSFETs", Microelectronic Engineering 28 (1995), pp. 431-434, 4 pages, Doc 1085.
Keys—"Low Distortion Mixers or RF Communications", Ph.D. Thesis, University of California—Berkeley, 1995, 135 pages, Doc 0219.
Kohama—"High Power DPDT Antenna Switch MMIC for Digital Cellular Systems", GaAs IC Symposium, 1995, pp. 75-78, 4 pages, Doc 0220.
Lovelace—"Silicon MOSFET Technology for RF Ics", IEEE 1995, pp. 1238-1241, 4 pages, Doc 0221.
Matsumoto—"Fully Depleted 30-V-Class Thin Film SOI Power MOSFET", IEDM 95-979, Dec. 10-13, 1995, pp. 38.6.1-38.6.4, 4 pages, Doc 0222.
McGrath—"A 1.9-GHz GaAs Chip Set for the Personal Handyphone System", IEEE Transaction on Microwave Theory and Techniques, 1995, pp. 1733-1744, 12 pages, Doc 0223.
Microwave Journal—"A Voltage Regulator for GaAs FETs", Microwave Journal 1995, 1 page, Doc 0224.
Miyatsuji—"A GaAs High Power RF Single Pole Dual Throw Switch IC for Digital Mobile Communication System", IEEE Journal of Solid-State Circuits, 1995, pp. 979-983, 5 pages, Doc 0226.
Sanders—"Statistical Modeling of SOI Devices for the Low Power Electronics Program", AET, Inc., 1995, pp. 1-109, 109 pages, Doc 0227.
Tokumitsu—"A Low-Voltage, High-Power T/R-Switch MMIC Using LC Resonators", IEEE Transactions on Microwave Theory and Techniques, vol. 43, No. 5, May 1995, pp. 997-1003, 7 pages, Doc 0228.
Morishita—"Leakage Mechanism Due to Floating Body and Countermeasure on Dynamic Retention Mode of SOI-DRAM", 1995 Symposium on VLSI Technology Digest of Technical Papers, Apr. 1995, pp. 141-142, 2 pages, Doc 0229.
Suh—"A Physical Change-Based Model for Non-Fully Depleted SOI MOSFETs and Its Use in Assessing Floating-Body Effects in SOI SMOS Circuits", IEEE Transactions on Electron Devices, vol. 42, No. 4, Apr. 1995, pp. 728-737, 10 pages, Doc 0230.
Cherne—U.S. Statutory Invention Registration No. H1435, published May 2, 1995, 12 pages, Doc 0232.
Ota—"High Isolation and Low Insertion Loss Switch IC Using GaAa MESFETS", IEEE Transactions on Microwave Theory and Techniques, vol. 43, No. 9, Sep. 1995, pp. 2175-2177, 3 pages, Doc 0233.
Chan—"Comparative Study of Fully Depleted and Body-Grounded Non Fully Depleted SOI MOSFETs for High Performance Analog and Mixed Signal Circuits", IEEE Transactions on Electron Devices, vol. 42, No. 11, Nov. 1995, pp. 1975-1981, 7 pages, Doc 0234.
Assaderaghi—"History Dependence of Non-Fully Depleted (NFD) Digital SOI Circuits", 1996 Symposium on VLSI Technology Digest of Technical Papers 13.1, 1996, pp. 122-123, 2 pages, Doc 0235.
Burghartz—"Integrated RF and Microwave Components in BiCMOS Technology", IEEE Transactions on Electron Devices, 1996, pp. 1559-1570, 12 pages, Doc 0236.
Colinge—"A Low Voltage Low Power Microwave SOI MOSFET", IEEE International SOI Conference, 1996, pp. 128-129, 2 pages, Doc 0237.
Douseki—"A 0.5v SIMOX-MTMCOS Circuit with 200ps Logic Gate", IEEE International Solid-State Circuits Conference 1996, pp. 84-85, 423, 3 pages, Doc 0238.
Eggert—"CMOS/SIMOX-RF-Frontend for 1.7 GHz", Solid State Circuits Conference, 1996, 4 pages, Doc 0239.
Gentinne—"Measurement and Two-Dimensional Simulation of Thin-Film SOI MOSFETs: Intrinsic Gate Capacitances at Elevated Temperatures", Solid-State Electronics, vol. 39, No. 11, pp. 1613-1619, 1996, 7 pages, Doc 0240.
Hagan (or Hagen)—Radio Frequency Electronics:, Cambridge University Press 1996, 194 pages, Doc 0241(A-B).
Imai—"Novel High Isolation FET Switches", IEEE Transactions on Microwave Theory and Techniques 1996, pp. 685-691, 7 pages, Doc 0242.
Intersil—"RF Amplifier Design Using HFA3046, HFA3096, HFA3127, HFA3128 Transistor Arrays", Intersil Corporation 1996, pp. 1-4, 4 pages, Doc 0243.
Kuroda—"A 0.9-V, 150-Mhz, 10-mW, 4 mm2, 2-D Discrete Cosine Transform Core Processor with Variable-Threshold-Voltage (VT) Scheme", Technical Paper, 1996 IEEE International Solid-State Circuits Conference, 1996 Digest of Technical Papers, pp. 166-167, 14 pages, Doc 0245.
Larson—"RF and Microwave Circuit Design for Wireless Communications", Artech House 1996, 218 pages, Doc 0246 (A-C).
Nakayama—"A 1.9 GHz Single-Chip RF Front-End GaAs MMIC for Persona Communications", Microwave and Millimeter-Wave Monolithic Circuits Symposium, 1996, pp. 69-72, 4 pages, Doc 0247.
Soyuer—"RF and Microwave Building Blocks in a Standard BiCMOS Technology", IBM T.J. Watson Research Center, 1996 IEEE, pp. 89-92, 4 pages, Doc 0249.
Suematsu—"L-Band Internally Matched Si-MMIC Front End", IEEE, 1996, pp. 2375-2378, 4 pages, Doc 0250.
Titus—"A Silicon BICMOS Transceiver Front-End MMIC Covering 900 and 1900 MHZ Applications", Hittite Microwave Corporation, IEEE 1996 Microwave and Millimeter-Wave Monolithic Circuits Symposium, pp. 73-75, 4 pages, Doc 0251.
Uda—"A High Performance and Miniturized Dual Use (antenna/local) GaAs SPDT Switch IC Operating at +3V/0V", Microwave Symposium Digest, 1996, pp. 141-144, 4 pages, Doc 0252.
Uda—"Miniturization and High Isolation of GaAs SPDT Switch IC Mounted in Plastic Package", 1996, 8 pages, Doc 0253.
Yamamoto—"A GaAs RF Transceiver IS for 1.9GHz Digital Mobile Communication Systems", ISSCC96, 1996, pp. 340-341,469, 3 pages, Doc 0254.
Fuse—"0.5V SOI CMOS Pass-Gate Logic", 1996 IEEE Intl. Solid-State Circuits Conference, pp. 88-89, 424, 3 pages, Doc 0257.
Iyama—"L-Band SPDT Switch Using Si-MOSFET", IEICE Trans. Electron, vol. E79-C, No. 5, May 1996, pp. 636-643, 8 pages, Doc 0260.
Pelella—"Low-Voltage Transient Bipolar Effect Induced by Dynamic Floating-Body Charging in Scaled PD/SOI MOSFETs", IEEE Electron Device Letters, vol. 17, No. 5, May 1996, 3 pages, Doc 0261.

(56) **References Cited**

OTHER PUBLICATIONS

Wei—"Measurements of Transient Effects in SOI DRAM/SRAM Access Transistors", IEEE Electron Device Letters, vol. 17, No. 5, May 1996, pp. 193-195, 3 pages, Doc 0262.
Wei—"Measurement and Modeling of Transient Effects in Partially Depleted SOI MOSFETs", M.S. Thesis, MIT, Jul. 1996, 76 pages, Doc 0265.
Lu—"Floating Body Effects in Partially Depleted SOI CMOS Circuits", ISPLED, Aug. 1996, pp. 1-6, 6 pages, Doc 0266.
Madihian—"A High Speed Resonance Type FET Transceiver Switch for Millimeter Wave Band Wireless Networks", 26th EuMC, 1996, pp. 941-944, 4 pages, Doc 1084.
Chung—"A New SOI Inverter for Low Power Applications", IEEE SOI Conference, Oct. 1996, pp. 20-21, 2 pages, Doc 0267.
Ueda—"Floating Body Effects on Propagation Delay in SOI/CMOS LSIs", IEEE SOI Conference, Oct. 1996, pp. 142-143, 2 pages, Doc 0269.
Kuroda—"A 0.9-V, 150-Mhz, 10-mW, 4 mm2, 2-D Discrete Cosine Transform Core Processor with Variable-Threshold-Voltage (VT) Scheme", IEEE Journal of Solid-State Circuits, vol. 31, No. 11, Nov. 1996, pp. 1770-1779, 10 pages, Doc 0270.
Botto—"Series Connected Soft Switched IGBTs for High Power, High Voltage Drives Applications: Experimental Results," IEEE 1997, pp. 3-7, 5 pages, Doc 0271.
Carr—"Secrets of RF Circuit Design", McGraw-Hill, 1997, 293 pages, Doc 0272 (A-D).
Caverly—"A Project Oriented Undergraduate CMOS Analog Microelectronic System Design Course", IEEE, 1997, pp. 87-88, 2 pages, Doc 0274.
Caverly—Distortion in Microwave Control Devices, 1997, 10 pages, Doc 0275.
Caverly—"Distortion Properties of Gallium Arsenide and Silicon RF and Microwave Switches", IEEE, 1997, pp. 153-156, 4 pages, Doc 0276.
Crols—"CMOS Wireless Transceiver Design", Kluwer Academic, 1997, 214 pages, Doc 0277 (A-C).
Eggert—"A SOI-RF-CMOS Technology on High Resistivity SIMOX Substrates for Microwave Applications to 5 GHz", IEEE Transactions on Electron Devices, 1997, pp. 1981-1989, 9 pages, Doc 0278.
Freeman—"Radio System Design for Telecommunications", Wiley, 1997, 461 pages, Doc 0279 (A-F).
Gibson—"The Communication Handbook", CRC Press, 1997, 812 pages, Doc 0280 (A-R).
Hickman—"Practical RF Handbook", Newnes 1997, 270 pages, Doc 0281 (A-D).
Huang—"TFSOI Can It Meet the Challenge of Single Ship Portable Wireless Systems", IEEE International SOI Conference, 1997, pp. 1-3, 3 pages, Doc 0282.
Ishida—"A Low Power GaAs Front End IC with Current Reuse Configuration Using 0.15 μm Gate GaAs MODFETs", IEEE 1997, pp. 669-672, 4 pages, Doc 0283.
Iwata—"Gate Over Driving CMOS Architecture for 0.5V Single Power Supply Operated Devices", IEEE 1997, pp. 290-291, 3, pages, Doc 0284.
Johnson—"A Model for Leakage Control by MOS Transistor Stacking", ECE Technical Papers, 1997, pp. 1-28, 34 pages, Doc 0285.
Johnson—"Advanced High-Frequency Radio Communication", Artech House 1997, 205 pages, Doc 0286 (A-C).
Johnson—"Silicon-On-Sapphire MOSFET Transmit/Receive Switch for L and S Band Transceiver Applications", Electronic Letters, 1997, pp. 1324-1326, 3 pages, Doc 0287.
Kanda—"High Performance 19 GHz Band GaAs FET Using LOXI (Layered Oxide Isolation)—MESFETs", IEEE, 1997, pp. 62-65, 4 pages.
Lossee—"RF Systems, Components, and Circuits Handbook", Artech House 1997, 314 pages, Doc 0290 (A-D).
Madihan—"A 2-V, 1-10GHz BiCMOS Transceiver Chip for Multimode Wireless Communications Networks", IEEE 1997, pp. 521-525, 5 pages, Doc 0291.
Nishijima—"A High Performance Transceiver Hybrid IC for PHS Hand Set Operating with Single Positive Voltage Supply", Microwave Symposium Digest 1997, pp. 1155-1158, 4 pages, Doc 0293.
Philips Semiconductors—"SA630 Single Pole Double Throw (SPDT) Switch", 1997, 14 pages, Doc 0294.
Razavi—"Next Generation RF Circuits and Systems", IEEE 1997, pp. 270-282, 13 pages, Doc 0295.
Schaper—"Communications, Computations, Control, and Signal-Processing", Kluwer Academic, 1997, 308 pages, Doc 0296 (A-D).
Suematsu—"On-Chip Matching SI-MMIC for Mobile Communication Terminal Application", IEEE 1997, pp. 9-12, 4 pages, Doc 0297.
Wada—"Active Body-Bias SOI-CMOS Driver Circuits", Symposium on VLSI Circuits Digest of Technical Papers, 1997, pp. 29-30, 2 pages, Doc 0298.
Fuse—"A 0.5V 200MHz 1-Stage 32b ALU Using a Body Bias Controlled SOI Pass-Gate Logic", IEEE Intl Solid-State Circuits Conference, Feb. 1997, 3 pages, Doc 0299.
Shimomura—"TP 4.3: A 1V 46ns 16Mb SOI-DRAM with Body Control Technique", 1997 IEEE Intl Solid-State Circuits Conference, Feb. 1997, 9 pages, Doc 0300.
Ueda—"A CAD Compatible SOI/CMOS Gate Array Having Body Fixed Partially Depleted Transistors", IEEE International Solid-State Circuits Conference, Feb. 8, 1997, pp. 288-289, 3 pages, Doc 0301.
Assaderaghi—"Dynamic Threshold Voltage MOSFET (DTMOS) for Ultra Low Voltage VLSI", IEEE Transactions on Electron Devices, vol. 44, No. 3, Mar. 1997, pp. 414-422.
Schlechtweg—"Multifunctional Integration Using HEMT Technology", Fraunhofer Institute for Applied Solid State Physics, (date uncertain, believed Mar. 1997), 18 pages, Doc 0306.
Rohde—"Optic/Millimeter-Wave Converter for 60 GHz Radio-Over-Fiber Systems", Fraunhofer-Institut fur Angerwandte Festkorperphysik Freiburg i. Br., Apr. 1997, pp. 1-5, 5 pages, Doc 0307.
Smuk—"Monolithic GaAs Multi-Throw Switches with Integrated Low Power Decoder/Driver Logic", May 1997, IEEE Radio Frequency Integrated Circuits, 4 pages, Doc 0308.
Suehle—"Low Electric Field Breakdown of Thin Si02 Films Under Static and Dynamic Stress", IEEE Transactions on Electron Devices, vol. 44, No. 5, May 1997, 8 pages, Doc 0309.
Suehle—"Low Electric Field Breakdown of Thin Si02 Films Under Static and Dynamic Stress", IEEE Transactions on Electron Devices, vol. 44, No. 5, May 1997. pp 801-808, 8 pages, Doc 0310.
Assaderaghi—"Transient Pass-Transistor Leakage Current in SOI MOSFETs", IEEE Electron Device Letters, vol. 18, No. 6, Jun. 1997, pp. 241-243, 3 pages, Doc 0312.
Chung—"A New SOI Inverter Using Dynamic Threshold for Low-Power Applications", IEEE Electron Device Letters, vol. 18, No. 6, Jun. 1997, pp. 248-250, 3 pages, Doc 0313.
Kuang—"SRAM Bitline Circuits on PD SOI: Advantages and Concerns", IEEE Journal of Solid State Circuits, vol. 32, No. 6, Jun. 1997, pp. 837-844, 8 pages, Doc 0314.
Smuk—"Monolithic GaAs Multi-Throw Switches with Integrated Low-Power Decoder-Driver Logic", Hitite Microwave Corporation, Jun. 1997, 4 pages, Doc 0317.
Wang—"Efficiency Improvement in Charge Pump Circuits", IEEE Journal of Solid-State Circuits, vol. 32, No. 6, Jun. 1997, pp. 852-860, 9 pages, Doc 0318.
Caverly—"A Silicon CMOS Monolithic RF and Microwave Switching Element", 27th European Microwave Conference, 1987, pp. 1046-1051, 10 pages, Doc 0166.
Douseki—"A 0.5-V MTCMOS/SIMOX Logic Gate", IEEE Journal of Solid-State Circuits, vol. 32, No. 10, Oct. 1997, 6 pages, Doc 0320.
Krishnan—"Efficacy of Body Ties Under Dynamic Switching Conditions in Partially Depleted SOI CMOS Technology", Proceedings IEEE Intl SOI Conference, Oct. 1997, pp. 140-141, 2 pages, Doc 0321.
Workman—"Dynamic Effects in BTG/SOI MOSFETs and Circuits Due to Distributed Body Resistance", Proceedings 1997 IEEE International SOI Conference, Oct. 1997, pp. 28-29, 2 pages, Doc 0322.

(56) **References Cited**

OTHER PUBLICATIONS

Shimomura—"A 1-V 46-ns 16-mb SOI-DRAM with Body Control Technique", IEEE Journal of Solid-State Circuits, vol. 32, No. 11, Nov. 1997, pp. 1712-1720, 9 pages, Doc 0323.
Philips Semiconductors—Product Specificate, IC17 Data Handbook, Nov. 7, 1997, pp. 1-14, 14 pages, Doc 0324.
Edwards—"The Effect of Body Contact Series Resistance on SOI CMOS Amplifier Stages", IEEE Transactions on Electron Devices, vol. 44, No. 12, Dec. 1997, pp. 2290-2294, 5 pages, Doc 0325.
Caverly—"CMOS RF Circuits for Integrated Wireless Systems", IEEE 1998, pp. 1-4, 4 pages, Doc 0328.
Caverly—"Development of a CMOS Cell Library for RF Wireless and Telecommunications Applications", VLSI Symposium, 1998, 6 pages, Doc 0329.
Caverly—"Nonlinear Properties of Gallium Arsenide and Silicon FET-Based RF and Microwave Switches", IEEE 1998, pp. 1-4, 4 pages, Doc 0330.
Choumei—A High Efficiency, 2V Single Supply Voltage Operation RF Front End MMIC for 1.9GHz Personal Handy Phone Systems:, IEEE, 1998, pp. 73-76, 4 pages, Doc 0331.
Henshaw—"Design of an RF Transceiver", IEEE Colloquium on Analog Signal Processing, 1998, 6 pages, Doc 0332.
Johnson—"Advanced Thin Film Silicon-on-Sapphire Technology: Microwave Circuit Applications", IEEE Transactions on Electron Devices, vol. 45, No. 5, May 1988, pp. 1047-1054, 8 pages, Doc 0334 (A-B).
Larson—"Integrated Circuit Technology Options for RFICs—Present Status and Future Directions", IEEE Journal of Solid-State Circuits, 1998, pp. 387-399, 13 pages, Doc 0335.
Maas—"The RF and Microwave Circuit Design Cookbook", Artech House 1998, 149 pages, Doc 0336 (A-B).
Masuda—"High Power Heterojunction GaAs Switch IC with P-1dB of More than 38dBm for GSM Application", IEEE, 1998 pp. 229-232, 4 pages, Doc 0337.
Matsumoto—"A Novel High Frequency Quasi-SOI Power MOSFET for Multi-Gigahertz Application", IEEE, 1998, pp. 945-948, 4 pages, Doc 0338.
Megahed—"Low Cost UTSi Technology for RF Wireless Applications", Peregrine Semiconductor Corporation, IEEE MTT-S Digest, 1998, pp. 981-984, 4 pages, Doc 0339.
Moye—"A Compact Broadband, Six-Bit MMIC Phasor with Integrated Digital Drivers+", IEEE 1990 Microwave and Millimeter-Wave Monolithic Circuits Symposium, 1998 IEEE, pp. 123-126, 4 pages, Doc 0341.
Nakayama—"A 1.9 GHz Single-Chip RF Front-End GaAs MMIC with Low-Distortion Cascade FET Mixer for Personal Handy-Phone System Terminals", IEEE, 1998, pp. 101-104, Doc 0342.
Park—"A Regulated, Charge Pump CMOS DC/DC Converter for Low Power Application", 1998, pp. 1-62, 62 pages, Doc 0343.
Razavi—"RF Microelectronics", Prentice-Hall, 1998, 179 pages, Doc 0344.
Schindler—"DC-20 GHZ N X M Passive Switches", Raytheon Co., 1998 IEEE MTT-S Digest, pp. 1001-1005, 5 pages, Doc 0345.
Smith—"Modern Communication Circuits", McGraw-Hill 1998, 307 pages, Doc 0347 (A-D).
Stuber—"SOI CMOS with High Performance Passive Components for Analog, RF and Mixed Signal Designs", IEEE International SOI Conference, 1998, pp. 99-100, 2 pages, Doc 0348.
Tsutsumi—"A Single Chip PHS Front End MMIC with a True Single +3 Voltage Supply", IEEE Radio Frequency Integrated Circuits Symposium, 1998, pp. 105-108, 4 pages, Doc 0349.
Yamamoto—"Design and Experimental Results of a 2V-Operation Single Chip GaAs T/R MMIC Front-End for 1.9 GHz Personal Communications", IEEE 1998, pp. 7-12, 6 pages, Doc 0350.
Wei—"Effect of Floating-Body Charge on SOI MOSFET Design", IEEE Transaction on Electron Devices, vol. 45, No. 2, Feb. 1998, 9 pages, Doc 0352.
Koh—"Body-Contracted SOI MOSFET Structure and its Application to DRAM", IEEE Transactions on Electron Devices, vol. 45, No. 5, May 1998, pp. 1063-1070, 8 pages, Doc 0354.
Kawakyu—"A 2-V Operation Resonant Type T/R Switch with Low Distortion Characteristics for 1.9GHz PHS", IEICE Trans Electron, vol. E81-C, No. 6, Jun. 1998, pp. 862-867, 60 pages, Doc 0356.
Tseng—"Comprehensive Study on AC Characteristics in SOI MOSFETs for Analog Applications", 1998 Symposium on VLSI Technology Digest of Technical Papers, Jun. 1998, 2 pages, Doc 0357.
Tseng—"Comprehensive Study on AC Characteristics in SOI-MOSFETs for Analog Applications", 1998 Symposium on VLSI Technology Digest of Technical Papers, Jun. 1998, 2 pages, Doc 0355.
Mishra—"High Power Broadband Amplifiers for 1-18 GHz Naval Radar" University of California, Santa Barbara, pp. 1-9, Jul. 1, 1998, 9 pages, Doc 0358.
Rossek—"Direct Optical Control of a Microwave Phase Shifter Using GaAs Field-Effect Transistors", Communications Research Group, School of Electronic Engineering, Faculty of Technology, Middlesex University, Sep. 1998, 224 pages, Doc 0361.
Lee—"Effect of Body Structure on Analog Performance of SOI NMOSFETs", 1988 IEEE International SOI Conference, Oct. 1998, pp. 61-62, 2 pages, Doc 0365.
Pelella—"Control of Off-State Current in Scaled PD/SOI CMOS Digital Circuits", Proceedings IEEE Intl SOI Conference, Oct. 1998, pp. 147-148, 2 pages, Doc 0367.
Workman—"A Comparative Analysis of the Dynamic Behavior of BTG/SOI MOSFET's and Circuits with Distributed Body Resistance", IEEE Transactions and Electron Devices, vol. 45, No. 10, Oct. 1998, pp. 2138-2145, 8 pages, Doc 0368.
Mizutani—"Compact DC-60-GHz HJFET MMIC Switches using Ohmic Electrode-Sharing Technology", IEEE Transactions on Microwave Theory and Techniques, vol. 46, No. 11, Nov. 1998, pp. 1597-1603, 7 pages, Doc 0371.
Linear Technology—"LTC1550L/LTC1551L: Low Noise Charge Pump Inverters in MS8 Shrink Cell Phone Designs", published Dec. 1998, pp. 1-2, 2 pages, Doc 0372.
Sleight—"Transient Measurements of SOI Body Contact Effectiveness", IEEE Electron Device Letters, vol. 19, No. 12, Dec. 1998, pp. 499-501, 3 pages, Doc 0373.
Analog Devices—"CMOS, Low Voltage RF/Video, SPST Switch", Analog Devices, Inc. 1999, pp. 1-10, 10 pages, Doc 0376.
Caverly—"High Power Gallium Nitride Devices for Microwave and RF Control Applications", 1999, pp. 1-30, 30 pages, Doc 0377.
Caverly—"Linear and Nonlinear Characteristics of the Silicon CMOS Monolithic 50-Omega Microwave and RF Control Element", IEEE Journal of Solid-State Circuits, vol. 34, No. 1, Jan. 1999, pp. 124-126, 3 pages, Doc 0378.
Derossi—"A Routing Switch Based on a Silicon-on-Insulator Mode Mixer", IEEE Photonics Technology Letters, 1999, pp. 194-196, 3 pages, Doc 0380.
Doyama—"Class E Power Amplifier for Wireless Transceivers", University of Toronto, 1999, pp. 1-59, 59 pages, Doc 0382.
Flandre—"Fully Depleted SOI CMOS Technology for Low Voltage Low Power Mixed Digital/Analog/Microwave Circuits", Analog Integrated Circuits and Signal Processing, 1999, pp. 213-228, 16 pages, Doc 0383.
Gil—"A High Speed and Low Power SOI Inverter Using Active Body-Bias", Solid-State Electronics, vol. 43, 1999, pp. 791-799, 9 pages, Doc 0384.
Harris—"CMOS Analog Switches", 1999, pp. 1-9, 9 pages, Doc 0385.
Harris Corporation—HI-5042 thru HI-5051 Datasheet, 1999, 9 pages, Doc 0386.
Hess—"Transformerless Capacitive Coupling of Gate Signals Operation of Power MOS Devices", IEEE 1999, pp. 673-675, 3 pages, Doc 0387.
Hu—"A Unified Gate Oxide Reliability Model", IEEE 37th Annual International Reliability Physic Symposium, 1999, pp. 47-51, 5 pages, Doc 0388.
Intersil—"Radiation Hardened CMOS Dual DPST Analog Switch", Intersil 1999, pp. 1-2, 2 pages, Doc 0391.
Lee—"CMOS RF: (Still) No Longer an Oxymoron (Invited)", IEEE Radio Frequency Integrated Circuits Symposium, 1999, pp. 3-6, 4 pages, Doc 0392.

(56) **References Cited**

OTHER PUBLICATIONS

Lindert—"Dynamic Threshold Pass-Transistor Logic for Improved Delay at Lower Power Supply Voltages", IEEE Journal of Solid-State Circuits, vol. 34, No. 1, Jan. 1999, pp. 85-89, 5 pages, Doc 0394.
Madihan—"CMOS RF Ics for 900MHz—2.4GHz Band Wireless Communications Networks", IEEE Radio Frequency Integrated Circuits Symposium, 1999, pp. 13-16, 4 pages, Doc 0395.
Masuda—"RF Current Evaluation of Ics by MP-10L", NEC Research and Development, vol. 40-41, 1999, pp. 253-258, 7 pages, Doc 0400.
Miller—"Modern Electronic Communications", Prentice-Hall 1999, 414 pages, Doc 0401 (A-E).
Nagayama—"Low Insertion Los DP3T MMIC Switch for Dual Band Cellular Phones", IEEE Journal of Solid State Circuits 1999, pp. 1051-1055, 5 pages, Doc 0402.
Newman—"Radiation Hardened Power Electronics", Intersil Corporation, 1999, pp. 1-4, 4 pages, Doc 0403.
Pelella—"Analysis and Control of Hysteresis in PD/SOI CMOS", University of Florida, Gainesville, FL, 1999, IEEE, p. 34.5.1-34.5.4, 4 pages, Doc 0404.
Reedy—"Single Chip Wireless Systems Using SOI", IEEE International SOI Conference, 1999, pp. 8-11, 4 pages, Doc 0405.
Shahidi—"Partially Depleted SOI Technology for Digital Logic", IEEE Intl Solid-State Circuits Conference, 1999, pp. 426-427, 2 pages, Doc 0408.
Smuk—"Multi-Throw Plastic MMIC Switches Up to 6GHz with Integrated Positive Control Logic", IEEE 1999, pp. 259-262, 4 pages, Doc 0409.
Tseng—"Characterization of Floating Body and Body-Grounded Thin Film Silicon-on-Insulator MOSFETs for Analog Circuit Applications", Ph.D Thesis, UCLA, 1999, 240 pages, Doc 0410.
Wambacq—"A Single Package Solution for Wireless Transceivers", IEEE 1999, pp. 1-5, 5 pages, Doc 0411.
Wei—"Large-Signal Model of Triple-Gate MESFET/PHEMT for Switch Applications", Alpha Industries, Inc., 1999 IEEE, pp. 745-748, 4 pages, Doc 0412.
McRory—"Transformer Coupled Stacked FET Power Amplifier", IEEE Journal of Solid State Circuits, vol. 34, No. 2, Feb. 1999, pp. 157-161, 5 pages, Doc 0413.
Pelloie—"WP 25.2: SOI Technology Performance and Modeling", 1999 IEEE Intl. Solid-State Circuits Conference, Feb. 1999, 9 pages, Doc 0414.
Shoucair—"Modeling, Decoupling and Suppression of MOSFET Distortion Components", IEEE Proceeding Circuit Devices Systems, vol. 146, No. 1, Feb. 1999, 7 pages, Doc 0415.
Takamiya—"High-Performance Accumulated Black-Interface Dynamic Threshold SOI MOSFET (AB-DTMOS) with Large Body Effect at Low Supply Voltage", Japanese Journal of Applied Physics, vol. 38 (1999), Part 1, No. 4B, Apr. 1999, pp. 2483-2486, 4 pages, Doc 0416.
Ernst—"Detailed Analysis of Short-Channel SOI DT-MOSFET", Laboratoire de Physique des Composants a Semiconducteurs, Enserg, France, Sep. 1999, pp. 380-383, 4 pages, Doc 0421.
Hsu—"Comparison of Conventional and Thermally-Stable Cascose (TSC) A;GaAs/GaAs HBTs for Microwave Power Applications", Journal of Solid-State Electronics, V. 43, Sep. 1999, 2 pages, Doc 0422.
Ferlet-Cavrois—"High Frequency Characterization of SOI Dynamic Threshold Voltage MOS (DTMOS) Transistors", 1999 IEEE International SOI Conference, Oct. 1999, pp. 24-25, 2 pages, Doc 0423.
Kuang—"A Dynamic Body Discharge Technique for SOI Circuit Applications", IEEE International SOI Conference, Oct. 1999, pp. 77-78, 2 pages, Doc 0424.
Adan—"Linearity and Low Noise Performance of SOI MOSFETs for RF Applications", IEEE International SOI Conference, 2000, pp. 30-31, 2 pages, Doc 0426.
Bernstein—"SOI Circuit Design Concepts", Springer Science + Business Media 2000, 239 pages, Doc 0427 (A-B).
Bolam—"Reliability Issues for Silicon-on-Insulator", IBM Microelectronics Division, IEEE 2000, p. 6.4.1-6.4.4, 4 pages, Doc 0428.
Bullock—"Transceiver and System Design for Digital Communication", Noble 2000, 142 pages, Doc 0431 (A-B).
Caverly—"High Power Gallium Nitride Devices for Microwave and RF Control Applications", 2000, pp. 1-33, 35 pages, Doc 0432.
Caverly—"On-State Distortion in High Electron Mobility Transistor Microwave and RF Switch Control Circuits", IEEE Transactions on Microwave Theory and Techniques, 2000, pp. 98-103, 6 pages. Doc 0433.
Caverly—"SPICE Modeling of Microwave and RF Control Diodes", IEEE 2000, pp. 28-31, 4 pages, Doc 0434.
Cristoloveanu—"State-of-the-art and Future of Silicon on Insulator (SOI) Technologies, Materials and Devices", Microelectronics Reliability 40 (2000), pp. 771-777, 7 pages, Doc 0435.
Giugni—"A Novel Multi-Port Microwave/Millimeter-Wave Switching Circuit", Microwave Conference, 2000, 4 pages, Doc 0436.
Hittite Microwave—"Positive Bias GaAs Multi-Throw Switches with Integrated TTL Decoders", Hittite Microwave, 2000, 5 pages, Doc 0438.
Hittite Microwave—"Wireless Symposium 2000 is Stage for New Product Introductions", Hittite Microwave 2000, pp. 1-8, 8 pages, Doc 0439.
Huang—"A 900-MHz T/R Switch with a 0.8-dB Insertion Loss Implemented in a 0.5- μm CMOS Process", IEEE Custom Integrated Circuits Conference, 2000, pp. 341-344, 4 pages, Doc 0440.
Kumar—"A Simple High Performance Complementary TFSOI BiCMOS Technology with Excellent Cross-Talk Isolation" IEEE International SOI Conference 2000, pp. 142-143, 2 pages, Doc 0444.
Lee—"Harmonic Distortion Due to Narrow Width Effects in Deep Submicron SOI-CMOS Device for Analog RF Applications", 2002 IEEE International SOI Conference, Oct. 2002, pp. 83-85, 3 pages, Doc 0445.
Montoriol—"3.6V and 4.8V GSM/DCS1800 Dual Band PA Application with DECT Capability Using Standard Motorola RFICs", 2000, p. 1-20, 20 pages, Doc 0446.
Silicon Wave—"Silicon Wave SiW1502 Radio Modem IC", Silicon Wave, 2000, pp. 1-21, 21 pages, Doc 0447.
Street—"R.F. Switch Design", The Institution of Electrical Engineers, 2000, pp. 4/1-4/7, 7 pages, Doc 0448.
Weigand—"An ASIC Driver for GaAs FET Control Components", Technical Feature, Applied Microwave & Wireless, 2000, pp. 42-48, 4 pages, Doc 0449.
Weisman—"The Essential Guide to RF and Wireless", Prentice-Hall 2000, 133 pages, Doc 0450 (A-B).
Hiramoto—"Low Power and Low Voltage MOSFETs with Variable Threshold Voltage Controlled by Back-Bias", IEICE Trans. Electron, vol. E83-C, No. 2, Feb. 2000, pp. 161-169, 9 pages, Doc 0437.
Lascari—"Accurate Phase Noise Prediction in PLL Synthesizers", Applied Microwave & Wireless, published May 2000, pp. 90-96, 4 pages, Doc 0452.
Lauterbach—"Charge Sharing Concept and New Clocking Scheme for Power Efficiency and Electromagnetic Emission Improvement of Boosted Charge Pumps", IEEE Journal of Solid-State Circuits, vol. 35, No. 5, May 2000, pp. 719-723, 5 pages, Doc 0453.
Yang—"Sub-100nm Vertical MOSFETs with Si1-x-y GexCy Source/Drains", a dissertation presented to the faculty of Princeton University, Jun. 2000, 272 pages, Doc 0455.
Wang—"A Novel Low-Voltage Silicon-on-Insulator (SOI) CMOS Complementary Pass-Transistor Logic (CPL) Circuit Using Asymmetrical Dynamic Threshold Pass-Transistor (ADTPT) Technique", Proceedings of the 43rd IEEE Midwest Symposium on Circuits and Systems, Aug. 2000, pp. 694-697, 4 pages, Doc 0458.
Eastman—"High Power, Broadband, Linear, Solid State Amplifier", 16th Quarterly Rep. under MURI Contract No. N00014-96-1-1223 for period Jun. 1, 2000 to Aug. 31, 2000, Sep. 2000, 8 pages, Doc 0459.
Rauly—"Investigation of Single and Double Gate SOI MOSFETs in Accumulation Mode for Enhanced Performances and Reduced Technological Drawbacks", Proceedings 30th European Solid-State Device Research Conference, Sep. 2000, pp. 540-543, 4 pages, Doc 0460.

(56) **References Cited**

OTHER PUBLICATIONS

Casu—"Comparative Analysis of PD-SOI Active Body-Biasing Circuits", IEEE Intl SOI Conference, Oct. 2000, pp. 94-95, 2 pages, Doc 0462.
Kuang—"A High-Performance Body-Charge-Modulated SOI Sense Amplifier", IEEE International SOI Conference, Oct. 2000, pp. 100-101, 2 pages, Doc 0463.
Saccamango—"An SOI Floating Body Charge Monitor Technique", IEEE International SOI Conference, Oct. 2000, pp. 88-89, 2 pages, Doc 0464.
Terauchi—"A Novel 4T SRAM Cell Using "Self-Body-Biased" SOI MOSFET Structure Operating as 0/5 Volt", IEEE International SOI Conference, Oct. 2000, pp. 108-109, 2 pages, Doc 0465.
Yeh—"High Performance 0.1 μm Partially Depleted SOI CMOSFET", 2000 IEEE International SOI Conference, Oct. 2000, pp. 68-69, 2 pages, Doc 0466.
Assaderaghi—"DTMOS: Its Derivatives and Variations, and Their Potential Applications", The 12th Intl Conference on Microelectronics, Nov. 2000, pp. 9-10, 2 pages, Doc 0467.
Mashiko—"Ultra-Low Power Operation of Partially-Depleted SOI/CMOS Integrated Circuits", IEICE Transactions on Electronic Voltage, No. 11, Nov. 2000, pp. 1697-1704, 8 pages, Doc 0468.
Nork—"New Charge Pumps Offer Low Input and Output Noise", Linear Technology Corporation, Design Notes, Design Note 243, published Nov. 2000, pp. 1-2, 2 pages, Doc 0469.
Rozeau—"SOI Technologies Overview for Low Power Low Voltage Radio Frequency Applications", Analog Integrated Circuits and Signal Processing, Nov. 2000, pp. 93-114, 22 pages, Doc 0470.
Ajjkuttira—"A Fully Integrated CMOS RFIC for Bluetooth Applications", IEEE International Solid-State Circuits Conference, 2001, pp. 1-3, 3 pages, Doc 0473.
Caverly—"Gallium Nitride-Based Microwave and RF Control Devices", 2001, 17 pages, Doc 0475.
Chang—"Investigations of Bulk Dynamic Threshold-Voltage MOSFET with 65 GHz "Normal-Mode" Ft and 220GHz "Over-Drive Mode" Ft for RF Applications", Institute of Electronics, National Chiao-Tung University, Taiwan, 2001 Symposium on VLSI Technology Digest of Technical Papers, pp. 89-90, 2 pages, Doc 0476.
Couch—"Digital and Analog Communication Systems", 2001, Prentice-Hall, 398 pages, Doc 0477 (A-E).
Darabi—"A 2.4GHz CMOS Transceiver for Bluetooth", IEEE, 2001, pp. 89-92, 3 pages, Doc 0479.
Drake—"Dynamic-Threshold Logic for Low Power VLSI Design", www.research.ibm.com/acas, 2001, 5 pages, Doc 0480.
Drozdovsky—"Large Signal Modeling of Microwave Gallium Nitride Based HFETs", Asia Pacific Microwave Conference, 2001, pp. 248-251, 4 pages, Doc 0481.
Dunga—"Analysis of Floating Body Effects in Thin Film SOI MOSFETs Using the GIDL Current Technique", Proceedings of the 8th International Symposium on Physical and Failure Analysis of Integrated Circuits, 2001, pp. 254-257, 4 pages, Doc 0482.
Fiorenza—"RF Power Performance of LDMOSFETs on SOI: An Experimental Comparison with Bulk Si MOSFETs", IEEE Radio Frequency Integrated Circuits Symposium, 2001, pp. 43-46, 4 pages, Doc 0483.
Fukuda—"SOI CMOS Device Technology", OKI Technical Review, Special Edition on 21st Century Solutions, 2001, pp. 54-57, 4 pages, Doc 0484.
Gould—"NMOS SPDT Switch MMIC with >48dB Isolation and 30dBm IIP3 for Applications within GSM and UMTS Bands", Bell Labs, 2001, pp. 1-4, 4 pages, Doc 0486.
Gu—"A High Performance GaAs SP3T Switch for Digital Cellular Systems", IEEE MTT-S Digest, 2001, pp. 241-244, 4 pages, Doc 0487.
Hittite Microwave—Floating Ground SPNT MMIC Switch Driver Techniques, 2001, 4 pages, Doc 0488.
Honeywell—"CMOS SOI Technology", 2001, pp. 1-7, 7 pages, Doc 0489.
Honeywell—"Honeywell SPDT Reflective RF Switch", Honeywell Advance Information, 2001, pp. 1-3, 3 pages, Doc 0490.
Huang—"A 2.4-GHz Single-Pole Double Throw T/R Switch with 0.8-dB Insertion Loss Implemented in a CMOS Process (slides)", Silicon Microwave Integrated Circuits and Systems Research, 2001, pp. 1-16, 16 pages, Doc 0492.
Huang—"A 2.4-GHz Single-Pole Double Throw T/R Switch with 0.8-dB Insertion Loss Implemented in a CMOS Process", Silicon Microwave Integrated Circuits and Systems Research, 2001, pp. 1-4, 4 pages, Doc 0493.
Huang—"Schottky Clamped MOS Transistors for Wireless CMOS Radio Frequency Switch Application", University of Florida, 2001, pp. 1-167, 167 pages, Doc 0494.
Itoh—"RF Technologies for Low Power Wireless Communications", Wiley, 2001, 244 pages, Doc 0495 (A-C).
Karandikar—"Technology Mapping for SOI Domino Logic Incorporating Solutions for the Parasitic Bipolar Effect", ACM 2001, pp. 1-14, 14 pages, Doc 0496.
Koh—"Low-Voltage SOI CMOS VLSI Devices and Circuits", Wiley Interscience, XP001090589, New York, 2001, 215 pages, Doc 0497 (A-C).
Koo—"RF Switches", Univ. Toronto, Elec. and Computer Engineering Dept. 2001, 12 pages, Doc 0498.
Kuo—"Low Voltage SOI CMOS VLSI Devices and Circuits", Wiley, 2001, pp. 57-60, 349-354, 215 pages, Doc 0499 (A-C).
Leenaerts—"Circuits Design for RF Transceivers", Kluwer Academic, 2001, 179 pages, Doc 0501 (A-B).
Marenk—"Layout Optimization of Cascode RF SOI Transistors", IEEE International SOI Conference, 2001, pp. 105-106, 2 pages, Doc 0502.
Misra—"Radio Frequency and Microwave Communication Circuits", Wiley 2001, 297 pages, Doc 0503 (A-C).
Morreale—The CRC Handbook of Modern Telecommunication:, CRC Press 2001, 228 pages, Doc 0504 (A-F).
Nakatani—"A Wide Dynamic Range Switched-LNA in SiGe BICMOS", IEEE Radio Frequency Integrated Circuits Symposium, 2001, pp. 223-226, 4 pages, Doc 0505.
Narendra—"Scaling of Stack Effects and its Application for Leakage Reduction", ISLPED 2001, 2001, pp. 195-200, 6 pages, Doc 0506.
Pozar—"Microwave and RF Design of Wireless Systems", Wiley 2001, 192 pages, Doc 0507 (A-B).
Reedy—"UTSi CMOS: A Complete RF SOI Solution", Peregrine Semiconductor Corporation, 2001, 6 pages, Doc 0509.
Salva (or Savla)—"Design and Simulation of a Low Power Bluetooth Transceiver", The University of Wisconsin, 2001, pp. 1-90, 90 pages, Doc 0510.
Sayre—"Complete Wireless Design", McGraw-Hill 2001, 284 pages, Doc 0511 (A-D).
Shimura—"High Isolation V-Band SPDT Switch MMIC for High Power Use", IEEE MTT-S International Microwave Symposium Digest, 2001, pp. 245-248, 4 pages, Doc 0512.
Sudhama—"Compact Modeling and Circuit Impact of Novel Frequency Dependence of Capacitance in RF MOSFETs", Nano Science and Technology Institute, Technical Proceedings of the 2001 Intl Conference of Modeling and Simulation of Microsystems, 4 pages, Doc 0513.
Wetzel—"Silicon-on-Sapphire Technology for Microwave Power Application", University of California, San Diego, 2001, 229 pages, Doc 0514 (A-B).
Cheng—"Gate-Channel Capacitance Characteristics in the Fully-Depleted SOI MOSFET", IEEE Transactions on Electron Devices, vol. 48, No. 2, Feb. 2001, pp. 388-391, 4 pages. Doc 0515.
Gritsch—"Influence of Generation/Recombination Effects in Simulations of Partially Depleted SOI MOSFETs", Solid-State Electronics 45 (2001), accepted Feb. 14, 2001, pp. 621-627, 7 pages, Doc 0516.
Huang—"A 0.5- μm CMOS T/R Switch for 900-MHz Wireless Applications", IEEE Journal of Solid-State Circuits, vol. 36, No. 3, Mar. 2001, pp. 486-492, 8 pages, Doc 0517.
Maxin Integrated Products—"Charge Pumps Shine in Portable Designs", published Mar. 15, 2001, pp. 1-16, 16 pages, Doc 0518.
Adriaensen—"Analysis and Potential of the Bipolar- and Hybrid-Mode Thin-Film SOI MOSFETs for High-Temperature Applica-

(56) **References Cited**

OTHER PUBLICATIONS

tions", Laboratoire de Macroelectronique, Universite Catholique de Louvain, May 2001, 5 pages, Doc 0519.
Chung—"SOI MOSFET Structure with a Junction Type Body Contact for Suppression of Pass Gate Leakage", IEEE Transactions on Electron Devices, vol. 48, No. 7, Jul. 2001, pp. 1360-1365, 6 pages, Doc 0520.
Burgener—"CMOS SOS Switches Offer Useful Features, High Integration", CMOS SOS Switches, Microwaves & RF, Aug. 2001, pp. 107-118, 7 pages, Doc 0523.
Casu—"Synthesis of Low-Leakage PD-SOI Circuits with Body Biasing", Intl Symposium on Low Power Electronics and Design, pp. 287-290, Aug. 6-7, 2001, 4 pages, Doc 0524.
Makioka—"Super Self Aligned GaAs RF Switch IC with 0.25dB Extremely Low Insertion Loss for Mobile Communication Systems", IEEE Transactions on Electron Devices, vol. 48, No. 8, August 2001, pp. 1510-1514, 2 pages, Doc 0525.
Dehan—"Alternative Architectures of SOI MOSFET for Improving DC and Microwave Characteristics", Microwave Laboratory, Universite Catholique de Louvain, Sep. 2001, 4 pages, Doc 0529.
Texas Instruments—"TPS60204, TPS60205, Regulated 3.3-V, 100-mA Low-Ripple Charge Pump Low Power DC/DC Converters", published Feb. 2001, rev. Sep. 2001, pp. 1-18, 18 pages, Doc 0530.
Casu—"High Performance Digital CMOS Circuits in PD-SOI Technology: Modeling and Design", Tesi di Dottorato di Recerca, Gennaio 2002, Politecnico di Torina, Corso di Dottorato di Ricerca in Ingegneria Elettronica e delle Communicazioni, 200 pages, Doc 0532.
De Boer—"Highly Integrated X-Band Multi-Function MMIC with Integrated LNA and Driver Amplifier", TNO Physics and Electronics Laboratory, 2002, pp. 1-4, 4 pages, Doc 0534.
Hanzo—"Adaptive Wireless Transceivers", Wiley, 2002, 379 pages, Doc 0535 (A-E).
Honeywell—"CMOS SOI RF Switch Family", 2002, pp. 1-4, 4 pages, Doc 0536.
Honeywell—"Honeywell SPDT Absorptive RF Switch", Honeywell, 2002, pp. 1-6, 6 pages, Doc 0537.
Jeon—"A New "Active" Predistorter with High Gain Using Cascose-FET Structures", IEEE Radio Frequency Integrated Circuits Symposium, 2002, pp. 253-256, 4 pages, Doc 0538.
Koudymov—"Low Loss High Power RF Switching Using Multifinger AlGaN/GaN MOSHFETs", University of South Carolina Scholar Commons, 2002, pp. 449-451, 5 pages, Doc 0539.
Lee—"Analysis of Body Bias Effect with PD-SOI for Analog and RF Application", Solid State Electron, vol. 46, 2002, pp. 1169-1176, 8 pages, Doc 0540.
Marshall—"SOI Design: Analog, Memory, and Digital Techniques", Kluwer Academic Publishers, 2002, 414 pages, Doc 0543.
Numata—"A +2.4/0 V Controlled High Power GaAs SPDT Antenna Switch IC for GSM Application", IEEE Radio Frequency Integrated Circuits Symposium, 2002, pp. 141-144, 4 pages, Doc 0544.
O—"CMOS Components for 802.11b Wireless LAN Applications", IEEE Radio Frequency Integrated Circuits Symposium, 2002, pp. 103-106, 4 pages, Doc 0545.
Ohnakado—"A 1.4dB Insertion Loss, 5GHz Transmit/Receive Switch Utilizing Novel Depletion-Layer Extended Transistors (DETs) in 0.18 μm CMOS Process", Symposium on VLSI Circuits Digest of Technical Papers, 2002, pp. 162-163, 2 pages, Doc 0546.
Peczalski—"RF/Analog/Digital SOI Technology GPS Receivers and Other Systems on a Chip", IEEE Aerospace Conference Proceedings, 2002, pp. 2013-2017, 5 pages, Doc 0547.
Shafi—"Wireless Communications in the 21st Century", Wiley, 2002, 230 pages, Doc 0548 (A-C).
Tinella—"A 0.7DB Insertion Loss CMOS—SOI Antenna Switch with More than 50dB Isolation Over the 2.5 to 5GHz Band", Proceeding of the 28th European Solid-State Circuits Conference, 2002, pp. 483-486, 4 pages, Doc 0549.
Van Der Pujie—"Telecommunication Circuit Design", Wiley 2002, 225 pages, Doc 0550 (A-C).
Hameau—"Radio-Frequency Circuits in Integration Using CMOS SOI 0.25 μm Technology", 2002 RF IC Design Workshop Europe, Mar. 2002, Grenoble, France, 6 pages, Doc 0551.
Harneau—"Radio-Frequency Circuit Integration Using CMOS SOI 0.25 μm Technology", 2002 RF IC Design Workshop Europe, Mar. 19-22, 2002, Grenoble, France, 6 pages, Doc 0552.
Raab—"Power Amplifiers and Transmitters for RF and Microwave", IEEE Transactions and Microwave Theory and Techniques, vol. 50, No. 3, pp. 814-826, Mar. 2002, 13 pages, Doc 0553.
Sivaram—"Silicon Film Thickness Considerations in SOI-DTMOS", IEEE Device Letters, vol. 23, No. 5, May 2002, pp. 276-278, 3 pages, Doc 0556.
Han—"A Simple and Accurate Method for Extracting Substrate Resistance of RF MOSFETs", IEEE Electron Device Letters, vol. 23, No. 7, Jul. 2002, pp. 434-436, 3 pages, Doc 0557.
Das—"A Novel Sub-1 V High Speed Circuit Design Technique in Partially Depleted SOI-CMOS Technology with Ultra Low Leakage Power", Proceedings of the 28th European Solid-State Circuits Conference, Sep. 2002, pp. 24-26, 22 pages, Doc 0559.
Das—"A Novel Sub-1 V High Speed Circuit Design Technique in Partially Depleted SOI-CMOS Technology with Ultra Low Leakage Power", Proceedings of the 28th European Solid-State Circuits Conference, Sep. 2002, pp. 267-270, 4 pages, Doc 0560.
Bahl—"Lumped Elements for RF and Microwave Circuits", Artech House, 2003. pp. 353-394, 58 pages, Doc 0563.
Das—"Ultra-Low-Leakage Power Strategies for Sub-1 V Vlsi: Novel Circuit Styles and Design Methodologies for Partially Depleted Silicon-on-Insulator (PD-SOI) CMOS Technology", Proceedings of the 16th Intl. Conference on VLSI Design, 2003, 6 pages, Doc 0564.
Ezzeddine—"The High Voltage/High Power FET (HiVP1)", 2003 IEEE Radio Frequency Integrated Circuits Symposium, 4 pages, Doc 0566.
Gu—"A 2.3V PHEMT Power SP3T Antenna Switch IC for GSM Handsets", IEEE GaAs Digest, 2003, pp. 48-51, 4 pages, Doc 0561.
Gu—"A High Power DPDT MMIC Switch for Broadband Wireless Applications", IEEE MTT-S Digest, 2003, pp. 173-176, 4 pages, Doc 0568.
Hirano—"Impact of Actively Body Bias Controlled (ABC) SOI SRAM by Using Direct Body Contact Technology for Low Voltage Application," IEEE, 2003, p. 2.4.1-2.4.4, 4 pages, Doc 0569.
Huang—"Hot Carrier Degradation Behavior in SOI Dynamic-Threshold-Voltage nMOSFETs (n-DTMOSFET) Measured by Gated-Diode Configuration", Microelectronics Reliability 43 (2003) pp. 707-711, 5 pages, Doc 0572.
Lederer—"Frequency Degradation of SOI MOS Device Output Conductance", Microwave Laboratory of Universite Catholique de Louvain, Belgium, IEEE 2003, pp. 76-77, 2 pages, Doc 0573.
Minoli—"Telecommunications Technology Handbook", Artech House 2003, 408 pages, Doc 0576 (A-F).
NEC—"RF & Microwave Device Overview 2003—Silicon and GaAs Semiconductors", NEC 2003, 73 pages, Doc 0577.
Numata—"A High Power Handling GSM Switch IC with New Adaptive Control Voltage Generator Circuit Scheme", IEEE Radio Frequency Integrates Circuits Symposium, 2003, pp. 233-236, 4 pages, Doc 0578.
Pylarinos—"Charge Pumps: An Overview", Proceedings of the IEEE International Symposium on Circuits and Systems, 2003, pp. 1-7, 7 pages, Doc 0579.
Ueda—"A 5GHz-Band On-Chip Matching CMOS MMIC, Front-End", 11th GAAS Symposium—Munich 2003, pp. 101-104, 4 pages, Doc 0580.
Ytterdal—"MOSFET Device Physics and Operation", Device Modeling for Analog and RF CMOS Circuit Design, 2003, John Wiley & Sons, Ltd., 46 pages, Doc 0581.
Su—"On the Body-Source Built-In Potential Lowering of SOI MOSFETs", IEEE Electron Device Letters, vol. 24, No. 2, Feb. 2003, pp. 90-92, 3 pages, Doc 0582.
Cho—"Comparative Assessment of Adaptive Body-Bias SOI Pass-Transistor Logic", Fourth Intl Symposium on Quality Electronic Design, Mar. 2003, pp. 55-60, 6 pages, Doc 0583.

(56) **References Cited**

OTHER PUBLICATIONS

Kim—"High-Performance V-Band Cascode HEMT Mixer and Downconverter Module", IEEE Transactions on Microwave Theory and Techniques, vol. 51, No. 3, p. 805-810, Mar. 2003, 6 pages, Doc 0584.
Terauchi—"A Self-Body-Bias" SOI MOSFET: A Novel Body-Voltage-Controlled SOI MOSFET for Low Voltage Applications, The Japan Society of Applied Physics, vol. 42 (2003), pp. 2014-2019, Part 1, No. 4B, April 2003, 6 pages, Doc 0587.
Dehan—"Partially Depleted SOI Dynamic Threshold MOSFET for Low-Voltage and Microwave Applications" 203rd Meeting of the Electrochemical Society—11th Int. Symp. on SOI technology and devices, Paris, France , 2003 1 page, Doc 1080.
Tinella—"A High Performance CMOS-SOI Antenna Switch for the 2.5-5-GHz Band", IEEE Journal of Solid-State Circuits, vol. 38, No. 7, Jul. 2003, pp. 1270-1283, 5 pages, Doc 0588.
Drake—"Analysis of the Impact of Gate-Body Signal Phase on DTMOS Inverters in 0.13 μm PD-SOI", Department of EECS, University of Michigan, Ann Arbor, MI, Sep./Oct. 2003, 16 pages, Doc 0591.
Drake—"Analysis of the Impact of Gate-Body Signal Phase on DTMOS Inverters in 0.13 μm PD-SOI", Department of EECS, University of Michigan, Ann Arbor, MI, Sep./Oct. 2003, 4 pages, Doc 0592.
Lederer—"Frequency Degradation of SOI MOS Device Output Conductance", Microwave Laboratory of Universite Catholique de Louvain, Belgium, Sep./Oct. 2003, 1 page, Doc 0593.
Bernstein—"Design and CAD Challenges in sub-90nm CMOS Technologies", IBL Thomas J. Watson Research Center, NY, Nov. 11-13, 2003, pp. 129-136, 8 pages, Doc 0595.
Drake—"Evaluation of Dynamic-Threshold Logic for Low-Power VLSI Design in 0.13 μm PD-SOI", University of Michigan, Ann Arbor, MI, Dec. 2003, 29 pages, Doc 0596.
Drake—Evaluation of Dynamic-Threshold Logic for Low-Power VLSI Design in 0.13 μm PD-SOI:, IFIP VLSI-SoC 2003, IFIP WG 10.5 International Conference on Very Large Scale Integration of System-on-Chip, Darmstadt, Germany, Dec. 1-3, 2003, 6 pages, Doc 0597.
Bonkowski—"Integration of Triple Band GSM Antenna Switch Module Using SOI CMOS", IEEE Radio Frequency Integrated Circuits Symposium, 2004, pp. 511-514, 4 pages, Doc 0598.
Gu—"Low Insertion Loss and High Linearity PHEMT SPDT and SP3T Switch Ics for WLAN 802.11a/b/g Application", 2004 IEEE Radio Frequency Integrated Circuits Symposium, 2004, pp. 505-508, 4 pages, Doc 0600.
Kelly—"Integrated Ultra CMIS Designs in GSM Front End", Wireless Design Magazine, 2004, pp. 18-22, 4 pages, Doc 0601.
Wang—"A Robust Large Signal Non-Quasi-Static MOSFET Model for Circuit Simulation", IEEE 2004 Custom Integrated Circuits Conference, pp. 2-1-1-2-1-4, 4 pages, Doc 0603.
Chao—"High-Voltage and High-Temperature Applications of DTMOS with Reverse Schottky Barrier on Substrate Contacts", vol. 25, No. 2, Feb. 2004, pp. 86-88, 3 pages, Doc 0605.
Bawedin—"Unusual Floating Body Effect in Fully Depleted MOSFETs", IMEP, Enserg, France and Microelectronics Laboratory, Universite Catholique de Louvain, Belgium, Oct. 2004, 22 pages, Doc 0614.
Damiano—"Integrated Dynamic Body Contact for H Gate PD SOI MOSFETs for High Performance/Low Power", IEEE SOI Conference, Oct. 2004, pp. 115-116, 2 pages, Doc 0615.
Goo—"History-Effect-Conscious SPICE Model Extraction for PD-SOI Technology", 2004 IEEE International SOI Conference, Oct. 2004, pp. 156-158, 3 pages, Doc 0616.
Kuang—A Floating-Body Charge Monitoring Technique for Partially Depleted SOI Technology:, International Journal of Electronics, vol. 91, No. 11, 2004, pp. 625-637, 13 pages, Doc 0618.
Wiatr—"Impact of Floating Silicon Film on Small-Signal Parameters of Fully Depleted SOI-MOSFETs Biased into Accumulation", Solid-State Electronics 49 (2005), revised Nov. 9, 2004, pp. 779-789, 11 pages, Doc 0619.
Perraud—"A Direct-Conversion CMOS Transceiver for the 802.11a/b/g WLAN Standard Utilizing a Vartesian Feedback Transmitter", IEEE Journal of Solid-State Circuits, vol. 39, No. 12, Dec. 2004, pp. 2226-2238, 13 pages, Doc 0621.
Dehan—"Dynamic Threshold Voltage MOS in Partially Depleted SOI Technology: A Wide Frequency Band Analysis", Solid-State Electronics 49 (2005), pp. 67-72, 6 pages, Doc 0622.
Darabi—"A Dual-Mode 802.11b/Bluetooth Radio in 0.35-m CMOS", IEEE Journal of Solid-State Circuits, vol. 40, No. 3, Mar. 2005, pp. 698-706, 10 pages, Doc 0624.
Lee—"Effects of Gate Structures on the RF Performance in PD SOI MESFETs", IEEE Microwave and Wireless Components Letters, vol. 15, No. 4, Apr. 2005, pp. 223-225, 3 pages, Doc 0625.
Sjoblom—"An Adaptive Impedance Tuning CMOS Circuit for ISM 2.4-GHz Band", IEEE Transactions on Circuits and Systems—I: Regular Papers, vol. 52, No. 6, Jun. 2005, pp. 1115-1124, 10 pages, Doc 0627.
Su—"On the Prediction of Geometry-Dependent Floating-Body Effect in SOI MOSFETs", IEEE Transactions on Electron Devices, vol. 52, No. 7, Jul. 2005, pp. 1662-1664, 3 pages, Doc 0630.
Defree—"Peregrine Trumpets HaRP", https://www.edn.com/electronics-news/4325802/Peregrine-Trumpets-HaRP, Oct. 7, 2005, 2 pages, Doc 7000.
Bernstein—"SOI Circuit Design Concepts", IBM Microelectronics 2007, 239 pages, Doc 0654.
Iijima—"Boosted Voltage Scheme with Active Body-Biasing Control on PD-SOI for Ultra Low Voltage Operation", IEICE Transactions on Electronics, Institute of Electronics, Tokyo, JP, vol. E90C, No. 4, Apr. 1, 2007, pp. 666-674, 9 pages, Doc 0655.
Willert-Porada—"Advances in Microwave and Radio Frequency Processing", 8th International Conference on Microwave and High-Frequency Heating, Oct. 2009, 408 pages, Doc 0714 (A-F).
Nguyen, Niki Hoang, Office Action received from the USPTO dated Jun. 1, 2016 for U.S. Appl. No. 14/845,154, 6 pgs.
Nguyen, Niki Hoang, Final Office Action received from the USPTO dated Mar. 8, 2017 for U.S. Appl. No. 14/845,154, 28 pgs.
Nguyen, Niki Hoang, Notice of Allowance received from the USPTO dated Apr. 10, 2017 for U.S. Appl. No. 14/845,154, 8 pgs.
Nguyen, Niki Hoang, Notice of Allowance received from the USPTO dated Aug. 9, 2017 for U.S. Appl. No. 14/845,154, 12 pgs.
Brindle, et al., Response filed in the USPTO dated Oct. 28, 2016 for U.S. Appl. No. 14/845,154, 9 pgs.
Brindle, et al., Response filed in the USPTO dated Mar. 24, 2017 for U.S. Appl. No. 14/845,154, 3 pgs.
Burgener, et al., Preliminary Amendment filed in the USPTO dated Nov. 17, 2017 for U.S. Appl. No. 15/656,953, 7 pgs.
Itoh, Tadashige , et al., English translation of Office Action received from the JPO dated Feb. 27, 2018 for appln. No. 2016-175339, 4 pgs.
Tieu, Binh Kien, Office Action received from the USPTO dated Mar. 7, 2018 for U.S. Appl. No. 15/656,953, 14 pgs.
Nguyen, Niki Hoang, Office Action received from the USPTO dated Mar. 9, 2018 for U.S. Appl. No. 15/693,182, 10 pgs.
Tieu, Binh Kien, Final Office Action received from the USPTO dated May 16, 2018 for U.S. Appl. No. 15/656,953, 12 pgs.
Tat, Binh C., Office Action received from the USPTO dated Jun. 4, 2018 for U.S. Appl. No. 15/419,898, 39 pgs.
Nguyen, Niki Hoang, Notice of Allowance received from the USPTO dated Jun. 21, 2018 for U.S. Appl. No. 15/693,182, 22 pgs.
F. Hameau and O. Rozeau, "Radio-Frequency Circuits Integration Using CMOS SOI 0.25 μm Technology", 2002 RF IC Design Workshop Europe, Mar. 19-22, 2002, Grenoble, France.
O. Rozeau et al., "SOI Technologies Overview for Low-Power Low-Voltage Radio-Frequency Applications," Analog Integrated Circuits and Signal Processing, 25, pp. 93-114, Boston, MA, Kluwer Academic Publishers, Nov. 2000.
C. Tinella et al., "A High-Performance CMOS-SOI Antenna Switch for the 2.55-GHz Band,"IEEE Journal of Solid-State Circuits, vol. 38, No. 7, Jul. 2003.
H. Lee et al., "Analysis of body bias effect with PD-SOI for analog and RF applications," Solid State Electron., vol. 46, pp. 1169-1176, 2002.

(56) **References Cited**

OTHER PUBLICATIONS

J.-H. Lee, et al., "Effect of Body Structure on Analog Performance of SOI NMOSFETs," Proceedings, 1998 IEEE International SOI Conference, Oct. 5-8, 1998, pp. 61-62.
C. F. Edwards, et al., The Effect of Body Contact Series Resistance on SOI CMOS Amplifier Stages, IEEE Transactions on Electron Devices, vol. 44, No. 12, Dec. 1997 pp. 2290-2294.
S. Maeda, et al., Substrate-bias Effect and Source-drain Breakdown Characteristics in Body-tied Short-channel SOI MOSFET's, IEEE Transactions on Electron Devices, vol. 46, No. 1, Jan. 1999 pp. 151-158.
F. Assaderaghi, et al., "Dynamic Threshold-voltage MOSFET (DTMOS) for Ultra-low Voltage VLSI," IEEE Transactions on Electron Devices, vol. 44, No. 3, Mar. 1997, pp. 414-422.
G. O. Workman and J. G. Fossum, "A Comparative Analysis of the Dynamic Behavior of BTG/SOI MOSFETs and Circuits with Distributed Body Resistance," IEEE Transactions on Electron Devices, vol. 45, No. 10, Oct. 1998 pp. 2138-2145.
T.-S. Chao, et al. "High-voltage and High-temperature Applications of DTMOS with Reverse Schottky Barrier on Substrate Contacts," IEEE Electron Device Letters, vol. 25, No. 2, Feb. 2004, pp. 86-88.
Wei, et al., "Measurement of Transient Effects in SOI DRAM/SRAM Access Transistors", IEEE Electron Device Letters, vol. 17, No. 5, May 1996.
Sleight, et al., "Transient Measurements of SOI Body Contact Effectiveness", IEEE Electron Device Letters, vol. 19, No. 12, Dec. 1998.
Chung, et al., "SOI MOSFET Structure with a Junction-Type Body Contact for Suppression of Pass Gate Leakage", IEEE Transactions on Electron Devices, vol. 48, No. 7, Jul. 2001.
Lee, et al., "Effects of Gate Structures on the RF Performance in PD SOI MOSFETs", IEEE Microwave and Wireless Components Letters, vol. 15, No. 4, Apr. 2005.
Hirano, et al., "Impact of Actively Body-bias Controlled (ABC) SOI SRAM by using Direct Body Contact Technology for Low-Voltage Application" IEEE, 2003, pp. 2.4.1-2.4.4.
Lee, et al., "Harmonic Distortion Due to Narrow Width Effects in Deep sub-micron SOI-CMOS Device for analog-RF Applications", 2002 IEEE International SOI Conference, Oct. 2002.
Orndorff, et al., "CMOS/SOS/LSI Switching Regulator Control Device", ISSCC 78, Feb. 17, 1978, IEEE International Solid-State Circuits Conference, pp. 234-235 and 282.
Kuo, et al., "Low-Voltage SOI CMOS VLSI Devices and Circuits", 2001, Wiley Interscience, New York, XP001090589, pp. 57-60 and 349-354.
Tat, Binh C., International Search Report and Written Opinion received from USRO dated Jul. 3, 2008 for application no. PCT/US06/36240, 10 pgs.
Tat, Binh C., Office Action received from USPTO dated Sep. 15, 2008 for application No. 11/520,912, 18 pgs.
Shingleton, Michael B., Office Action dated Oct. 7, 2008 received from the USPTO for application No. 11/881,816, 4 pgs.
Hoffmann, Niels, Communication from the EPO dated Feb. 4, 2009 for appln No. 06786943.8, 7 pgs.
Stuber, Michael, et al., photocopy of an Amendment dated Mar. 16, 2009 filed in the USPTO for appln. No. 11/520,912, 21 pages.
Shingleton, Michael B., Communication received from USPTO dated Apr. 28, 2009 for application No. 11/881,816, 3 pgs.
Tat, Binh C., Office Action received from USPTO dated Jul. 8, 2009 for application No. 11/520,912, 6 pgs.
Dribinsky, et al, Response filed in USPTO dated Aug. 28, 2009 for appln. No. 11/881,816, 5 pgs.
Photocopy of a translation of an Office Action dated Jul. 31, 2009 for Chinese appln. No. 200680025128.7, 3 pages.
Stuber, Michael, et al., Photocopy of a Response that was filed in the USPTO for application No. 11/520,912, dated Sep. 8, 2009, 3 pgs.
Tat, Binh C., Office Action received from the USPTO dated Dec. 10, 2009 for appln. No. 11/520,912, 19 pages.
Shingleton, Michael B., Office Action received from the USPTO dated Jan. 19, 2010 for appln. No. 11/881,816, 16 pgs.
Brindle, Chris, et al., Translation of a Response filed in the Chinese Patent Office for appln No. 200680025128.7 dated Nov. 30, 2009, 3 pages.
Morena, Enrico, Supplementary European Search Report for appln. No. 06814836.0, dated Feb. 17, 2010, 8 pages.
Kuang, J.B., et al., "A Floating-Body Charge Monitoring Technique for Partially Depleted SOI Technology", Int. J. Of Electronics, vol. 91, No. 11, Nov. 11, 2004, pp. 625-637.
Stuber, et al., Amendment filed in the USPTO for appln. No. 11/520,912, dated Jun. 10, 2010, 25 pages.
Sedra, Adel A., et al., "Microelectronic Circuits", Fourth Edition, University of Toronto, Oxford University Press, 1982, 1987, 1991 and 1998, pp. 374-375.
Tat, Binh C., Notice of Allowance received from the USPTO for appln. No. 11/520,912, dated Sep. 16, 2010, 13 pages.
Brindle, et al., Response filed in the EPO for application No. 06 814 836.0-1235 dated Oct. 12, 2010, 24 pages.
Nguyen, Tram Hoang, Office Action received from the USPTO dated Sep. 19, 2008 for appln. No. 11/484,370, 7 pgs.
Brindle, et al., Response filed in the USPTO dated Jan. 20, 2009 for appln. No. 11/484,370, 5 pgs.
Nguyen, Tram Hoang, Office Action received from the USPTO dated Apr. 23, 2009 for appln. No. 11/484,370, 11 pgs.
Brindle, et al., Response filed in the USPTO dated Aug. 24, 2009 for appln. No. 11/484,370, 5 pgs.
Nguyen, Tram Hoang, Office Action received from the USPTO dated Jan. 6, 2010 for appln. No. 11/484,370, 46 pgs.
Brindle, et al., Amendment filed in the USPTO dated Jul. 6, 2010 for appln. No. 11/484,370, 23 pgs.
Bolam, et al., "Reliability Issues for Silicon-on-Insulator", 2000 IEEE, IBM Microelectronics Division, pgs. 6.4.1-6.4.4, 4 pages.
Hu, et al., "A Unified Gate Oxide Reliability Model", IEEE 99CH36296, 37th Annual International Reliability Physics Symposium, San Diego, CA 1999, pp. 47-51.
Tieu, Binh Kien, Notice of Allowance received from the USPTO dated Aug. 1, 2018 for appln. No. 15/656,953, 13 pgs.

* cited by examiner

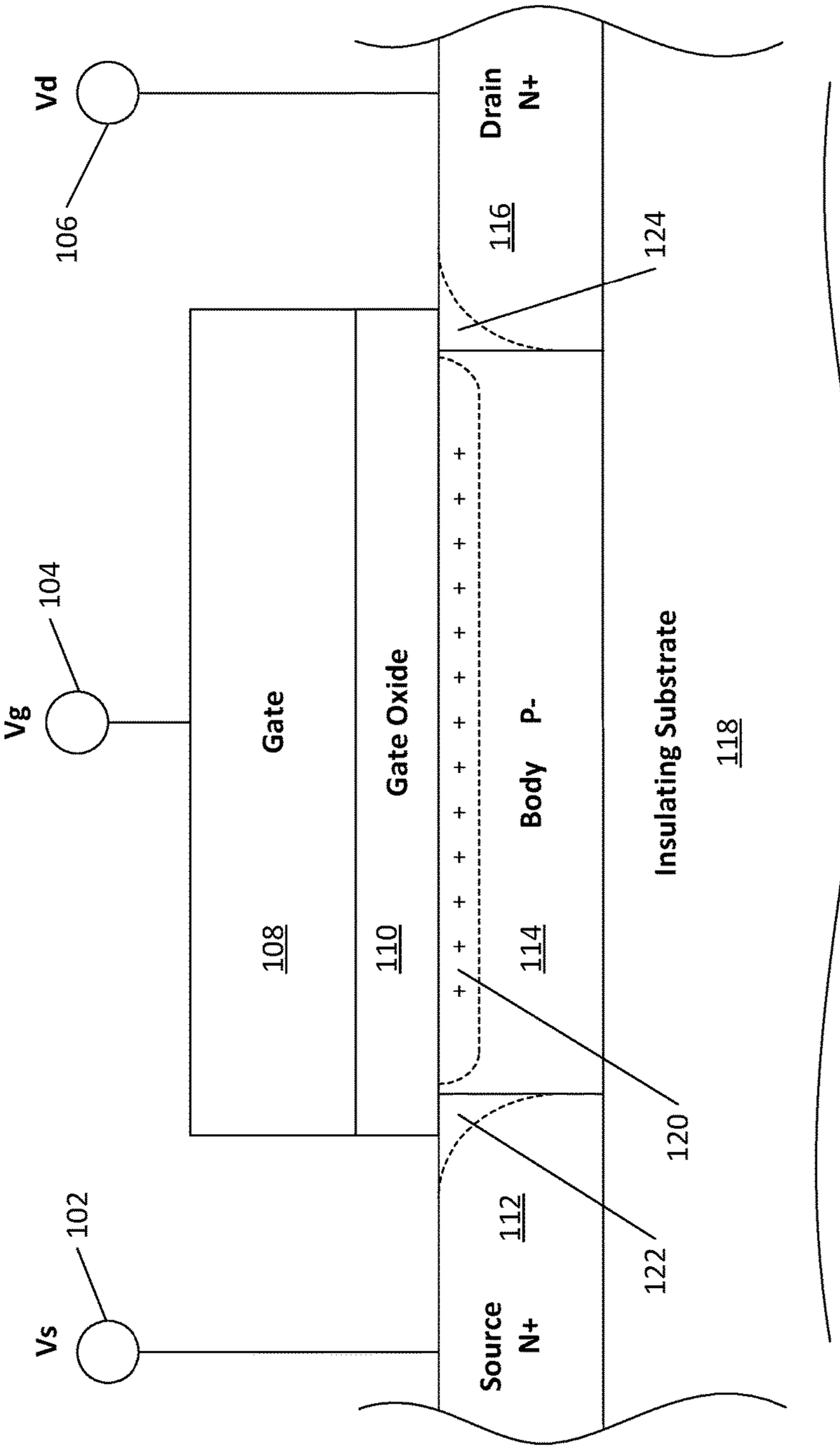

Figure 1 (Prior Art)

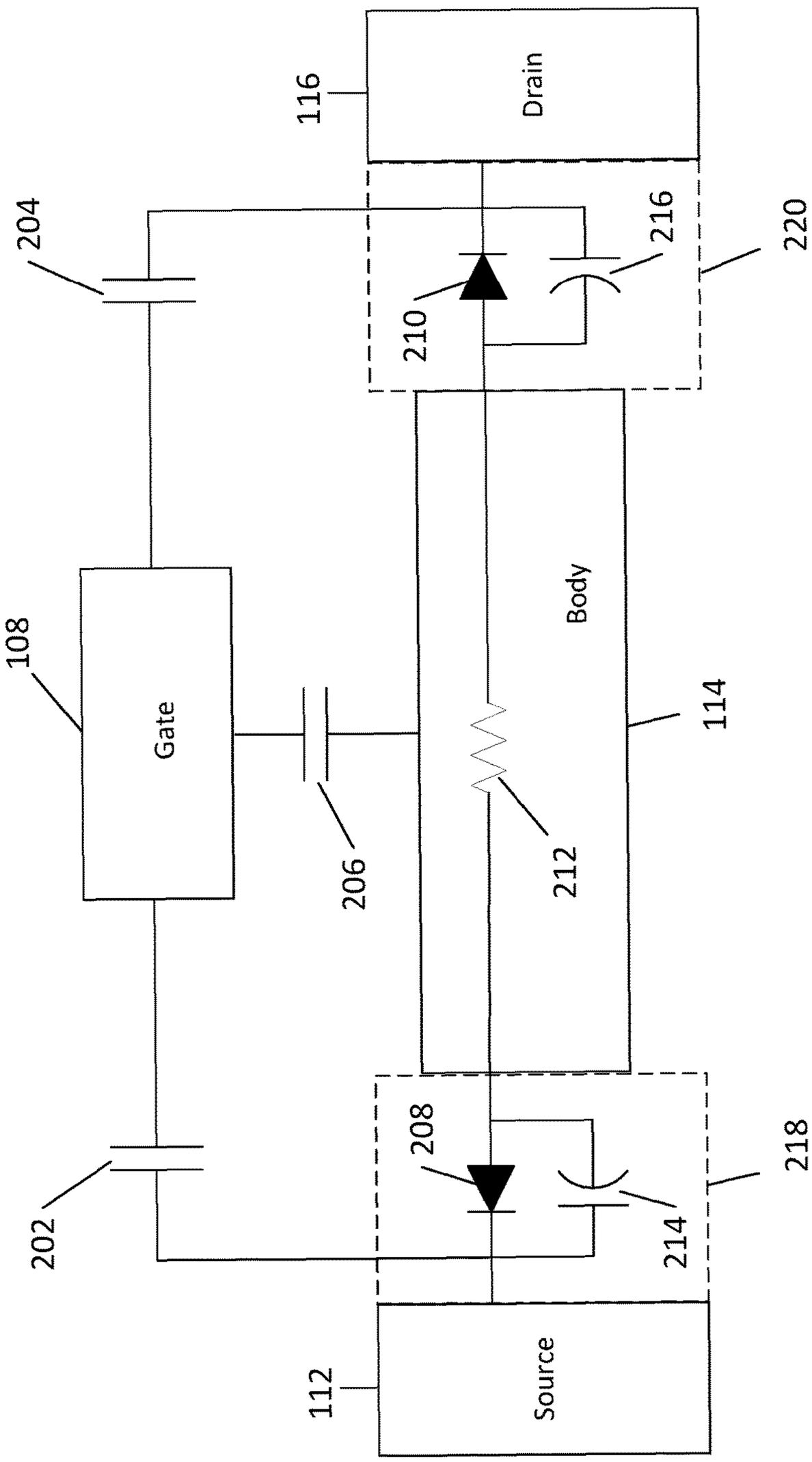
116
Drain
204
216
220
210
Body
108
Gate
114
206
212
208
218
214
202
112
Source
200

Figure 2A

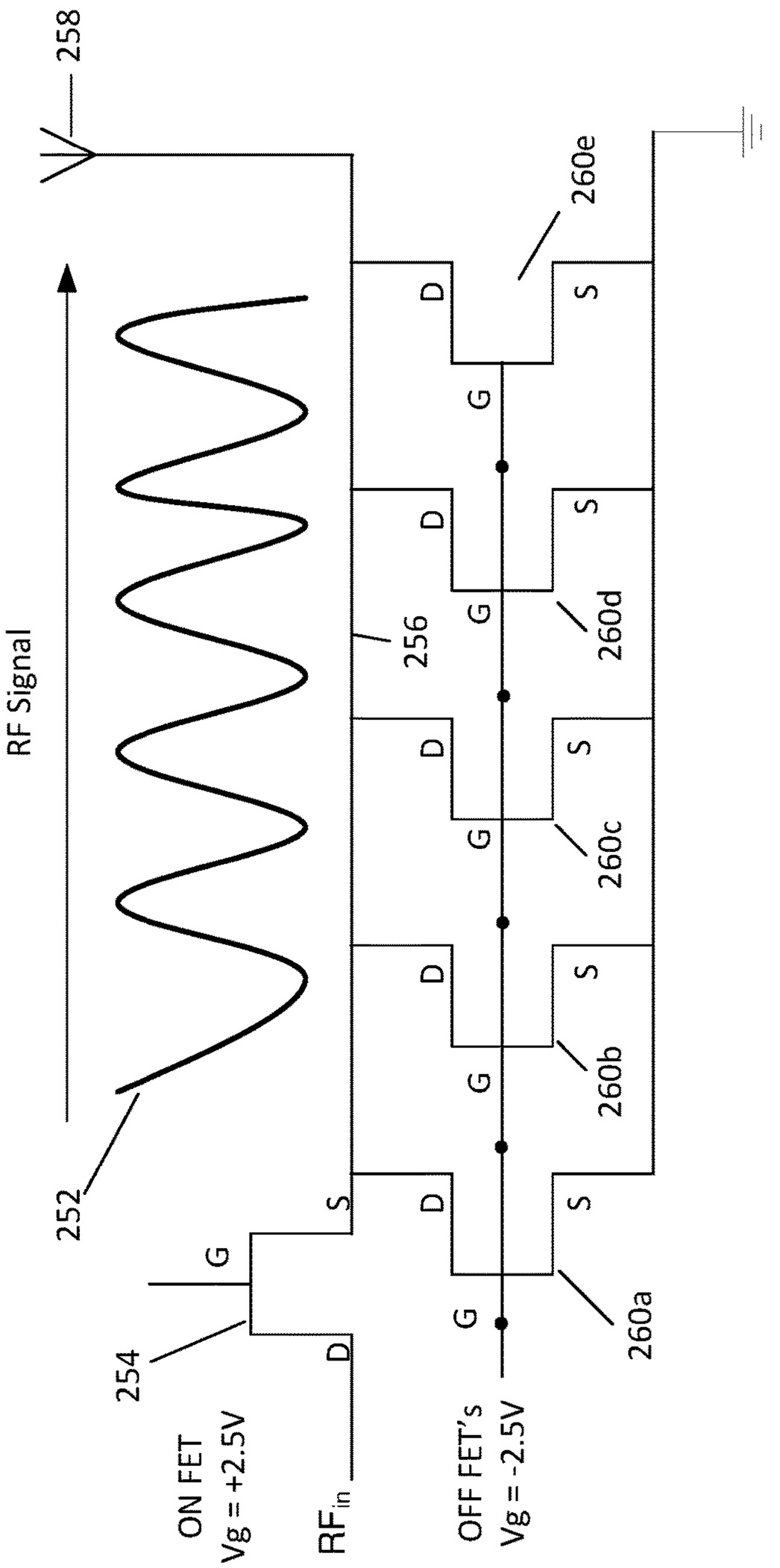
258
260e
D
S
G
RF Signal
252
256
260d
260c
260b
260a
254
ON FET
Vg = +2.5V
RFin
OFF FET's
Vg = -2.5V
250

FIGURE 2B

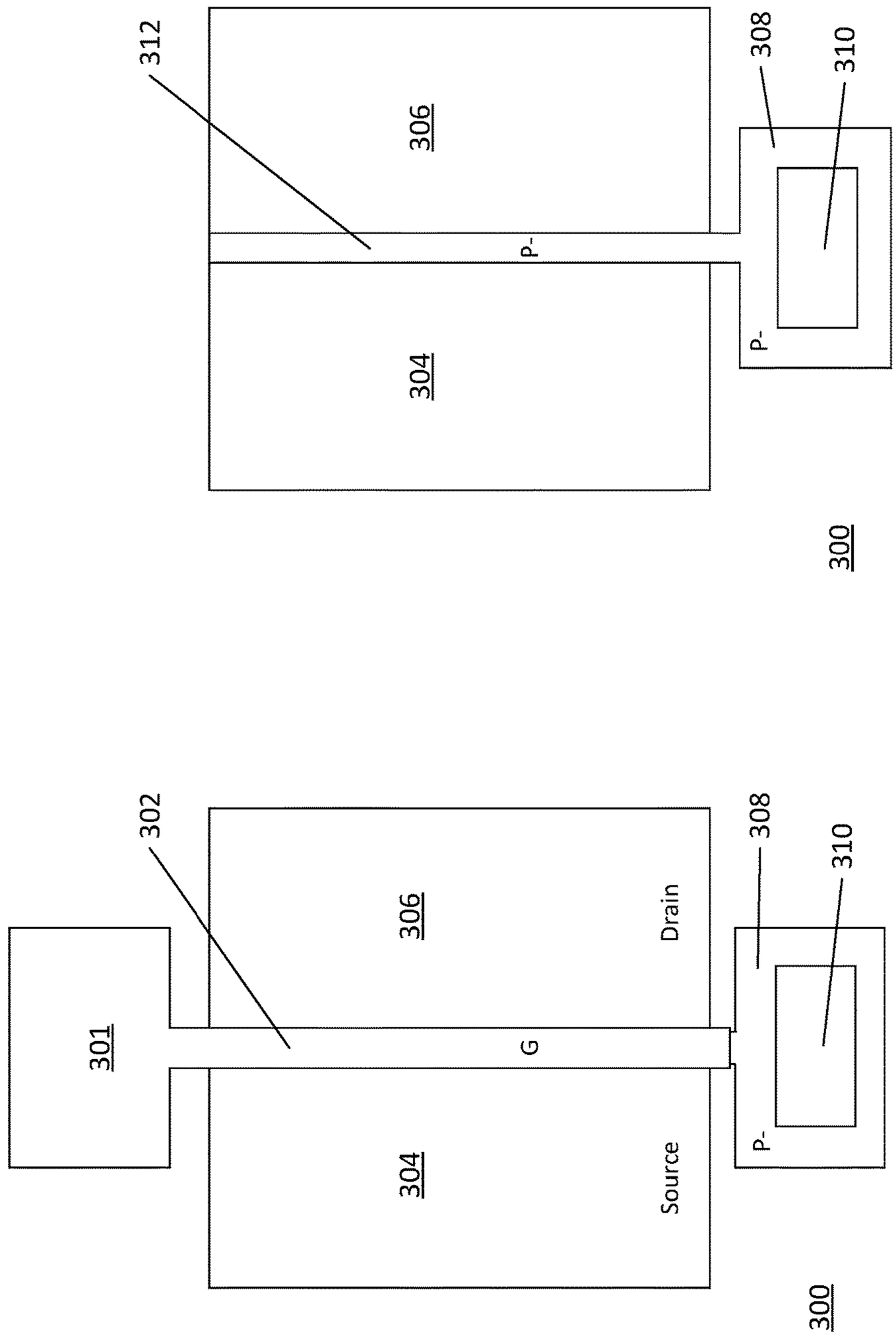

Figure 3B

Figure 3A

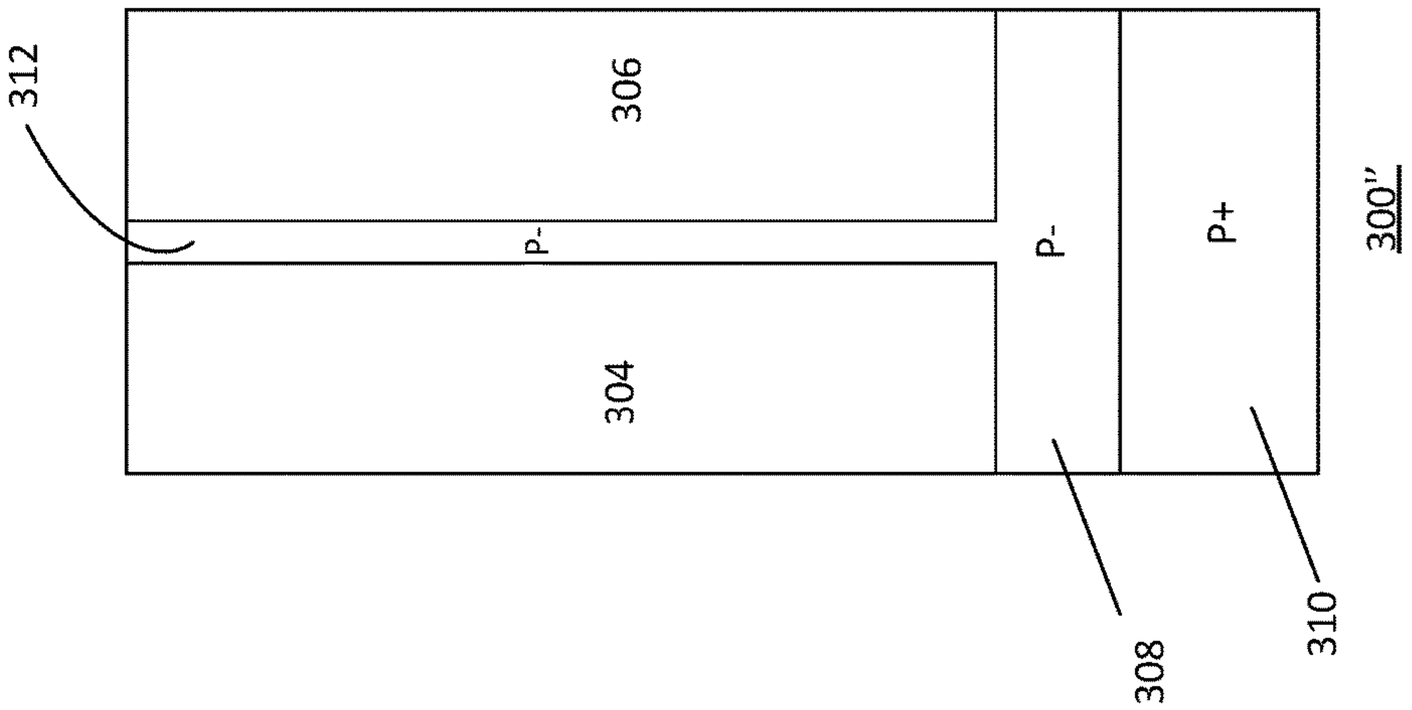

Figure 3D

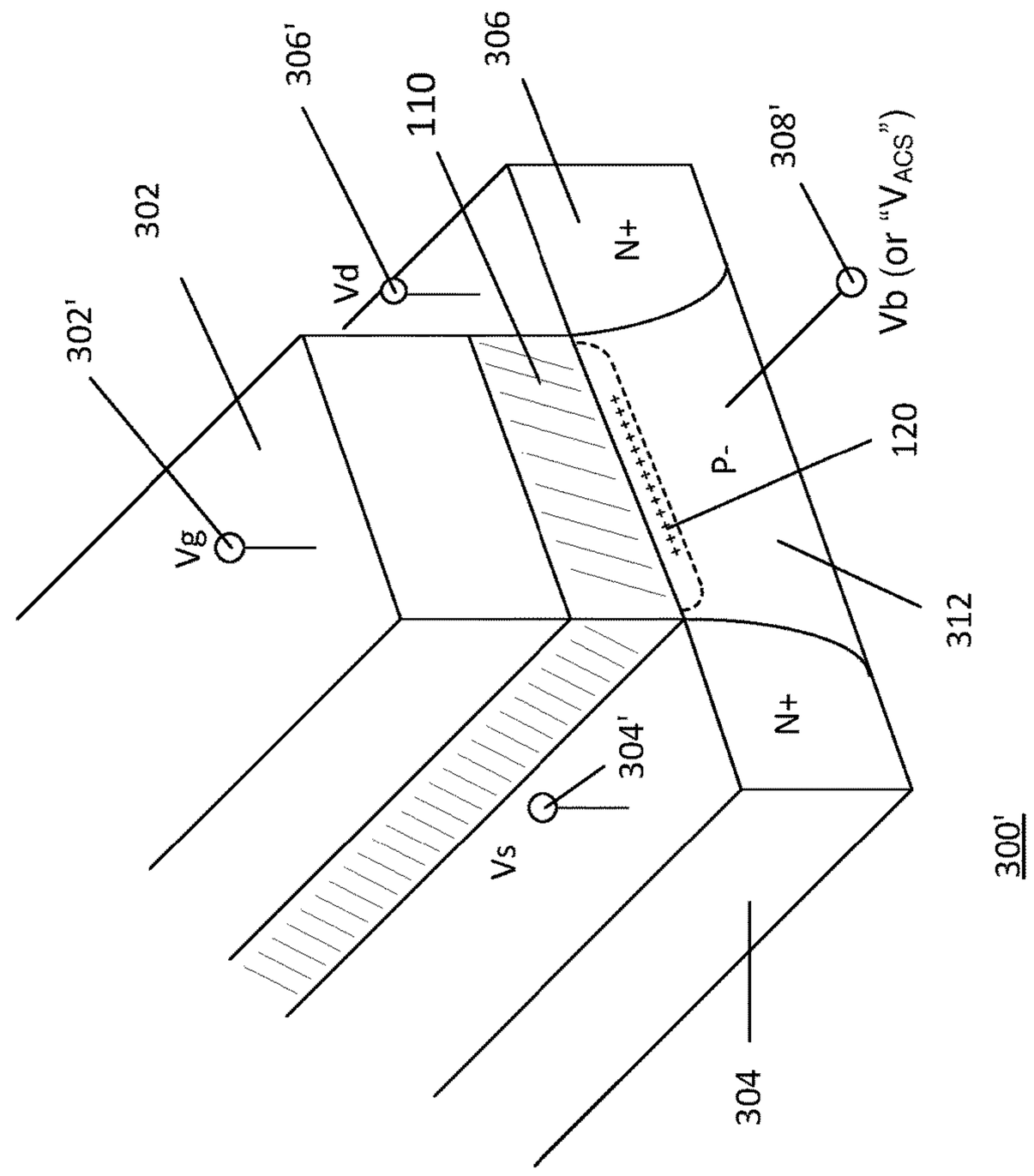

Figure 3C

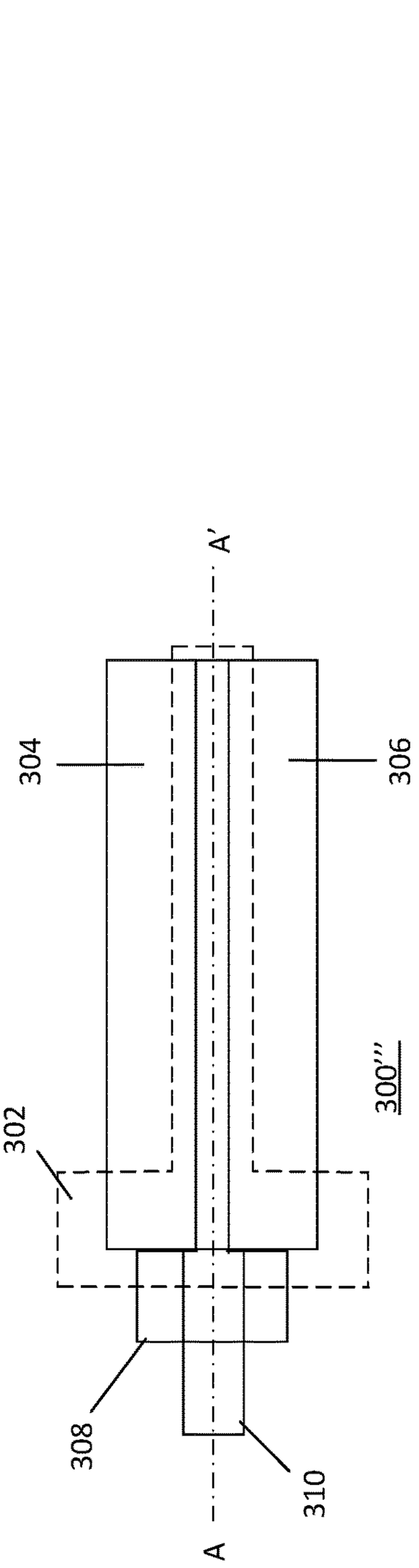

Figure 3E

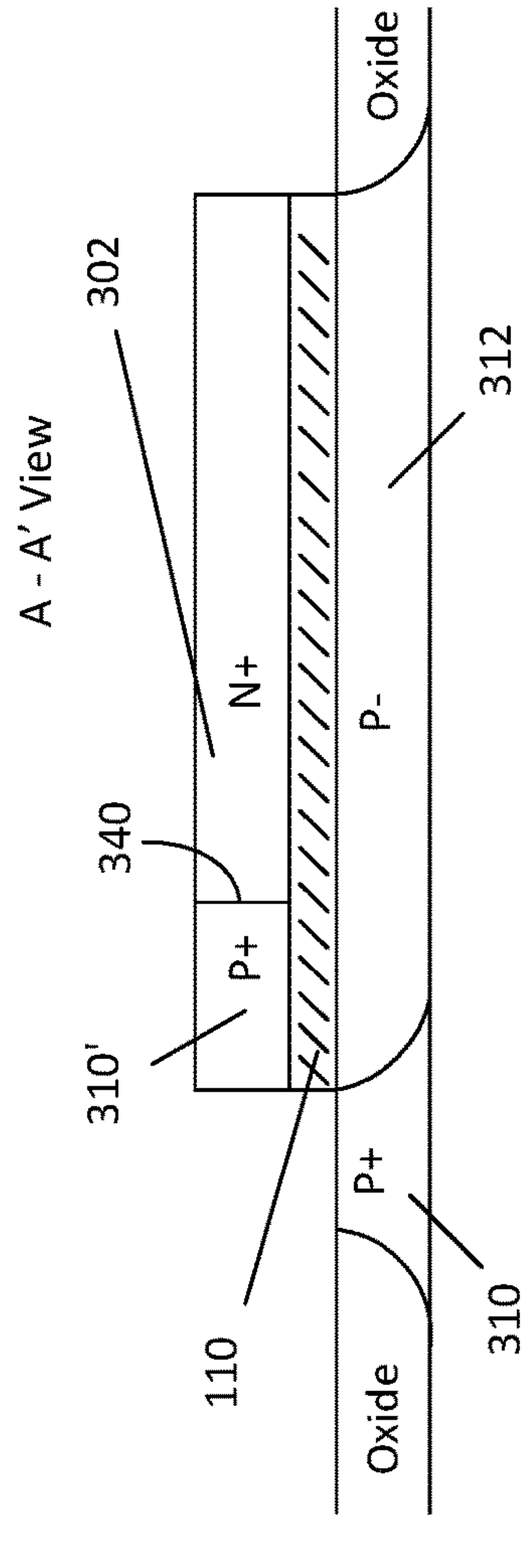

Figure 3F

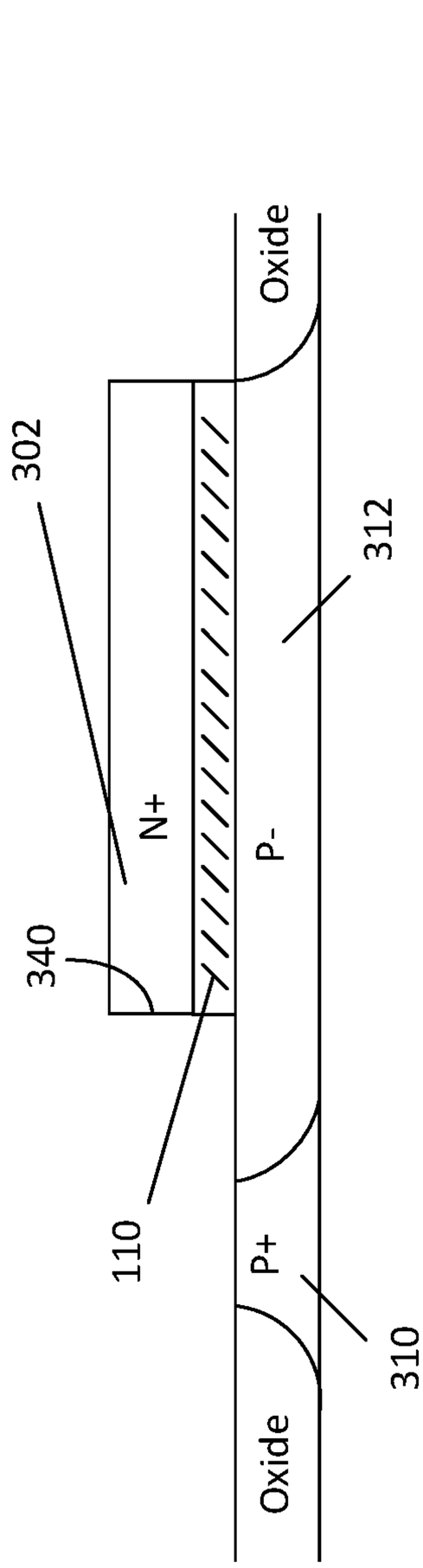

Figure 3G

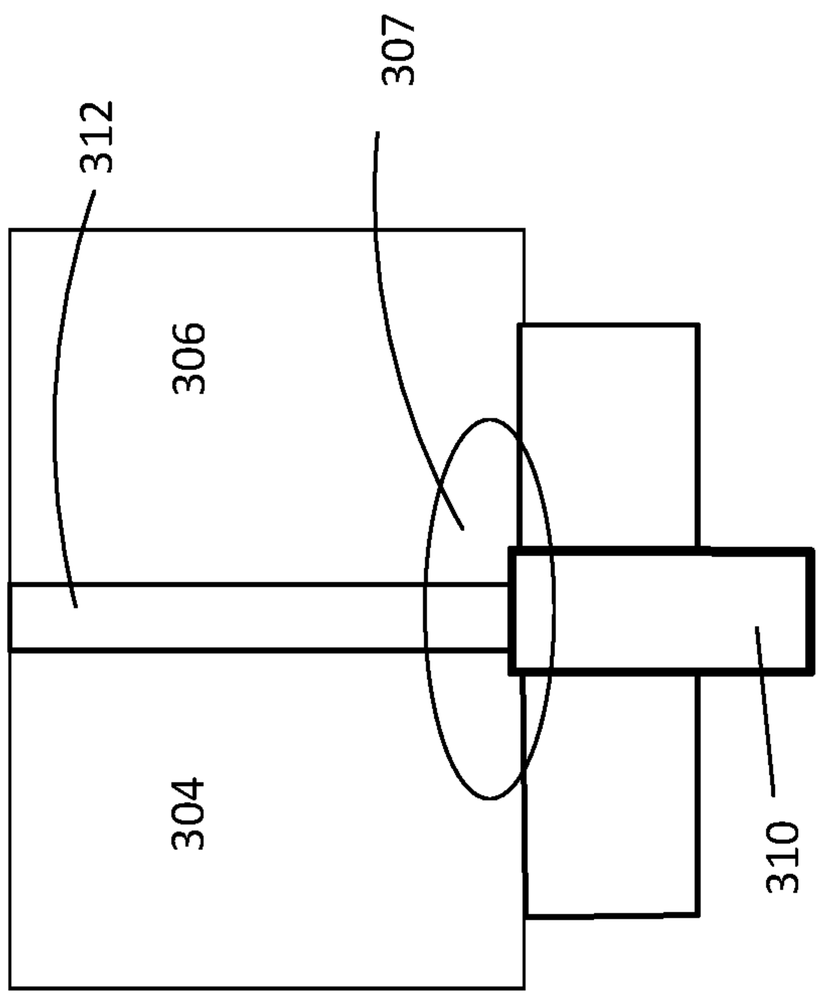

Figure 3H

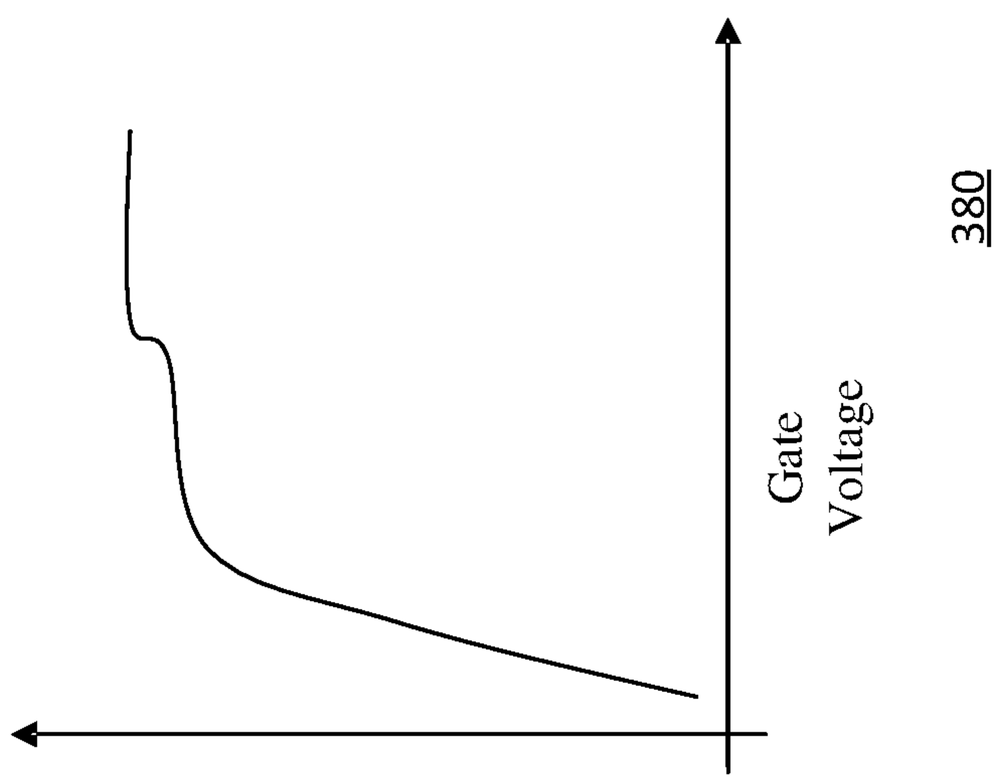

Figure 3I

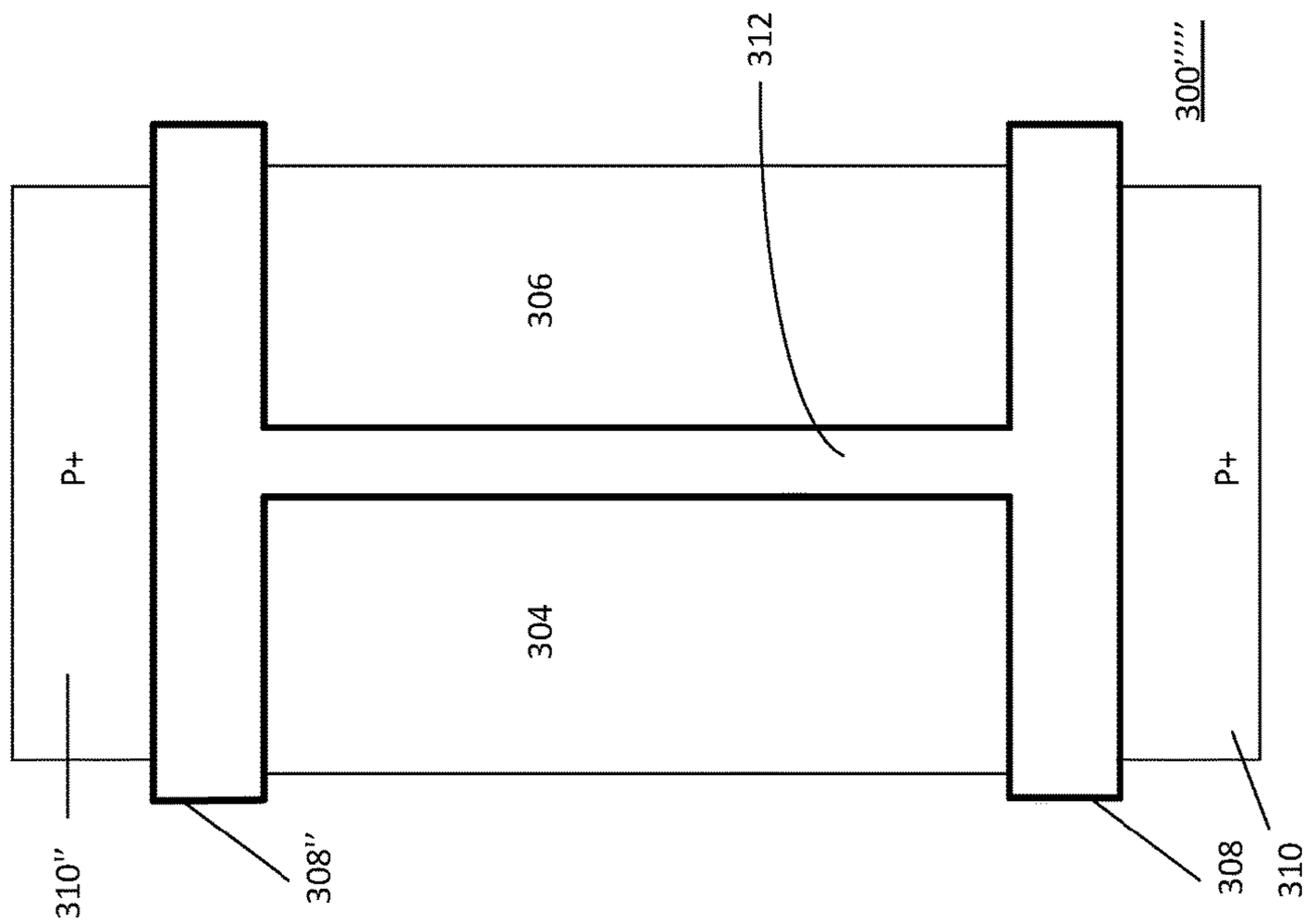

Figure 3K

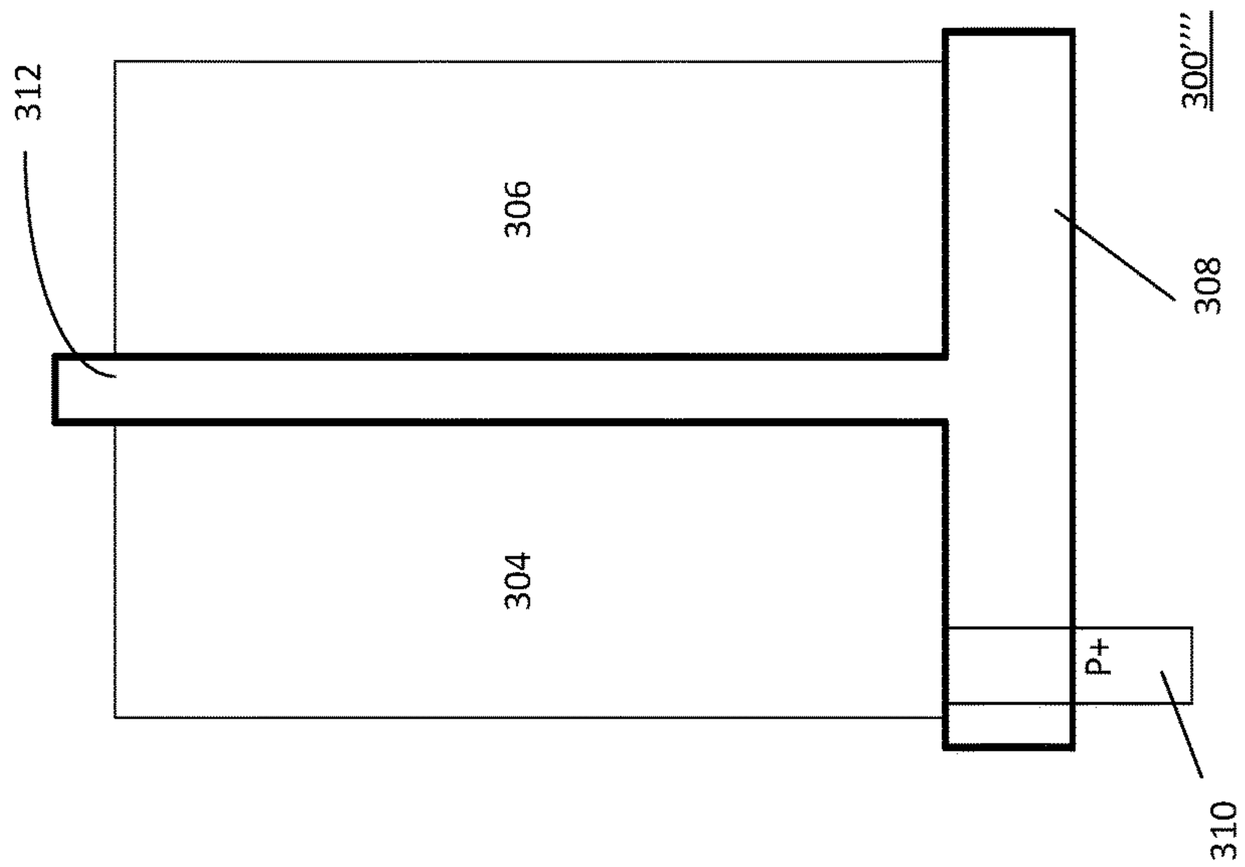

Figure 3J

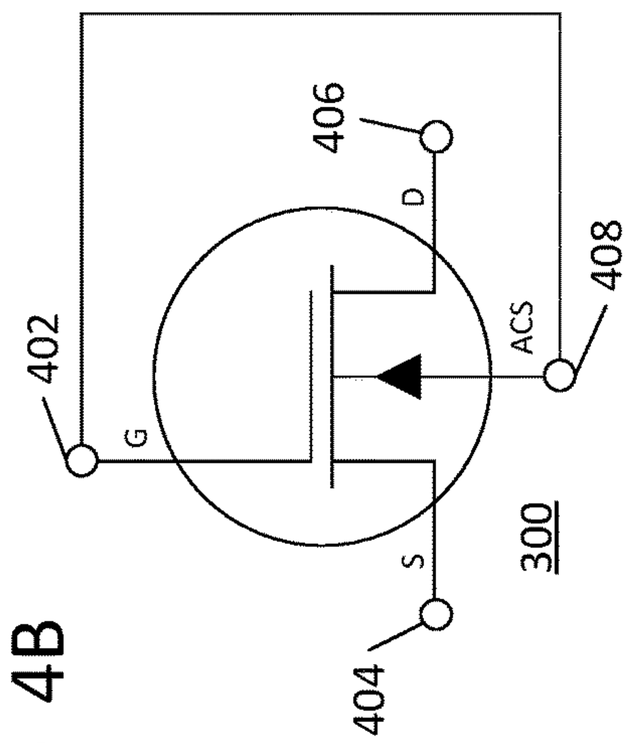

Figure 4B

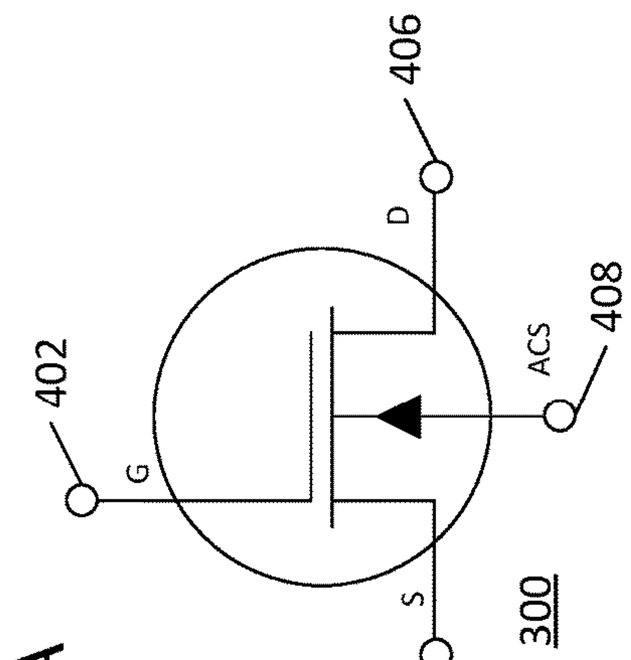

Figure 4A

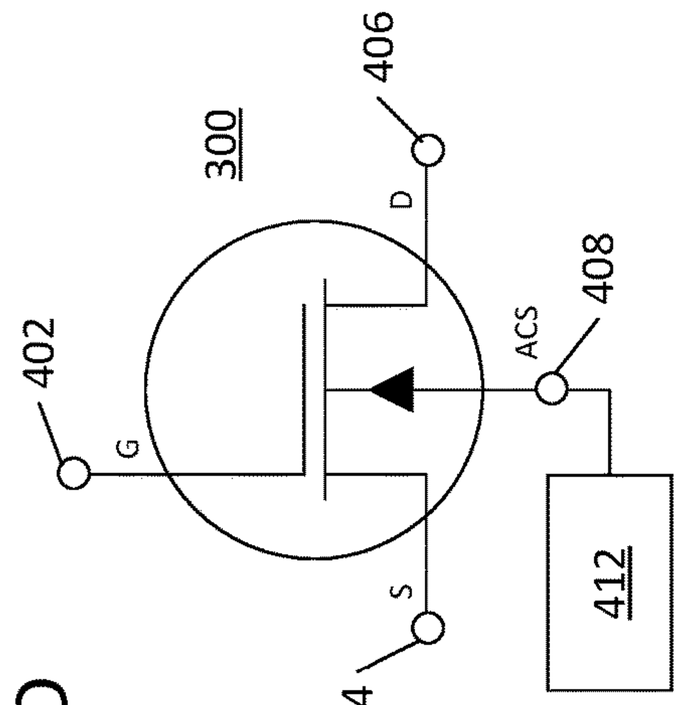

Figure 4D

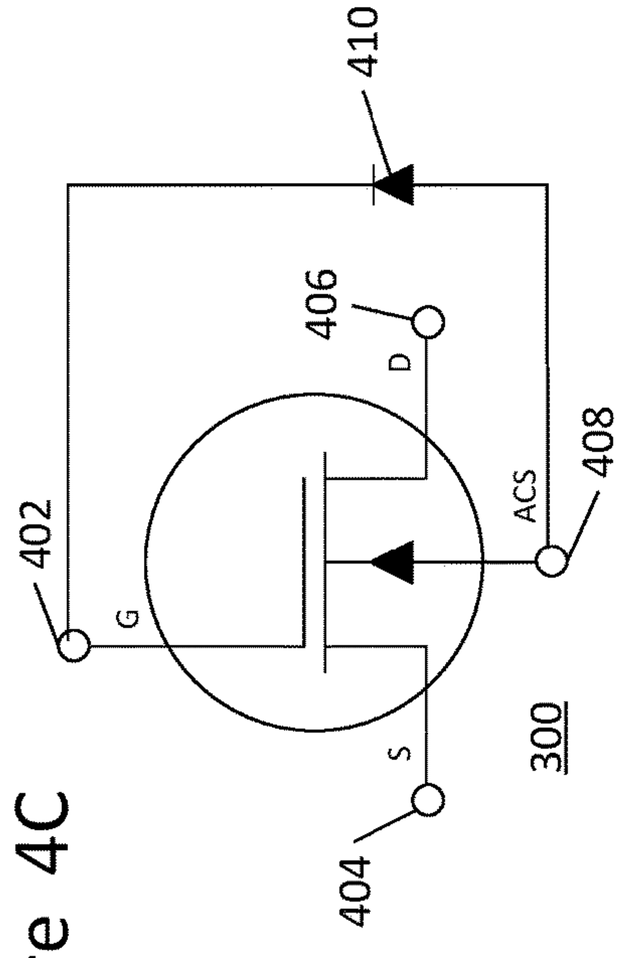

Figure 4C

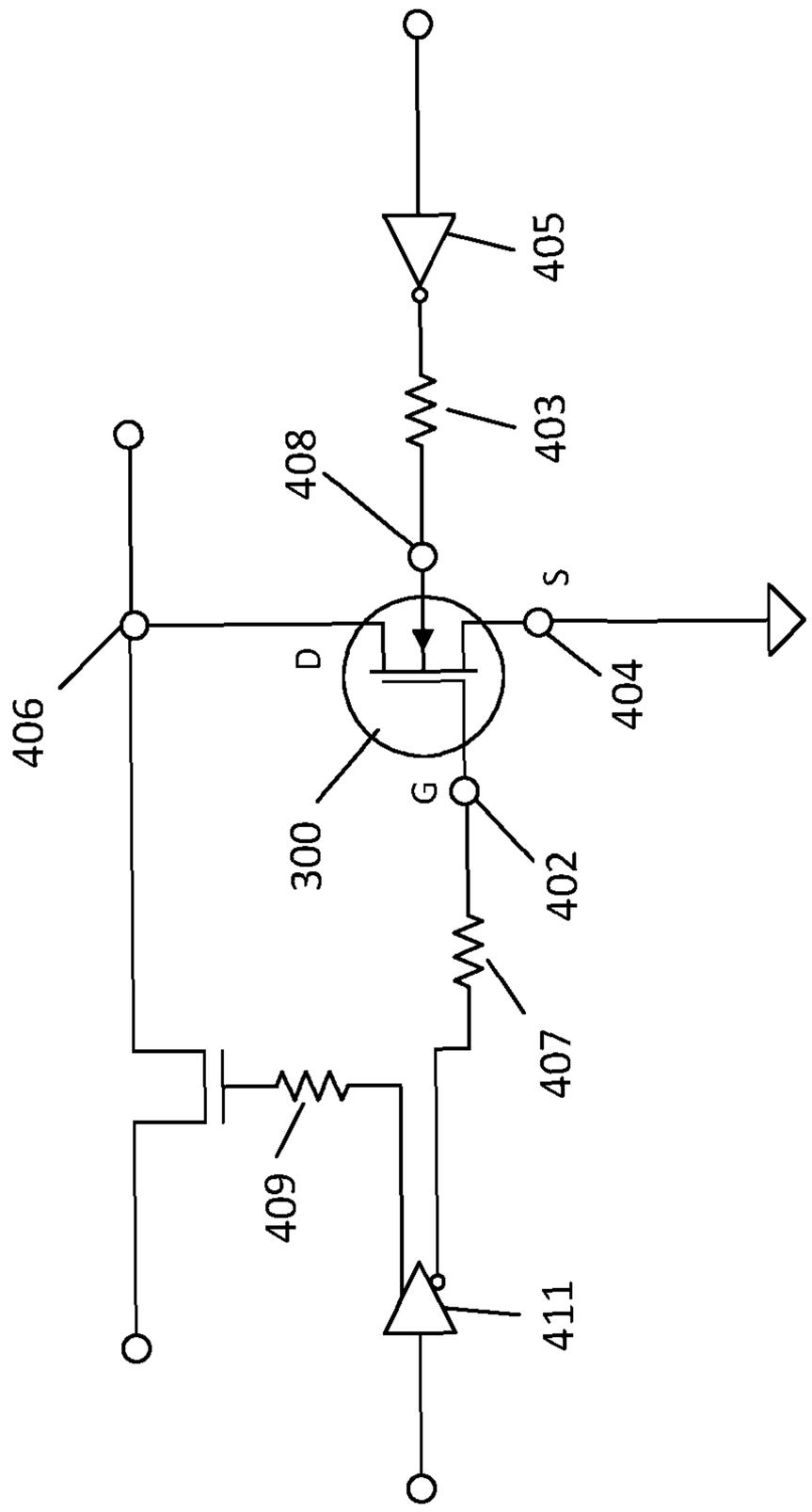

Figure 4E

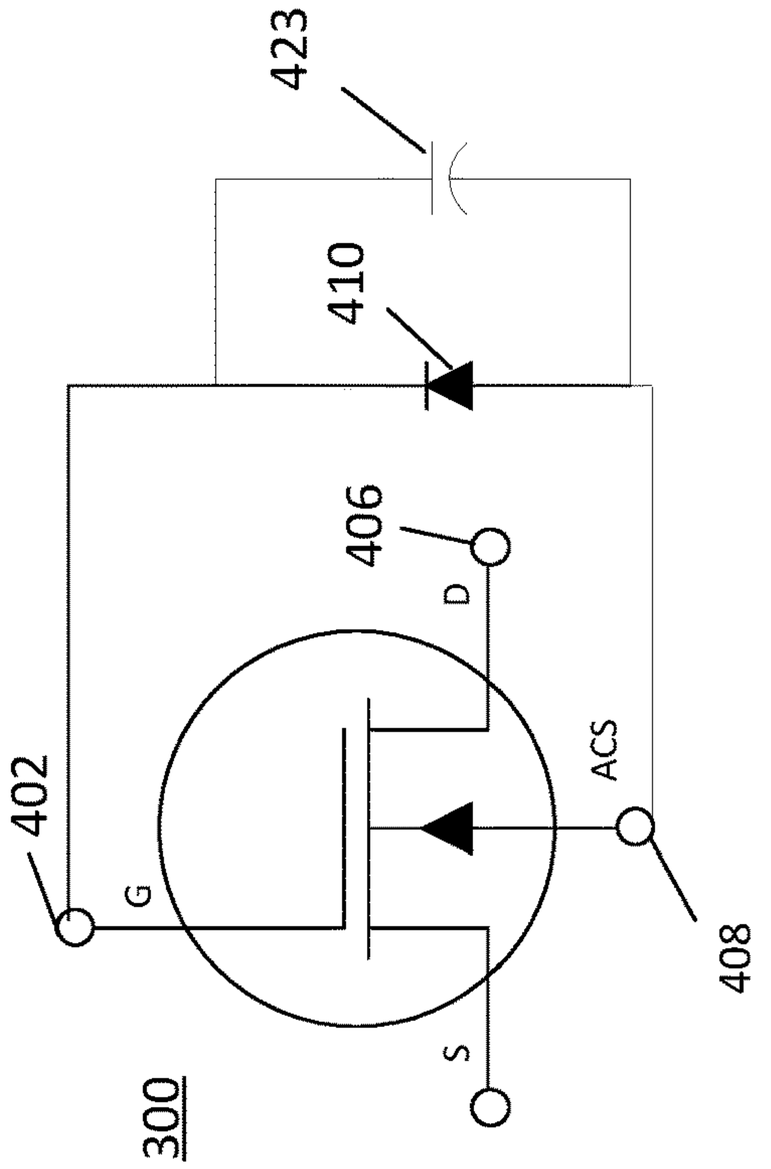

Figure 4G

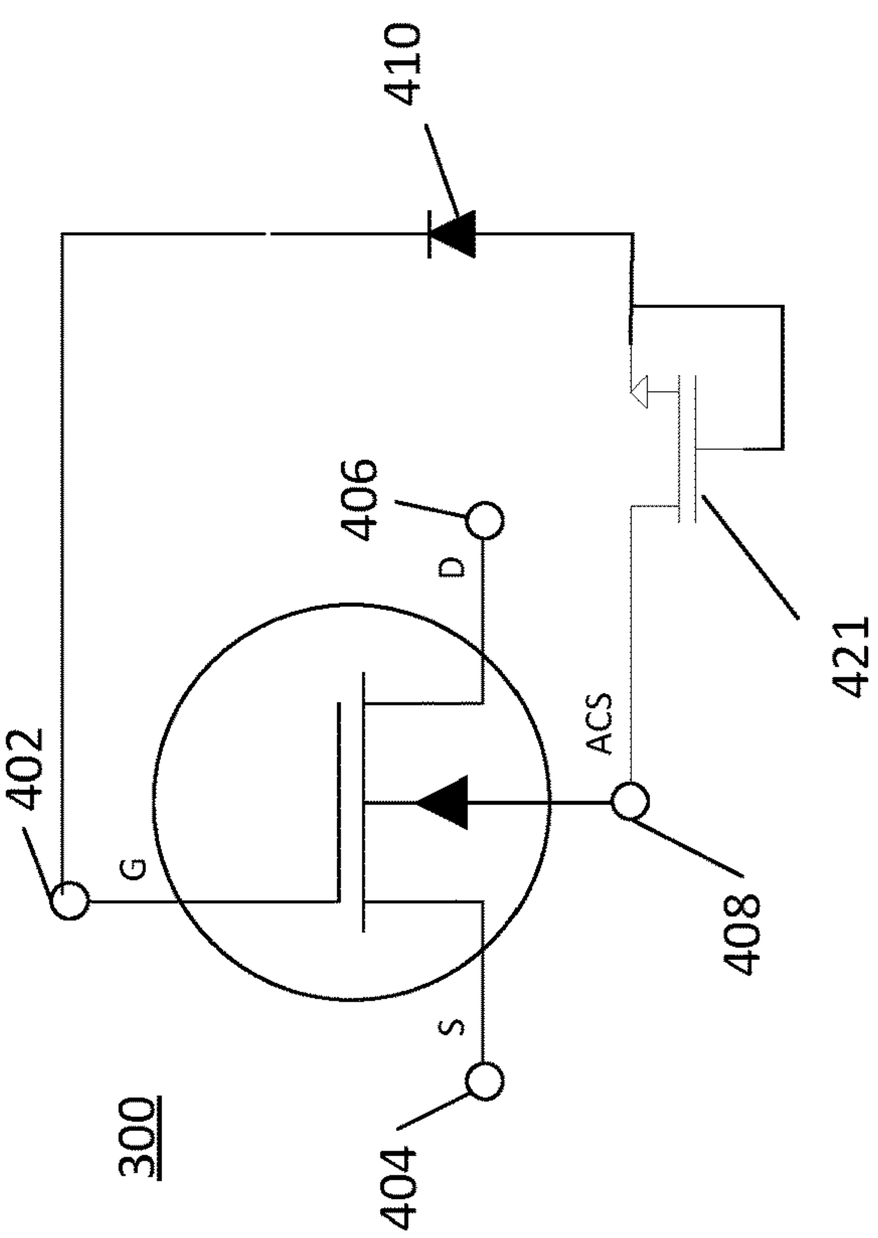

Figure 4F

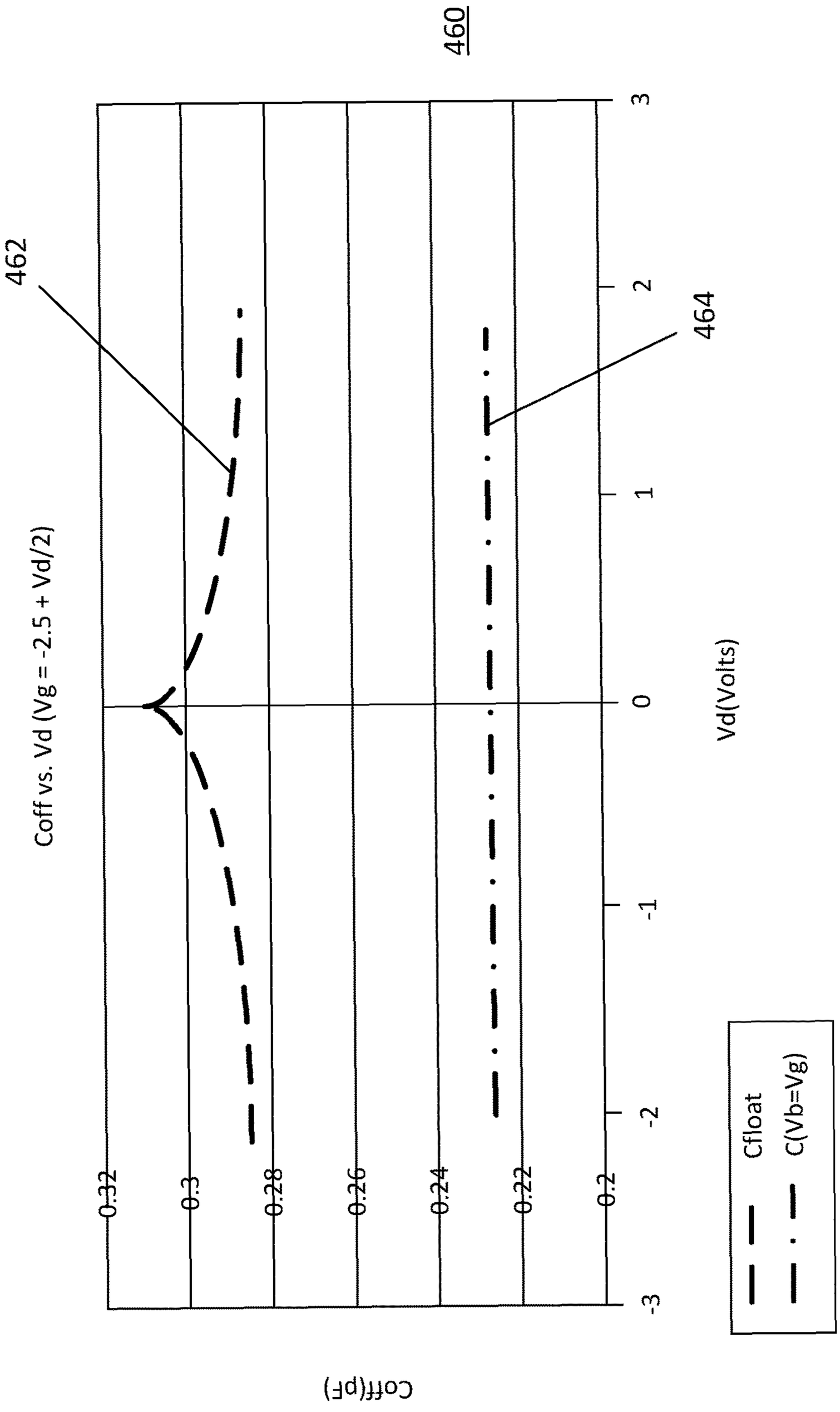
460
462
464
Coff vs. Vd (Vg = -2.5 + Vd/2)
Vd(Volts)
Coff(pF)
3
2
1
0
-1
-2
-3
0.32
0.3
0.28
0.26
0.24
0.22
0.2
Cfloat
C(Vb=Vg)

Figure 4H

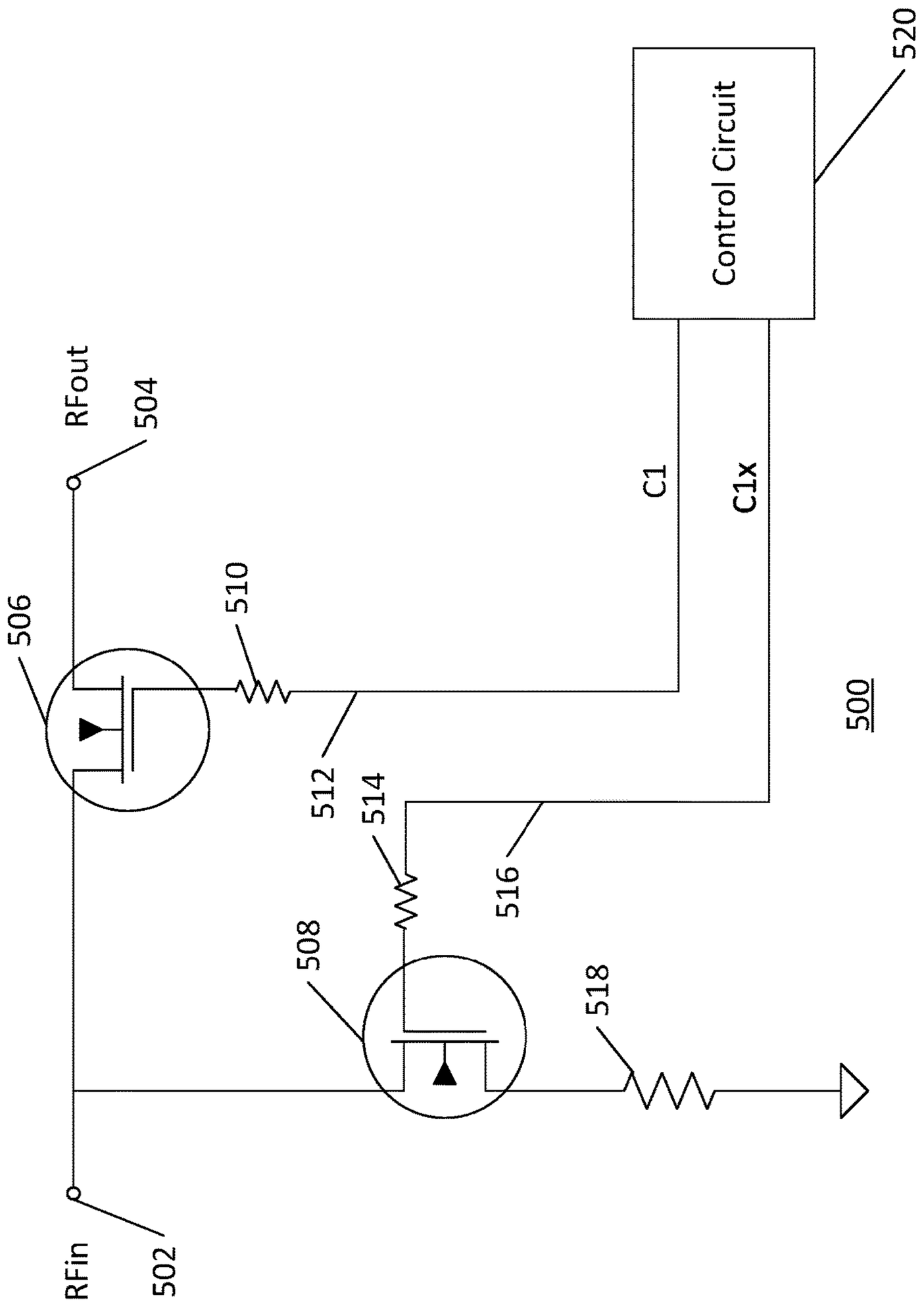
Control Circuit
520
RFout
504
506
510
C1
C1x
512
514
516
508
518
500
RFin
502

Figure 5A

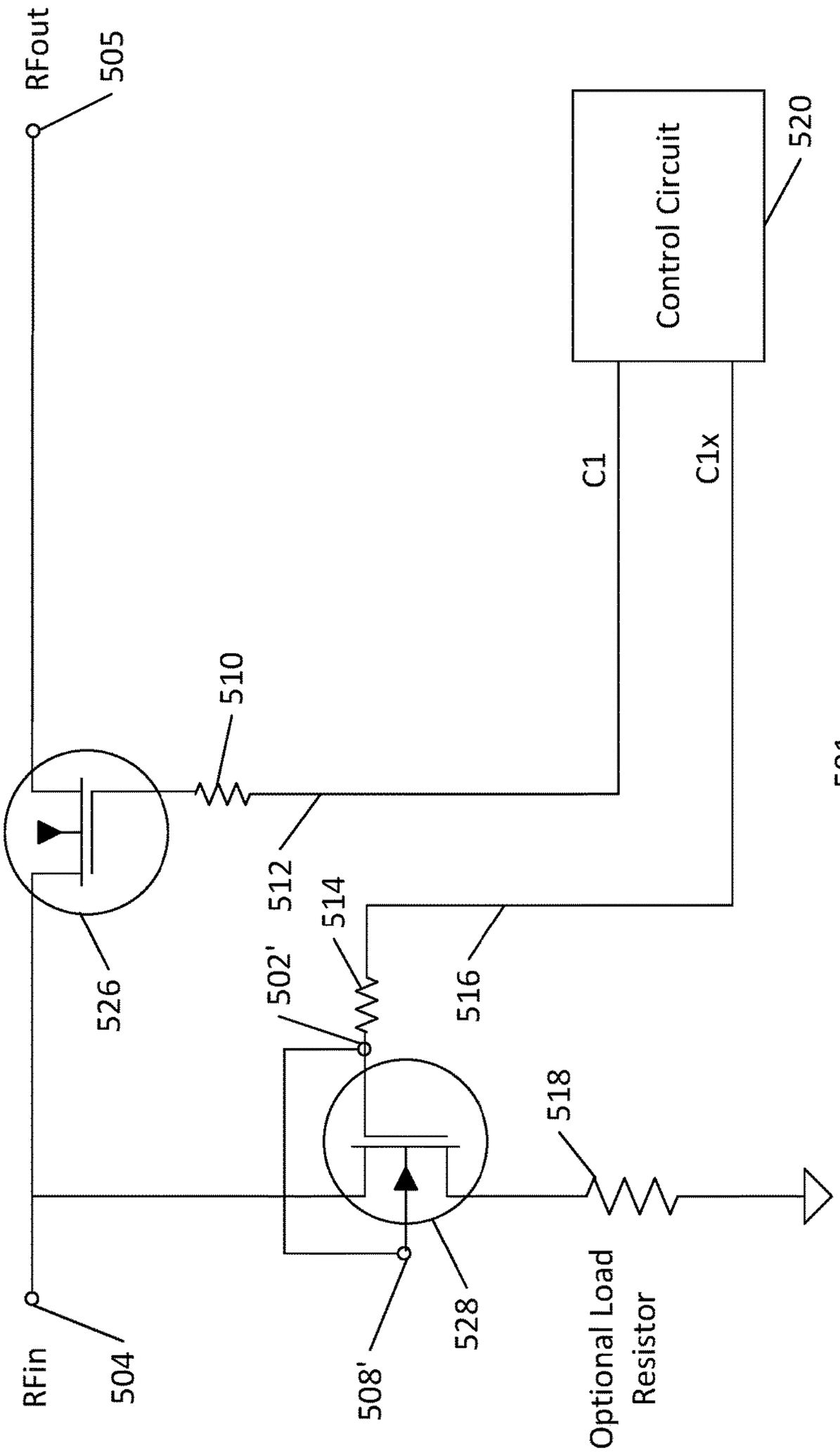
RFout
505
Control Circuit
520
C1
C1x
510
512
514
502'
526
516
518
501
RFin
504
508'
528
Optional Load
Resistor

Figure 5B

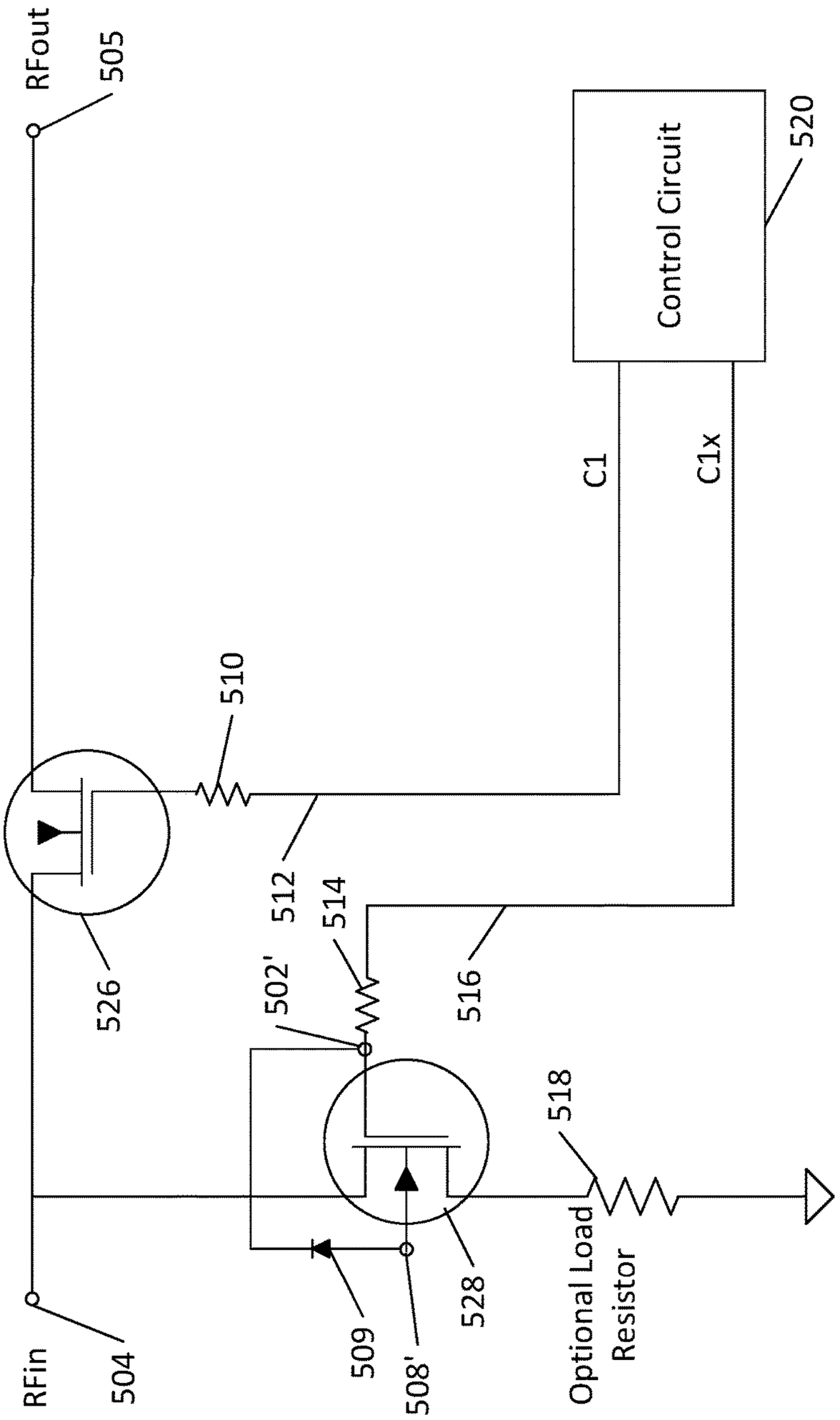
RFout
505
Control Circuit
520
C1
C1x
502
510
512
514
502'
516
526
518
Optional Load Resistor
528
509
508'
RFin
504

Figure 5C

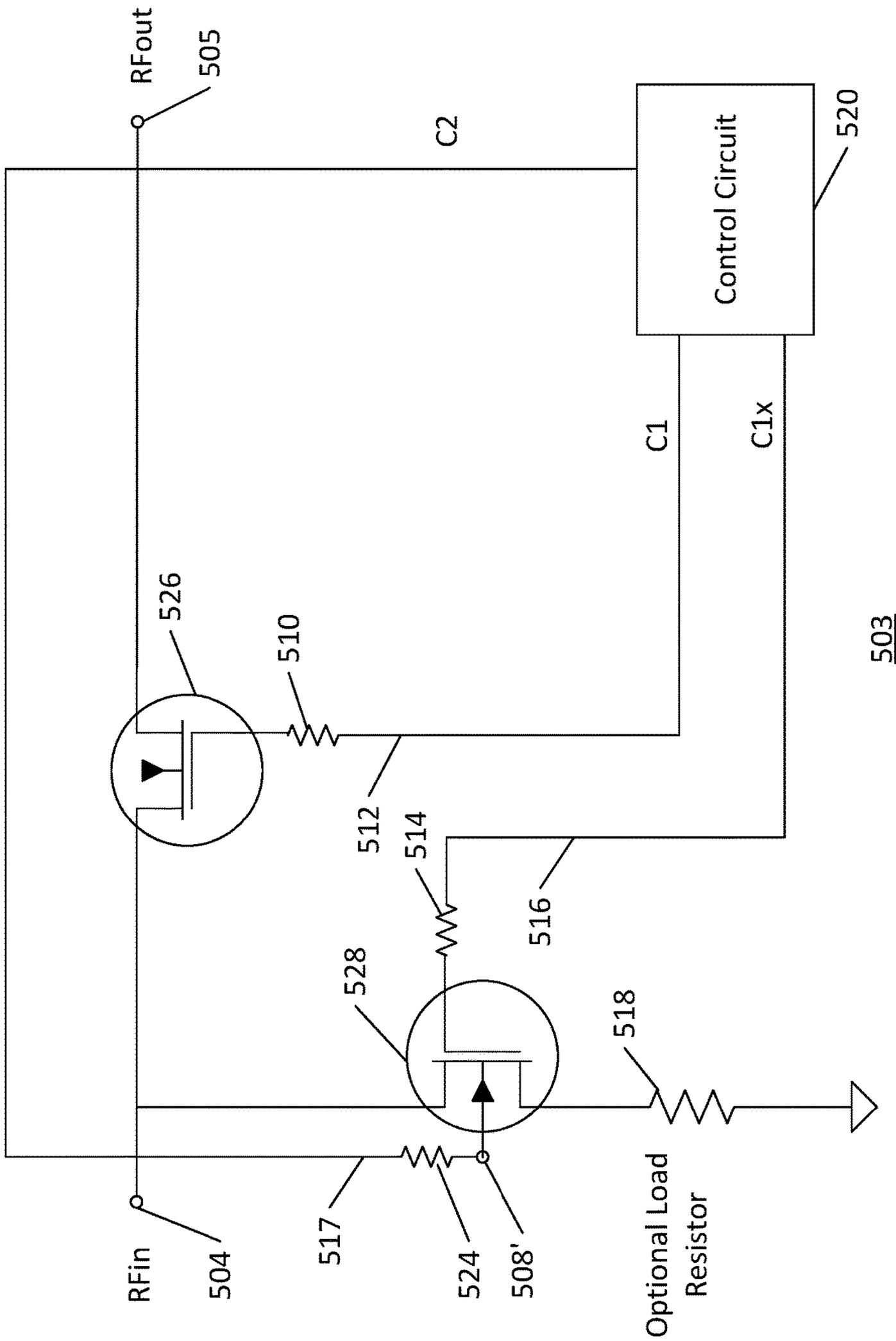
RFout
505
C2
Control Circuit
520
C1
C1x
526
510
512
514
516
528
518
503
RFin
504
517
524
508'
Optional Load
Resistor

Figure 5D

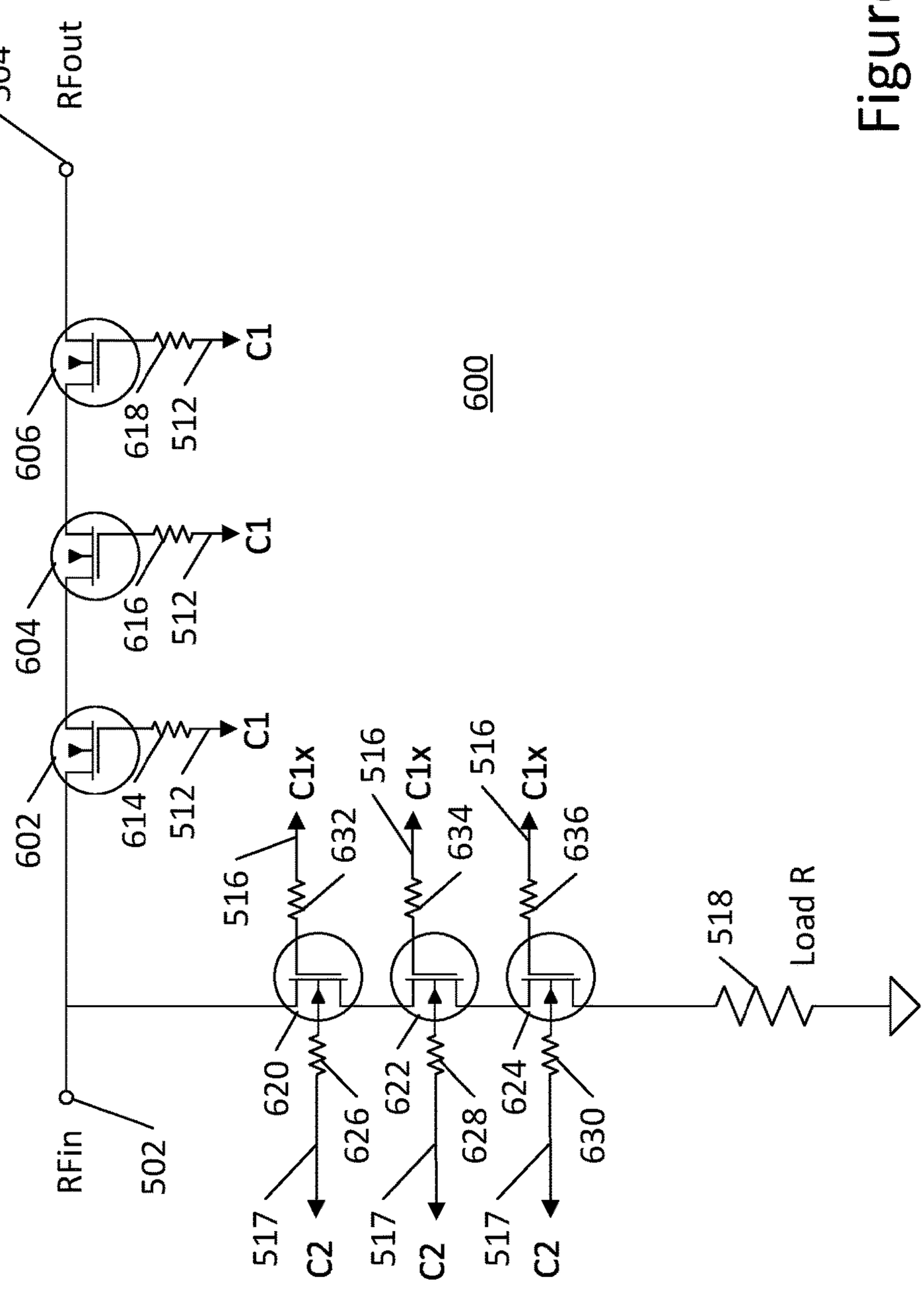
RFin
502
504
RFout
600
602
604
606
512
514
516
517
518
520
522
524
526
528
530
532
534
536
538
540
542
544
546
548
550
552
554
556
558
560
562
564
566
568
570
572
574
576
578
580
582
584
586
588
590
592
594
596
598
C1
C1x
C2
Load R

Figure 6

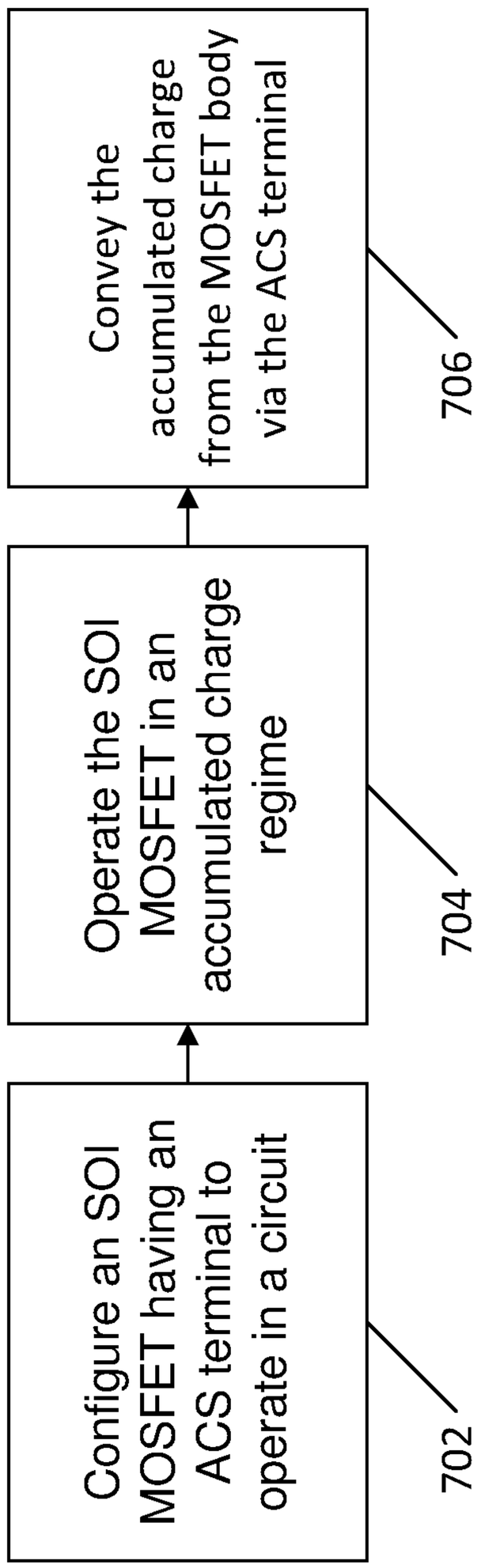
Configure an SOI MOSFET having an ACS terminal to operate in a circuit
702
Operate the SOI MOSFET in an accumulated charge regime
704
Convey the accumulated charge from the MOSFET body via the ACS terminal
706
700

Figure 7

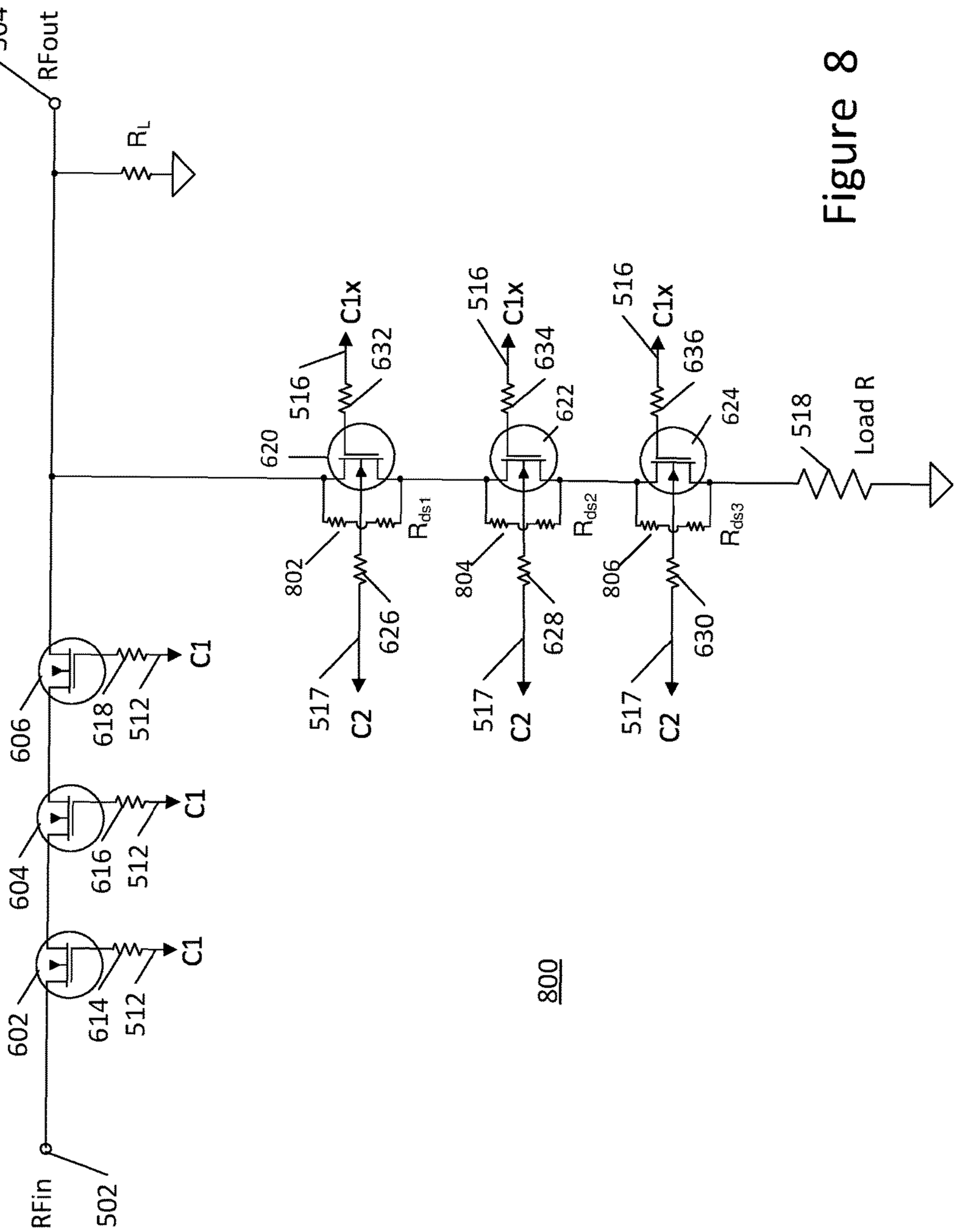
504
RFout
R_L
516
C1x
632
620
634
622
636
624
518
Load R
802
804
806
R_{ds1}
R_{ds2}
R_{ds3}
626
628
630
517
C2
606
618
512
C1
604
616
602
614
RFin
502
800

Figure 8

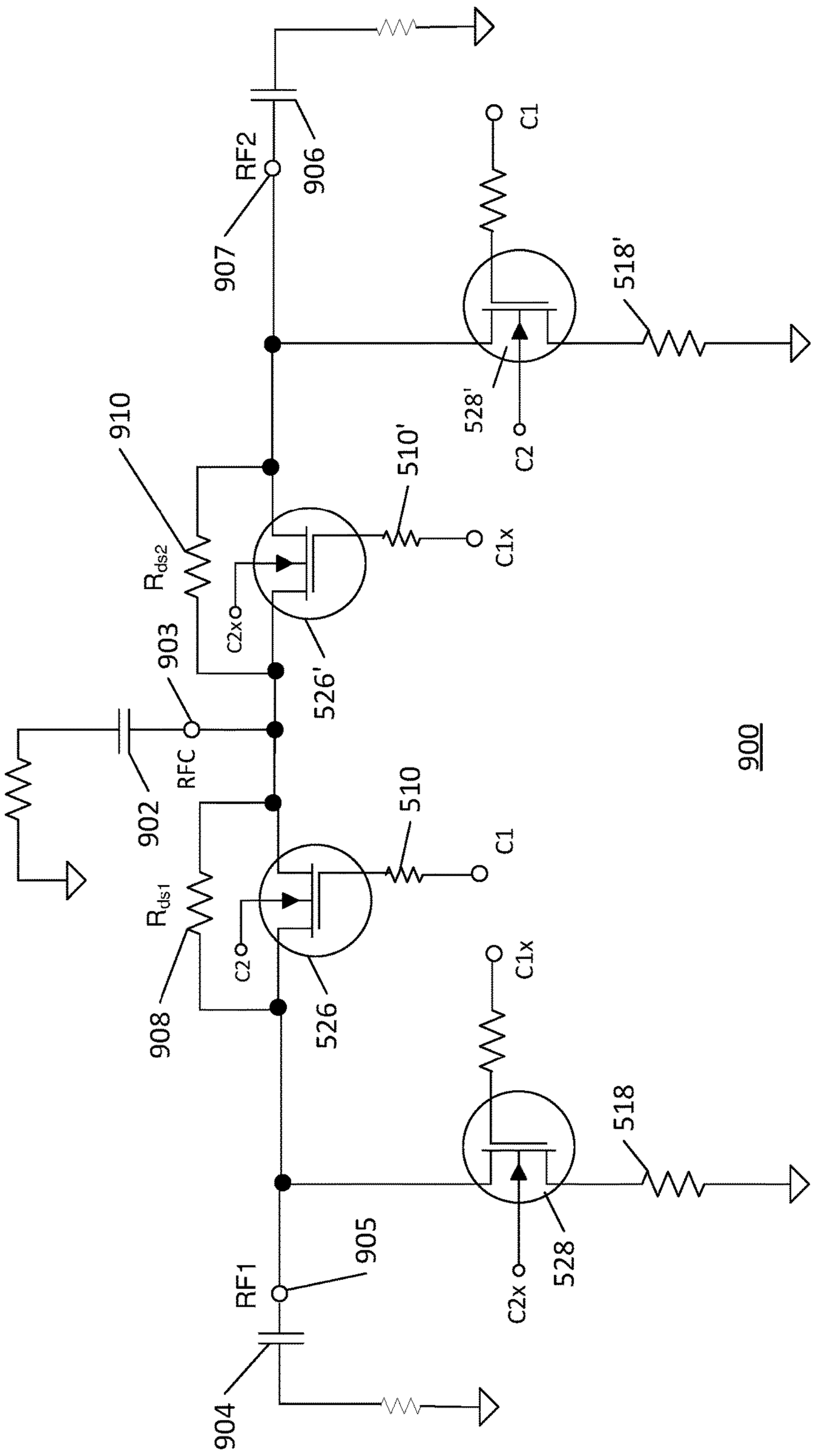
907
RF2
906
C1
518'
528'
C2
910
R_{ds2}
C2x
510'
C1x
526'
903
902
RFC
510
C1
R_{ds1}
908
C2
526
C1x
518
905
RF1
C2x
528
904
900

Figure 9

METHOD AND APPARATUS FOR USE IN IMPROVING LINEARITY OF MOSFETS USING AN ACCUMULATED CHARGE SINK

Matter enclosed in heavy brackets [ ] appears in the original patent but forms no part of this reissue specification; matter printed in italics indicates the additions made by reissue; a claim printed with strikethrough indicates that the claim was canceled, disclaimed, or held invalid by a prior post-patent action or proceeding.

This application *is a reissue of U.S. application Ser. No. 15/707,970, filed Sep. 18, 2017, now U.S. Pat. No. 10,153,763, which* is a continuation application of co-pending and commonly assigned U.S. application Ser. No. 14/845,154, "Method and Apparatus for use in Improving Linearity of MOSFETs using an Accumulated Charge Sink", filed Sep. 3, 2015, *now U.S. Pat. No. 9,780,775*; which is a continuation application of and commonly assigned U.S. application Ser. No. 13/850,251, "Method and Apparatus for use in Improving Linearity of MOSFETs using an Accumulated Charge Sink", filed Mar. 25, 2013, [issuing on Sep. 8, 2015 as] *now* U.S. Pat. No. 9,130,564, which application Ser. No. 13/850,251 is a continuation application of commonly assigned U.S. application Ser. No. 13/412,529, "Method and Apparatus for use in Improving Linearity of MOSFETs Using an Accumulated Charge Sink", filed Mar. 5, 2012, [issuing on Mar. 26, 2013 as] *now* U.S. Pat. No. 8,405,147, which application Ser. No. 13/412,529 is a Continuation of commonly assigned U.S. application Ser. No. 13/053,211, "Method and Apparatus for use in Improving Linearity of MOSFETs Using an Accumulated Charge Sink", filed Mar. 22, 2011, [issuing Mar. 6, 2012 as] *now* U.S. Pat. No. 8,129,787, which application Ser. No. 13/053,211 is a divisional application of commonly assigned U.S. application Ser. No. 11/484,370, "Method and Apparatus for use in Improving Linearity of MOSFETs Using an Accumulated Charge Sink", filed Jul. 10, 2006, [issuing Mar. 22, 2011 as] *now* U.S. Pat. No. 7,910,993; and application Ser. No. 11/484,370 (U.S. Pat. No. 7,910,993) claims the benefit of priority under 35 U.S.C. § 119 (e) to commonly-assigned U.S. Provisional Application No. 60/698,523, filed Jul. 11, 2005, entitled "Method and Apparatus for use in Improving Linearity of MOSFETs using an Accumulated Charge Sink"; and [this application] *U.S. application Ser. No. 15/707,970* is also a continuation of commonly assigned [pending] U.S. application Ser. No. 15/419,898 filed Jan. 30, 2017, which is a continuation application of commonly assigned U.S. application Ser. No. 13/948,094 filed Jul. 22, 2013 (U.S. Pat. No. 9,608,619 issued Mar. 28, 2017), which is a continuation application of commonly assigned U.S. application Ser. No. 13/028,144 filed Feb. 15, 2011 (U.S. Pat. No. 8,954,902 issued Feb. 10, 2015), which is a divisional of commonly assigned U.S. application Ser. No. 11/520,912 filed Sep. 14, 2006 (U.S. Pat. No. 7,890,891 issued Feb. 15, 2011), which is a continuation-in-part of U.S. application Ser. No. 11/484,370, filed Jul. 10, 2006 (U.S. Pat. No. 7,910,993 issued Mar. 22, 2011), and which *application* Ser. No. 11/520,912 [application] claims priority to U.S. provisional applications 60/718,260 filed Sep. 15, 2005 and 60/698,523 filed Jul. 11, 2005; and [this Continuation application] *U.S. application Ser. No. 15/707,970* is also related to U.S. application Ser. No. 11/881,816 filed Jul. 26, 2007 which is a CIP of *application* Ser. No. 11/520,912 and a CIP of *application* Ser. No. 11/484,370; and the contents of all of the above cited provisional applications, pending applications, and issued patents, including their associated appendices, are hereby incorporated by reference herein in their entirety.

BACKGROUND

1. Field

The present invention relates to metal-oxide-semiconductor (MOS) field effect transistors (FETs), and particularly to MOSFETs fabricated on Semiconductor-On-Insulator ("SOI") and Semiconductor-On-Sapphire ("SOS") substrates. In one embodiment, an SOI (or SOS) MOSFET is adapted to control accumulated charge and thereby improve linearity of circuit elements.

2. Description of Related Art

Although the disclosed method and apparatus for use in improving the linearity of MOSFETs are described herein as applicable for use in SOI MOSFETs, it will be appreciated by those skilled in the electronic device design arts that the present teachings are equally applicable for use in SOS MOSFETs. In general, the present teachings can be used in the implementation of MOSFETs using any convenient semiconductor-on-insulator technology, including silicon-on-insulator technology. For example, the inventive MOSFETs described herein can be implemented using compound semiconductors on insulating substrates. Such compound semiconductors include, but are not limited to, the following: Silicon Germanium (SiGe), Gallium Arsenide (GaAs), Indium Phosphide (InP), Gallium Nitride (GaN), Silicon Carbide (SiC), and II-VI compound semiconductors, including Zinc Selenide (ZnSe) and Zinc Sulfide (ZnS). The present teachings also may be used in implementing MOSFETs fabricated from thin-film polymers. Organic thin-film transistors (OTFTs) utilize a polymer, conjugated polymers, oligomers, or other molecules to form the insulting gate dielectric layer. The present inventive methods and apparatus may be used in implementing such OTFTs.

It will be appreciated by those skilled in the electronic design arts that the present disclosed method and apparatus apply to virtually any insulating gate technology, and to integrated circuits having a floating body. As those skilled in the art will appreciate, technologies are constantly being developed for achieving "floating body" implementations. For example, the inventors are aware of circuits implemented in bulk silicon wherein circuit implementations are used to "float" the body of the device. In addition, the disclosed method and apparatus can also be implemented using silicon-on-bonded wafer implementations. One such silicon-on-bonded wafer technique uses "direct silicon bonded" (DSB) substrates. Direct silicon bond (DSB) substrates are fabricated by bonding and electrically attaching a film of single-crystal silicon of differing crystal orientation onto a base substrate. The present disclosure therefore contemplates embodiments of the disclosed method and apparatus implemented in any of the developing floating body implementations. Therefore, references to and exemplary descriptions of SOI MOSFETs herein are not to be construed as limiting the applicability of the present teachings to SOI MOSFETs only. Rather, as described below in more detail, the disclosed method and apparatus find utility in MOSFETs implemented in a plurality of device technologies, including SOS and silicon-on-bonded wafer technologies.

As is well known, a MOSFET employs a gate-modulated conductive channel of n-type or p-type conductivity, and is accordingly referred to as an "NMOSFET" or "PMOSFET", respectively. FIG. **1** shows a cross-sectional view of an exemplary prior art SOI NMOSFET **100**. As shown in FIG. **1**, the prior art SOI NMOSFET **100** includes an insulating substrate **118** that may comprise a buried oxide layer, sapphire, or other insulating material. A source **112** and drain **116** of the NMOSFET **100** comprise N+ regions (i.e., regions that are heavily doped with an "n-type" dopant material) produced by ion implantation into a silicon layer positioned above the insulating substrate **118**. (The source and drain of PMOSFETs comprise P+ regions (i.e., regions heavily doped with "p-type" dopant material)). The body **114** comprises a P− region (i.e., a region that is lightly doped with a "p-type" dopant), produced by ion implantation, or by dopants already present in the silicon layer when it is formed on the insulating substrate **118**. As shown in FIG. **1**, the NMOSFET **100** also includes a gate oxide **110** positioned over the body **114**. The gate oxide **110** typically comprises a thin layer of an insulating dielectric material such as SiO_2. The gate oxide **110** electrically insulates the body **114** from a gate **108** positioned over the gate oxide **110**. The gate **108** comprises a layer of metal or, more typically, polysilicon.

A source terminal **102** is operatively coupled to the source **112** so that a source bias voltage "Vs" may be applied to the source **112**. A drain terminal **106** is operatively coupled to the drain **116** so that a drain bias voltage "Vd" may be applied to the drain **116**. A gate terminal **104** is operatively coupled to the gate **108** so that a gate bias voltage "Vg" may be applied to the gate **108**.

As is well known, when a voltage is applied between the gate and source terminals of a MOSFET, a generated electric field penetrates through the gate oxide to the transistor body. For an enhancement mode device, a positive gate bias creates a channel in the channel region of the MOSFET body through which current passes between the source and drain. For a depletion mode device, a channel is present for a zero gate bias. Varying the voltage applied to the gate modulates the conductivity of the channel and thereby controls the current flow between the source and drain.

For an enhancement mode MOSFET, for example, the gate bias creates a so-called "inversion channel" in a channel region of the body **114** under the gate oxide **110**. The inversion channel comprises carriers having the same polarity (e.g., "P" polarity (i.e., hole carriers), or "N" polarity (i.e., electron carriers) carriers) as the polarity of the source and drain carriers, and it thereby provides a conduit (i.e., channel) through which current passes between the source and the drain. For example, as shown in the SOI NMOSFET **100** of FIG. **1**, when a sufficiently positive voltage is applied between the gate **108** and the source **112** (i.e. a positive gate bias exceeding a threshold voltage V_{th}), an inversion channel is formed in the channel region of the body **114**. As noted above, the polarity of carriers in the inversion channel is identical to the polarity of carriers in the source and drain. In this example, because the source and drain comprise "n-type" dopant material and therefore have N polarity carriers, the carriers in the channel comprise N polarity carriers. Similarly, because the source and drain comprise "p-type" dopant material in PMOSFETs, the carriers in the channel of turned on (i.e., conducting) PMOSFETs comprise P polarity carriers.

Depletion mode MOSFETs operate similarly to enhancement mode MOSFETs, however, depletion mode MOSFETs are doped so that a conducting channel exists even without a voltage being applied to the gate. When a voltage of

appropriate polarity is applied to the gate the channel is depleted. This, in turn, reduces the current flow through the depletion mode device. In essence, the depletion mode device is analogous to a "normally closed" switch, while the enhancement mode device is analogous to a "normally open" switch. Both enhancement and depletion mode MOSFETs have a gate voltage threshold, V_{th}, at which the MOSFET changes from an off-state (non-conducting) to an on-state (conducting).

No matter what mode of operation an SOI MOSFET employs (i.e., whether enhancement or depletion mode), when the MOSFET is operated in an off-state (i.e., the gate voltage does not exceed V_{th}), and when a sufficient nonzero gate bias voltage is applied with respect to the source and drain, an "accumulated charge" may occur under the gate. The "accumulated charge", as defined in more detail below and used throughout the present application, is similar to the "accumulation charge" described in the prior art literature in reference to MOS capacitors. However, the prior art references describe "accumulation charge" as referring only to bias-induced charge existing under a MOS capacitor oxide, wherein the accumulation charge is of the same polarity as the majority carriers of the semiconductor material under the capacitor oxide. In contrast, and as described below in more detail, "accumulated charge" is used herein to refer to gate-bias induced carriers that may accumulate in the body of an off-state MOSFET, even if the majority carriers in the body do not have the same polarity as the accumulated charge. This situation may occur, for example, in an off-state depletion mode NMOSFET, wherein the accumulated charge may comprise holes (i.e., having P polarity) even though the body doping is N− rather than P−.

For example, as shown in FIG. **1**, when the SOI NMOSFET **100** is biased to operate in an off-state, and when a sufficient nonzero voltage is applied to the gate **108**, an accumulated charge **120** may accumulate in the body **114** underneath and proximate the gate oxide **110**. The operating state of the SOI NMOSFET **100** shown in FIG. **1** is referred to herein as an "accumulated charge regime" of the MOSFET. The accumulated charge regime is defined in more detail below. The causes and effects of the accumulated charge in SOI MOSFETs are now described in more detail.

As is well known, electron-hole pair carriers may be generated in MOSFET bodies as a result of several mechanisms (e.g., thermal, optical, and band-to-band tunneling electron-hole pair generation processes). When electron-hole pair carriers are generated within an NMOSFET body, for example, and when the NMOSFET is biased in an off-state condition, electrons may be separated from their hole counterparts and pulled into both the source and drain. Over a period of time, assuming the NMOSFET continues to be biased in the off-state, the holes (resulting from the separated electron-hole pairs) may accumulate under the gate oxide (i.e., forming an "accumulated charge") underneath and proximate the gate oxide. A similar process (with the behavior of electrons and holes reversed) occurs in similarly biased PMOSFET devices. This phenomenon is now described with reference to the SOI NMOSFET **100** of FIG. **1**.

When the SOI NMOSFET **100** is operated with gate, source and drain bias voltages that deplete the channel carriers in the body **114** (i.e., the NMOSFET **100** is in the off-state), holes may accumulate underneath and proximate the gate oxide **110**. For example, if the source bias voltage Vs and the drain bias voltage Vd are both zero (e.g., connected to a ground contact, not shown), and the gate bias voltage Vg comprises a sufficiently negative voltage with

respect to ground and with respect to V_{th}, holes present in the body **114** become attracted to the channel region proximate the gate oxide **110**. Over a period of time, unless removed or otherwise controlled, the holes accumulate underneath the gate oxide **110** and result in the accumulated charge **120** shown in FIG. **1**. The accumulated charge **120** is therefore shown as positive "+" hole carriers in FIG. **1**. In the example given, Vg is negative with respect to Vs and Vd, so electric field regions **122** and **124** may also be present.

Accumulated Charge Regime Defined

The accumulated charge is opposite in polarity to the polarity of carriers in the channel. Because, as described above, the polarity of carriers in the channel is identical to the polarity of carriers in the source and drain, the polarity of the accumulated charge **120** is also opposite to the polarity of carriers in the source and drain. For example, under the operating conditions described above, holes (having "P" polarity) accumulate in off-state NMOSFETs, and electrons (having "N" polarity) accumulate in off-state PMOSFETs. Therefore, a MOSFET device is defined herein as operating within the "accumulated charge regime" when the MOSFET is biased to operate in an off-state, and when carriers having opposite polarity to the channel carriers are present in the channel region. Stated in other terms, a MOSFET is defined as operating within the accumulated charge regime when the MOSFET is biased to operate in an off-state, and when carriers are present in the channel region having a polarity that is opposite the polarity of the source and drain carriers.

For example, and referring again to FIG. **1**, the accumulated charge **120** comprises hole carriers having P or "+" polarity. In contrast, the carriers in the source, drain, and channel (i.e., when the FET is in the on-state) comprise electron carriers having N or "−" polarity. The SOI NMOSFET **100** is therefore shown in FIG. **1** as operating in the accumulated charge regime. It is biased to operate in an off-state, and an accumulated charge **120** is present in the channel region. The accumulated charge **120** is opposite in polarity (P) to the polarity of the channel, source and drain carriers (N).

In another example, wherein the SOI NMOSFET **100** comprises a depletion mode device, V_{th} is negative by definition. According to this example, the body **114** comprises an N− region (as contrasted with the P− region shown in FIG. **1**). The source and drain comprise N+ regions similar to those shown in the enhancement mode MOSFET **100** of FIG. **1**. For Vs and Vd both at zero volts, when a gate bias Vg is applied that is sufficiently negative relative to V_{th} (for example, a Vg that is more negative than approximately −1 V relative to V_{th}), the depletion mode NMOSFET is biased into an off-state. If biased in the off-state for a sufficiently long period of time, holes may accumulate under the gate oxide and thereby comprise the accumulated charge **120** shown in FIG. **1**.

In other examples, Vs and Vd may comprise nonzero bias voltages. In some embodiments, Vg must be sufficiently negative to both Vs and Vd (in order for Vg to be sufficiently negative to V_{th}, for example) in order to bias the NMOSFET in the off-state. Those skilled in the MOSFET device design arts shall recognize that a wide variety of bias voltages may be used to practice the present teachings. As described below in more detail, the present disclosed method and apparatus contemplates use in any SOI MOSFET device biased to operate in the accumulated charge regime.

SOI and SOS MOSFETs are often used in applications in which operation within the accumulated charge regime adversely affects MOSFET performance. As described below in more detail, unless the accumulated charge is removed or otherwise controlled, it detrimentally affects performance of SOI MOSFETs under certain operating conditions. One exemplary application, described below in more detail with reference to the circuits shown in FIGS. **2**B and **5**A, is the use of SOI MOSFETs in the implementation of radio frequency (RF) switching circuits. As described below with reference to FIGS. **2**B and **5**A in more detail, the inventors have discovered that unless the accumulated charge is removed or otherwise controlled, under some operating conditions, the accumulated charge adversely affects the linearity of the SOI MOSFET and thereby increases harmonic distortion and intermodulation distortion (IMD) caused by the MOSFET when used in the implementation of certain circuits. In addition, as described below in more detail, the inventors have discovered that removal or control of the accumulated charge improves the drain-to-source breakdown voltage (i.e., the "BVDSS") characteristics of the SOI MOSFETs.

Therefore, it is desirable to provide techniques for adapting and improving SOI (and SOS) MOSFETs, and circuits implemented with the improved SOI MOSFETs, in order to remove or otherwise control the accumulated charge, and thereby significantly improve SOI MOSFET performance. It is desirable to provide methods and apparatus for use in improving the linearity characteristics in SOI MOSFETs. The improved MOSFETs should have improved linearity, harmonic distortion, intermodulation distortion, and BVDSS characteristics as compared with prior art MOSFETs, and thereby improve the performance of circuits implemented with the improved MOSFETs. The present teachings provide such novel methods and apparatus.

SUMMARY

Apparatuses and methods are provided to control accumulated charge in SOI MOSFETs, thereby improving nonlinear responses and harmonic and intermodulaton distortion effects in the operation of the SOI MOSFETs.

In one embodiment, a circuit having at least one SOI MOSFET is configured to operate in an accumulated charge regime. An accumulated charge sink (ACS), operatively coupled to the body of the SOI MOSFET, receives accumulated charge generated in the body, thereby reducing the nonlinearity of the net source-drain capacitance of the SOI MOSFET.

In one embodiment, the ACS comprises a high impedance connection to the MOSFET body, with an exemplary impedance greater than 10^6 ohm.

BRIEF DESCRIPTION OF THE DRAWINGS

FIG. **1** is a cross-sectional view of an exemplary prior art SOI NMOSFET.

FIG. **2**A is a simplified schematic of an electrical model showing the off-state impedance characteristics of the exemplary prior art SOI NMOSFET of FIG. **1**.

FIG. **2**B is a schematic of an exemplary simplified RF switching circuit implemented using prior art SOI MOSFETs such as the prior art SOI NMOSFET of FIG. **1**.

FIGS. **3**A and **3**B are simplified schematic diagrams of a top view of an improved SOI NMOSFET adapted to control accumulated charge in accordance with the present teachings.

FIG. **3**C is a cross-sectional perspective schematic of an improved SOI NMOSFET adapted to control accumulated charge showing gate, source, drain and accumulated charge sink (ACS) terminals.

FIG. **3**D is a simplified top view schematic of an improved SOI NMOSFET adapted to control accumulated charge having an accumulated charge sink (ACS) electrically coupled to a P+ region.

FIG. **3**E is a simplified top view schematic of an improved SOI SOI NMOSFET adapted to control accumulated charge and showing a cross-sectional view line A-A' taken along approximately a center of the SOI NMOSFET.

FIG. **3**F is a cross-sectional view of the improved SOI NMOSET of FIG. **3**E taken along the A-A' view line of FIG. **3**E.

FIG. **3**G is a cross-sectional view of the improved SOI NMOSET of FIGS. **3**A-**3**B.

FIG. **3**H is a simplified top view schematic of an SOI NMOSFET illustrating a region of increased threshold voltage that can occur in prior art MOSFETs and in some embodiments of the improved SOI MOSFET due to manufacturing processes.

FIG. **3**I is a plot of inversion channel charge as a function of applied gate voltage when a region of increased threshold voltage is present in an SOI MOSFET.

FIG. **3**J is a simplified top view schematic of an improved SOI NMOSFET adapted to control accumulated charge and configured in a "T-gate" configuration.

FIG. **3**K is a simplified top view schematic of an improved SOI NMOSFET adapted to control accumulated charge and configured in an "H-gate" configuration.

FIG. **4**A is a simplified schematic of an improved SOI NMOSFET adapted to control accumulated charge embodied as a four terminal device.

FIG. **4**B is a simplified schematic of an improved SOI NMOSFET adapted to control accumulated charge, embodied as a four terminal device, wherein an accumulated charge sink (ACS) terminal is coupled to a gate terminal.

FIG. **4**C is a simplified schematic of an improved SOI NMOSFET adapted to control accumulated charge, embodied as a four terminal device, wherein an accumulated charge sink (ACS) terminal is coupled to a gate terminal via a diode.

FIG. **4**D is a simplified schematic of an improved SOI NMOSFET adapted to control accumulated charge, embodied as a four terminal device, wherein an accumulated charge sink (ACS) terminal is coupled to a control circuit.

FIG. **4**E is a simplified schematic of an exemplary RF switch circuit implemented using the four terminal ACC NMOSFET of FIG. **4**D, wherein the ACS terminal is driven by an external bias source.

FIG. **4**F is a simplified schematic of an improved SOI NMOSFET adapted to control accumulated charge, embodied as a four terminal device, wherein an accumulated charge sink (ACS) terminal is coupled to a clamping circuit.

FIG. **4**G is a simplified schematic of an improved SOI NMOSFET adapted to control accumulated charge, embodied as a four terminal device, wherein an accumulated charge sink (ACS) terminal is coupled to a gate terminal via a diode in parallel with a capacitor.

FIG. **4**H shows plots of the off-state capacitance (C_{off}) versus applied drain-to-source voltages for SOI MOSFETs operated in the accumulated charge regime, wherein a first plot shows the off-state capacitance C_{off} of a prior art SOI MOSFET, and wherein a second plot shows the off-state capacitance C_{off} of the improved ACC SOI MOSFET made in accordance with the present teachings.

FIG. **5**A is a schematic of an exemplary prior art single pole, single throw (SPST) radio frequency (RF) switch circuit.

FIG. **5**B is a schematic of an RF switch circuit adapted for improved performance using accumulated charge control, wherein the gate of a shunting SOI NMOSFET is coupled to an accumulated charge sink (ACS) terminal.

FIG. **5**C is a schematic of an RF switch circuit adapted for improved performance using accumulated charge control, wherein the gate of a shunting SOI NMOSFET is coupled to an accumulated charge sink (ACS) terminal via a diode.

FIG. **5**D is a schematic of an RF switch circuit adapted for improved performance using accumulated charge control, wherein the accumulated charge sink (ACS) terminal is coupled to a control circuit.

FIG. **6** is a schematic of an RF switch circuit including stacked MOSFETs, adapted for improved performance using accumulated charge control, wherein the accumulated charge sink (ACS) terminals of the shunting stacked MOSFETs are coupled to a control signal.

FIG. **7** shows a flowchart of an exemplary method of improving the linearity of an SOI MOSFET device using an accumulated charge sink in accordance with the present disclosure.

FIG. **8** shows a simplified circuit schematic of an exemplary embodiment of an RF switch circuit made in accordance with the present disclosure, wherein the RF switch circuit includes drain-to-source resistors between the drain and source of the ACC MOSFETs.

FIG. **9** shows a simplified schematic of an exemplary single-pole double-throw (SPDT) RF switch circuit made in accordance with the present disclosure, wherein drain-to-source resistors are shown across the switching ACC SOI MOSFETs.

Like reference numbers and designations in the various drawings indicate like elements.

DETAILED DESCRIPTION

As noted above, those skilled in the electronic device design arts shall appreciate that the teachings herein apply equally to NMOSFETs and PMOSFETs. For simplicity, the embodiments and examples presented herein for illustrative purposes include only NMOSFETs, unless otherwise noted. By making well known changes to dopants, charge carriers, polarity of bias voltages, etc., persons skilled in the arts of electronic devices will easily understand how these embodiments and examples may be adapted for use with PMOSFETs.

Non-Linearity and Harmonic Distortion Effects of Accumulated Charge in an SOI NMOSFET

As described above in the background, no matter what mode of operation the MOSFET employs (i.e., enhancement mode or depletion mode), under some circumstances, when a MOSFET is operated in an off-state with a nonzero gate bias voltage applied with respect to the source and drain, an accumulated charge may occur under the gate. According to the present teachings, as described above when the MOSFET is in an off-state, and when carriers are present in the channel region having a polarity that is opposite the polarity of the source and drain carriers, the MOSFET is defined herein as operating in the accumulated charge regime.

According to the present teachings, the inventors have observed that, when used in certain circuit implementations, MOSFETs operating in the accumulated charge regime exhibit undesirable non-linear characteristics that adversely impact circuit performance. For example, as described below in more detail with reference to FIG. **2**A, the accumulated charge **120** (FIG. **1**) adversely affects the linearity of off-state SOI MOSFETs, and more specifically, it

adversely affects the linearity of contributing capacitances to the drain-to-source capacitance (Cds). For an SOI MOSFET operating in an off-state, Cds is referred to as C_{off}. The contributing capacitances to C_{off} are described below in reference to FIG. **2**A for bias conditions wherein the gate bias Vg is provided by a circuit having an impedance that is large compared to the impedances of the contributing capacitances. As described below with reference to FIGS. **2**B and **5**A, this, in turn, adversely affects harmonic distortion, intermodulation distortion, and other performance characteristics of circuits implemented with the SOI MOSFETs. These novel observations, not taught or suggested by the prior art, may be understood with reference to the electrical model shown in FIG. **2**A.

FIG. **2**A is a simplified schematic of an electrical model **200** showing the off-state impedance (or conversely, conductance) characteristics of the exemplary prior art SOI NMOSFET **100** of FIG. **1**. More specifically, the model **200** shows the impedance characteristics from the source **112** to the drain **116** when the NMOSFET **100** is operated in the off-state. Because the drain-to-source off-state impedance characteristic of the NMOSFET **100** is primarily capacitive in nature, it is referred to herein as the drain-to-source off-state capacitance (C_{off}). For the exemplary description herein, the gate **108** is understood to be biased at a voltage Vg by a circuit (not shown) that has an impedance that is large compared to the impedances of the contributing capacitances described in reference to FIG. **2**A. Persons skilled in the electronic arts will understand how this exemplary description may be modified for the case wherein the impedance of the circuit providing the Vg bias is not large compared to the impedances of the contributing capacitances.

As shown in FIG. **2**A, the junction between the source **112** and the body **114** (i.e., a source-body junction **218**) of the off-state NMOSFET **100** can be represented by a junction diode **208** and a junction capacitor **214**, configured as shown. Similarly, the junction between the drain **116** and the body **114** (i.e., the drain-body junction **220**) of the off-state NMOSFET **100** can be represented by a junction diode **210** and a junction capacitor **216**, configured as shown. The body **114** is represented simply as an impedance **212** that is present between the source-body junction **218** and the drain-body junction **220**.

A capacitor **206** represents the capacitance between the gate **108** and the body **114**. A capacitor **202** represents the capacitance between the source **112** and the gate **108**, and another capacitor **204** represents the capacitance between the drain **116** and the gate **108**. A substrate capacitance due to the electrical coupling between the source **112** and the drain **116** (through the insulating substrate **118** shown in FIG. **1**) is taken to be negligibly small in the exemplary description set forth below, and therefore is not shown in the electrical model **200** of FIG. **2**A.

As described above, when the NMOSFET **100** is in the off-state, and when the accumulated charge **120** (FIG. **1**) is not present in the body **114** (i.e., the NMOSFET **100** is not operating within the accumulated charge regime), the body **114** is depleted of charge carriers. In this case the body impedance **212** is analogous to the impedance of an insulator, and the electrical conductance through the body **114** is very small (i.e., the NMOSFET **100** is in the off-state). Consequently, the principal contributions to the drain-to-source off-state capacitance C_{off} are provided by the capacitors **202** and **204**. The capacitors **202** and **204** are only slightly voltage dependent, and therefore do not significantly contribute to a nonlinear response that adversely affects harmonic generation and intermodulation distortion characteristics.

However, when the NMOSFET **100** operates within the accumulated charge regime, and the accumulated charge **120** is therefore present in the body **114**, mobile holes comprising the accumulated charge produce p-type conductivity between the source-body junction **218** and the drain-body junction **220**. In effect, the accumulated charge **120** produces an impedance between the source-body junction **218** and the drain-body junction **220** that is significantly less than the impedance between the junctions in the absence of the accumulated charge. If a Vds voltage is applied between the drain **116** and the source **112**, the mobile holes redistribute according to the electrical potentials that result within the body **114**. DC and low-frequency current flow through the SOI NMOSFET **100** is prevented by the diode properties of the source-body junction **218** and the drain-body junction **220**, as represented by the junction diodes **208** and **210**, respectively. That is, because the junction diodes **208** and **210** are anti-series (i.e., "back-to-back") in this case, no DC or low-frequency currents flow through the SOI NMOSFET **100**. However, high-frequency currents may flow through the SOI NMOSFET **100** via the capacitances of the source-body junction **218** and the drain-body junction **220**, as represented by the junction capacitors **214** and **216**, respectively.

The junction capacitors **214** and **216** are voltage dependent because they are associated with junctions between n-type and p-type regions. This voltage dependence results from the voltage dependence of the width of the depletion region of the junction between the n-type and p-type regions. As a bias voltage is applied to the NMOSFET, the width of the depletion region of the junction between the n-type and p-type regions is varied. Because the capacitance of the junction depends on the width of the junction depletion region, the capacitance also varies as a function of the bias applied across the junction (i.e., the capacitance is also voltage dependent).

Further, the capacitors **202** and **204** may also have a voltage dependence caused by the presence of the accumulated charge **120**. Although the complex reasons for this voltage dependence are not described in detail herein, persons skilled in the arts of electronic devices shall understand that electric field regions (e.g., electric field regions **122** and **124** described above with reference to FIG. **1**) may be affected by the response of the accumulated charge and its response to an applied Vds, thereby causing a voltage dependence of capacitors **202** and **204**. An additional nonlinear effect may occur due to a direct capacitance (not shown) between the source **112** and the drain **116**. Although this direct capacitance would usually be expected to be negligible for most SOI MOSFETs, it may contribute for SOI MOSFETs having very short spacing between the source and drain. The contribution of this direct capacitance to C_{off} is also voltage-dependent in the presence of an accumulated charge, for reasons that are analogous to the voltage dependencies of the capacitors **202** and **204** as described above.

The voltage dependencies of the junction capacitors **214** and **216**, the gate-to-source and gate-to-drain capacitors **202**, **204**, respectively, and the direct capacitance (not shown), cause nonlinear behavior in off-state capacitance C_{off} of the MOSFET when AC voltages are applied to the NMOSFET **100**, thereby producing undesirable generation of harmonic distortions and intermodulation distortion (IMD). The relative contributions of these effects are complex, and depend

on fabrication processes, biases, signal amplitudes, and other variables. However, those skilled in the electronic device design arts shall understand from the teachings herein that reducing, removing, or otherwise controlling the accumulated charge provides an overall improvement in the nonlinear behavior of C_{off}. In addition, because the body impedance **212** is significantly decreased in the presence of the accumulated charge **120**, the magnitude of C_{off} may be increased when the FET operates in the accumulated charge regime. Reducing, removing, or otherwise controlling the accumulated charge also mitigates this effect.

In addition, the accumulated charge does not accumulate in the body in an instant as soon as the FET transitions from an on-state (conducting state) to an off-state (non-conducting state). Rather, when the FET transitions from the on-state to the off-state, it begins to accumulate charge in the body of the MOSFET, and the amount of accumulated charge increases over time. The accumulation of the accumulated charge therefore has an associated time constant (i.e., it does not instantly reach a steady-state level of accumulated charge). The accumulated charge accumulates slowly in the FET body. The depleted FET has a C_{off} associated with it which is increased with an increasing amount of accumulated charge. In terms of FET performance, as the C_{off} increases with an increasing amount of accumulated charge in the FET body, drift occurs in the FET insertion loss (i.e., the FET becomes more "lossy"), isolation (the FET becomes less isolating) and insertion phase (delay in the FET is increased). Reducing, removing, or otherwise controlling the accumulated charge also mitigates these undesirable drift effects.

The inventors have observed that the nonlinear behavior of the MOSFET off-state capacitance C_{off} adversely affects the performance of certain circuits implemented with the prior art SOI MOSFETs. For example, when an RF switch is implemented using the prior art SOI MOSFETs, such as the prior art SOI NMOSFET **100** of FIG. **1**, the above-described non-linear off-state characteristics of the prior art MOSFETs adversely affect the linearity of the switch. As described below in more detail, RF switch linearity is an important design parameter in many applications. Improved switch linearity leads to improved suppression of harmonic and intermodulation (IM) distortion of signals processed by the switch. These improved switch characteristics can be critically important in some applications such as use in cellular communication devices.

For example, the well known GSM cellular communication system standard imposes stringent linearity, harmonic and intermodulation suppression, and power consumption requirements on front-end components used to implement GSM cell phones. One exemplary GSM standard requires that all harmonics of a fundamental signal be suppressed to below −30 dBm at frequencies up to 12.75 GHz. If harmonics are not suppressed below these levels, reliable cell phone operation can be significantly adversely impacted (e.g., increased dropped calls or other communication problems may result due to harmonic and intermodulation distortion of the transmit and receive signals). Because the RF switching function is generally implemented in the cell phone front-end components, improvements in the RF switch linearity, harmonic and intermodulation suppression, and power consumption performance characteristics is highly desirable. A description of how the non-linear behavior of the off-state capacitance C_{off} of the prior art MOSFETs adversely affects these RF switch characteristics is now described with reference to FIG. **2**B.

Harmonic Distortion Effects on RF Switch Circuits Implemented Using Prior Art SOI MOSFETs

FIG. **2**B illustrates an exemplary simplified RF switch circuit **250** implemented using prior art MOSFETs such as the prior art SOI NMOSFET **100** described above with reference to FIG. **1**. A detailed description of the operation and implementation of RF switch circuits is provided in commonly assigned U.S. Pat. No. 6,804,502 which is hereby incorporated herein by reference in its entirety for its teachings on RF switch circuits. As shown in FIG. **2**B, the prior art RF switch **250** includes a single "pass" or "switching" MOSFET **254** operatively coupled to five shunting MOSFETs **260**a-**260**e.

The MOSFET **254** acts as a pass or switching transistor and is configured, when enabled, to selectively couple an RF input signal (applied to its drain, for example) to an RF antenna **258** via a transmission path **256**. The shunting MOSFETs, **260**a-**260**e, when enabled, act to alternatively shunt the RF input signal to ground. As is well known, the switching MOSFET **254** is selectively controlled by a first switch control signal (not shown) coupled to its gate, and the shunting MOSFETs, **260**a-**260**e are similarly controlled by a second switch control signal (not shown) coupled to their gates. The switching MOSFET **254** is thereby enabled when the shunting MOSFETs **260**a-**260**e are disabled, and vice versa. As shown in the exemplary embodiment of the RF switch **250** of FIG. **2**B, the switching MOSFET **254** is enabled by applying a gate bias voltage of +2.5V (via the first switch control signal). The shunting MOSFETs **260**a-**260**e are disabled by applying a gate bias voltage of −2.5V (via the second switch control signal).

When the switch **250** is configured in this state, the RF signal **252** propagates through the switching MOSFET **254**, through the transmission path **256**, and to the antenna **258**. As described above with reference to FIG. **2**A, when the shunting MOSFETS **260**a-**260**e comprise prior art SOI (or SOS) MOSFETs, such as the SOI NMOSFET **100** (FIG. **1**), an accumulated charge can occur in the SOI MOSFET bodies (i.e., when the SOI MOSFETs operate in the accumulated charge regime as described above). The accumulated charge can produce nonlinear behavior in the off-state capacitance C_{off} of the SOI MOSFETs when AC voltages are applied to the MOSFETs.

More specifically, when the accumulated charge is present in the channel regions of the off-state SOI MOSFETs **260**a-**260**e it responds to variations in the RF signals applied to their respective drains. As the time varying RF signal propagates along the transmission path **256**, the RF signal applies time varying source-to-drain bias voltages to the SOI MOSFETs **260**a-**260**e. The time varying source-to-drain bias voltages creates movement of the accumulated charge within the channel regions of the SOI MOSFETs **260**-**260**e. The movement of the accumulated charge within the channel regions of the SOI MOSFETs causes variations in the drain-to-source off-state capacitance of the SOI MOSFETs **260**a-**260**e. More specifically, the movement of the accumulated charge within the channel regions causes a voltage dependence of the drain-to-source off-state capacitance as described above with reference to FIG. **2**A. The voltage dependent variations in the off-state capacitance of the SOI MOSFETs **260**a-**260**e is the dominant cause of harmonic distortion and IMD of the RF signal as it propagates through the RF switch **250**.

As noted above, harmonic distortion and IMD of the RF signal is a major disadvantage of the prior art RF switch circuits implemented using the prior art SOI MOSFET devices. For many applications, harmonics and IMD of the

RF signal must be suppressed to levels that heretofore have been difficult or impossible to achieve using prior art SOI MOSFET devices. In GSM devices, for example, at a maximum operating power of +35 dBm, prior art switches typically have only a 6 dB margin to the GSM third order harmonics suppression requirement of less than −30 dBm. Very low even order harmonic distortion is also desirable in GSM systems as the second order harmonic of the GSM transmit band also resides in the DCS receive band. Suppression of odd order (e.g., third order) harmonics of the RF signal, however, is desirable and improvements in that regard are needed.

In addition, as is well known, presence of an accumulated charge in the bodies of floating body (e.g., SOI) MOSFETs can also adversely affect the drain-to-source breakdown voltage (BVDSS) performance characteristics of the floating body MOSFETs. As is well known, floating-body FETs demonstrate drain-to-source breakdown voltage problems, also known as BVDSS, wherein the drain-to-source "punch-through" voltage is reduced by a parasitic bipolar action. The parasitic bipolar action is caused when holes are generated in the channel and the holes have nowhere to dissipate (i.e., because the body is floating, the holes have no means for escaping the body). As a consequence, the potential of the MOSFET body is increased, which effectively reduces the threshold voltage. In turn, this condition causes the MOSFET device to experience increased leakage, thereby generating more holes in the body, and thereby exacerbating the BVDSS problem (as a result of this positive feedback condition).

The present disclosed method and apparatus for improving linearity of SOI (and SOS) MOSFET devices overcomes the above-described disadvantages of the prior art. Once the accumulated charge is recognized as a major source of harmonic distortion, IMD and compression/saturation in off-state SOI MOSFET devices, and in circuits (such as RF circuits) implemented with these devices, it becomes clear that reduction, removal, and/or control of the accumulated charge improves the harmonic suppression characteristics of these devices. In addition, reduction, removal, and/or control of the accumulated charge also improve the BVDSS performance characteristics by preventing the parasitic bipolar action from occurring. Improvements in BVDSS lead to consequent improvements in device linearity. Several exemplary structures and techniques for controlling the accumulated charge in SOI MOSFETs are described in detail in the next section.

Method and Apparatus for Improving the Linearity of MOSFETs Using Accumulated Charge Sinks (ACS)—Overview

As described below in more detail, the present disclosure describes methods and apparatuses for improving semiconductor device linearity (e.g., reducing adverse harmonic distortion and IMD effects) in SOI MOSFETs. In one exemplary embodiment, the method and apparatus improves the linearity and controls the harmonic distortion and IMD effects of the MOSFET devices by reducing the accumulated charge in the bodies of the MOSFET devices. In one embodiment, the present method and apparatus reduces or otherwise controls the accumulated charge in the MOSFET bodies using an accumulated charge sink (ACS) that is operatively coupled to the MOSFET body. In one embodiment, the present method and apparatus entirely removes all of the accumulated charge from the bodies of the MOSFET devices. In one described embodiment, the MOSFET is biased to operate in an accumulated charge regime, and the ACS is used to entirely remove, reduce, or otherwise control, the accumulated charge and thereby reduce harmonic distortions and IMD that would otherwise result. Linearity is also improved in some embodiments by removing or otherwise controlling the accumulated charge thereby improving the floating body MOSFET BVDSS characteristics.

As noted in the background section above, persons skilled in the electronic device design and manufacture arts shall appreciate that the teachings herein apply equally to MOSFETs fabricated on Semiconductor-On-Insulator ("SOI") and Semiconductor-On-Sapphire ("SOS") substrates. The present teachings can be used in the implementation of MOSFETs using any convenient semiconductor-on-insulator technology. For example, the inventive MOSFETs described herein can be implemented using compound semiconductors fabricated on insulating substrates, such as GaAs MOSFETs. As noted above, the present method and apparatus may also be applied to silicon-germanium (SiGe) SOI MOSFETs. For simplicity, the embodiments and examples presented herein for illustrative purposes include only NMOSFETs, unless otherwise noted. By making well known changes to dopants, charge carriers, polarity of bias voltages, etc., persons skilled in the electronic device design arts will easily understand how these embodiments and examples may be adapted for use with PMOSFETs.

As noted above, the present disclosure is particularly applicable to FETs and associated applications benefiting from a fully depleted channel when the FET is operated in the off-state, wherein an accumulated charge may result. The disclosed method and apparatus for use in improving the linearity of MOSFETs also finds applicability for use with partially depleted channels. As known to those skilled in the art, the doping and dimensions of the body vary widely. In an exemplary embodiment, the body comprises silicon having a thickness of approximately 100 angstroms to approximately 2,000 angstroms. In a further exemplary embodiment, dopant concentration within the FET bodies ranges from no more than that associated with intrinsic silicon to approximately 1×10^{18} active dopant atoms per cm^3, resulting in fully-depleted transistor operation. In a further exemplary embodiment, dopant concentration within the FET bodies ranges from 1×10^{18} to 1×10^{19} active dopant atoms per cm^3 and/or the silicon comprising the body ranges from a thickness of 2000 angstroms to many micrometers, resulting in partially-depleted transistor operation. As will be appreciated by those skilled in the electronic design and manufacturing arts, the present disclosed method and apparatus for use in improving linearity of MOSFETs can be used in MOSFETs implemented in a wide variety of dopant concentrations and body dimensions. The present disclosed method and apparatus therefore is not limited for use in MOSFETs implemented using the exemplary dopant concentrations and body dimensions as set forth above.

According to one aspect of the present disclosure, accumulated charge within a FET body is reduced using control methodologies and associated circuitry. In one embodiment all of the accumulated charge is removed from the FET body. In other embodiments, the accumulated charge is reduced or otherwise controlled. In one embodiment, holes are removed from the FET body, whereas in another embodiment, electrons are removed from the FET body, as described below in more detail. By removing holes (or electrons) from the FET body using the novel and nonobvious teachings of the present disclosure, voltage induced variations in the parasitic capacitances of the off-state FETs are reduced or eliminated, thereby reducing or eliminating nonlinear behavior of the off-state FETs. In addition, as described above with reference to FIG. **2**A, because the body impedance is greatly increased when the accumulated

charge is reduced or controlled, there is a beneficial overall reduction in the magnitude of the FET off-state capacitances. Also, as described above, removing or otherwise controlling the accumulated charge in floating body MOSFETs improves the BVDSS characteristics of the FET and thereby improves the linearity of the floating body MOSFET.

Accumulated charge control not only facilitates a beneficial overall reduction in the FET off-state capacitance C_{off} (as described above with reference to FIG. **2**A and below with reference to FIG. **4**H), it also facilitates a reduction in C_{off} variations that can occur over time in the presence of a time varying V_{ds} bias voltage. Thus, a reduction of undesirable harmonics generation and intermodulation distortion in RF switch circuits is obtained using SOI MOSFETs made in accordance with the present disclosure. Improved SOI MOSFET power handling, linearity, and performance are achieved by devices made in accordance with the present teachings. While the methods and apparatuses of the present disclosure are capable of fully removing accumulated charge from the FET bodies, those skilled in the electronic device design arts shall appreciate that any reduction of accumulated charge is beneficial.

Reductions in harmonics and intermodulation distortion are generally beneficial in any semiconductor system, either bulk semiconductor or semiconductor-on-insulator (SOI) systems. SOI systems include any semiconductor architecture employing semiconductor-containing regions positioned above an underlying insulating substrate. While any suitable insulating substrate can be used in a SOI system, exemplary insulating substrates include silicon dioxide (e.g., a buried oxide layer supported by a silicon substrate, such as that known as Separation by Implantation of Oxygen (SIMOX)), bonded wafer (thick oxide), glass, and sapphire. As noted above, in addition to the commonly used silicon-based systems, some embodiments of the present disclosure may be implemented using silicon-germanium (SiGe), wherein the SiGe is used equivalently in place of Si.

A wide variety of ACS implementations and structures can be used to practice the present disclosed method and apparatus. In accordance with one embodiment of the present method and apparatus, an ACS is used to remove or otherwise control accumulated charge (referenced as **120** in FIG. **1** described above) from the MOSFETs when the MOSFETs are configured to operate in the accumulated charge regime. By adapting the SOI (or SOS) MOSFETs in accordance with the present teachings, improved Accumulated Charge Control (ACC) MOSFETs are realized. The ACC MOSFETs are useful in improving performance of many circuits, including RF switching circuits. Various characteristics and possible configurations of the exemplary ACC MOSFETs are described in detail below with reference to FIGS. **3**A-**3**K. This section also describes how the exemplary ACS implementations of the present disclosure differ from the body contacts of the prior art.

The ACC MOSFET is shown schematically embodied as a four-terminal device in FIG. **4**A. FIGS. **4**B-**4**G show various exemplary simple circuit configurations that can be used in removing the accumulated charge from the ACC MOSFET when it operates in an accumulated charge regime. The operation of the simplified circuit configurations is described in more detail below with reference to FIGS. **4**A-**4**G. The improvement in off-state capacitance C_{off} of the ACC MOSFETs, as compared with the off-state capacitance of the prior art SOI MOSFETs, is described below with reference to FIG. **4**H.

The operation of various exemplary RF switch circuits implemented using the ACC MOSFETs of the present disclosure is described below with reference to the circuit schematics of FIGS. **5**B-**5**D. Further, an exemplary RF switch circuit using stacked ACC MOSFETs (for increased power handling) of the present disclosure is described below with reference to FIG. **6**. An exemplary method of improving the linearity of an SOI MOSFET using an accumulated charge sink (ACS) is described with reference to FIG. **7**. Finally, exemplary fabrication methods that may be used to manufacture the ACC MOSFET are described. The various exemplary ACS implementations and structures that can be used to practice the disclosed method and apparatus are now described with reference to FIGS. **3**A-**3**K.

Controlling Accumulated Charge Using an Accumulated Charge Sink (ACS)

FIGS. **3**A and **3**B are simplified schematic diagrams of a top view of an Accumulated Charge Control (ACC) SOI NMOSFET **300** adapted to control accumulated charge **120** (FIG. **1**) in accordance with the present disclosure. In the exemplary embodiment, a gate contact **301** is coupled to a first end of a gate **302**. A gate oxide (not shown in FIG. **3**A but shown in FIG. **1**) and a body **312** (shown in FIG. **3**B) are positioned under the gate **302**. In the exemplary NMOSFET **300** shown, a source **304** and a drain **306** comprise N+ regions. In the exemplary embodiment, the ACC NMOSFET **300** includes an accumulated charge sink (ACS) **308** comprising a P− region. The ACS **308** is coupled to and is in electrical communication with the body **312** which also comprises a P− region. An electrical contact region **310** provides electrical connection to the ACS **308**. In some embodiments, the electrical contact region **310** comprises a P+ region. As shown in FIG. **3**A, the electrical contact region **310** is coupled to and is in electrical communication with the ACS **308**.

Those skilled in the arts of electronic devices shall understand that the electrical contact region **310** may be used to facilitate electrical coupling to the ACS **308** because in some embodiments it may be difficult to make a direct contact to a lightly doped region. In addition, in some embodiments the ACS **308** and the electrical contact region **310** may be coextensive. In another embodiment, the electrical contact region **310** comprises an N+ region. In this embodiment, the electrical contact region **310** functions as a diode connection to the ACS **308**, which prevents positive current flow into the ACS **308** (and also prevents positive current flow into the body **312**) under particular bias conditions, as described below in more detail.

FIG. **3**B is an alternative top view of the ACC SOI NMOSFET **300** of FIG. **3**A, illustrating the ACC NMOSFET **300** without its gate contact **301**, gate **302**, and gate oxide being visible. This view allows the body **312** to be visible. FIG. **3**B shows the coupling of the ACS **308** to one end of the body **312**. In one embodiment, the body **312** and the ACS **308** comprise a combined P− region that may be produced by a single ion-implantation step. In another embodiment, the body **312** and ACS **308** comprise separate P− regions that are coupled together.

As is well known to those skilled in the electronic device design arts, in other embodiments, the ACC NMOSFET **300** of FIGS. **3**A and **3**B can be implemented as an ACC PMOSFET simply by reversing the dopant materials used to implement the various FET component regions (i.e., replace p-type dopant material with n-type dopant material, and vice versa). More specifically, in an ACC PMOSFET, the source and drain comprise P+ regions, and the body comprises an N− region. In this embodiment, the ACS **308** also comprises an N− region. In some embodiments of the ACC PMOSFET, the electrical contact region **310** may comprise an N+

region. In other embodiments of the ACC PMOSFETs, the region **310** comprises a P+ region, which functions as a diode connection to the ACS **308** and thereby prevents current flow into the ACS **308** under particular bias conditions.

Prior Art Body Contacts Distinguished from the Disclosed ACS

According to the present disclosure, the ACS **308** used to implement ACC SOI MOSFETs includes novel features in structure, function, operation and design that distinguish it from the so-called "body contacts" (also sometimes referred to as "body ties", usually when the "body contact" is directly connected to the source) that are well known in the prior art.

Exemplary references relating to body contacts used in prior art SOI MOSFETs include the following: (1) F. Hameau and O. Rozeau, Radio-Frequency Circuits Integration Using CMOS SOI 0.25 μm Technology," 2002 RF IC Design Workshop Europe, 19-22 Mar. 2002, Grenoble, France; (2) J. R. Cricci et al., "Silicon on Sapphire MOS Transistor," U.S. Pat. No. 4,053,916, Oct. 11, 1977; (3) O. Rozeau et al., "SOI Technologies Overview for Low-Power Low-Voltage Radio-Frequency Applications," Analog Integrated Circuits and Signal Processing, 25, pp. 93-114, Boston, Mass., Kluwer Academic Publishers, November 2000; (4) C. Tinella et al., "A High-Performance CMOS-SOI Antenna Switch for the 2.5-5-GHz Band, "IEEE Journal of Solid-State Circuits, Vol. 38, No. 7, July, 2003; (5) H. Lee et al., "Analysis of body bias effect with PD-SOI for analog and RF applications," Solid State Electron., Vol. 46, pp. 1169-1176, 2002; (6) J.-H. Lee, et al., "Effect of Body Structure on Analog Performance of SOI NMOSFETs," Proceedings, 1998 IEEE International SOI Conference, 5-8 Oct. 1998, pp. 61-62; (7) C. F. Edwards, et al., The Effect of Body Contact Series Resistance on SOI CMOS Amplifier Stages," IEEE Transactions on Electron Devices, Vol. 44, No. 12, December 1997 pp. 2290-2294; (8) S. Maeda, et al., Substrate-bias Effect and Source-drain Breakdown Characteristics in Body-tied Short-channel SOI MOSFET' s," IEEE Transactions on Electron Devices, Vol. 46, No. 1, January 1999 pp. 151-158; (9) F. Assaderaghi, et al., "Dynamic Threshold-voltage MOSFET (DTMOS) for Ultra-low Voltage VLSI," IEEE Transactions on Electron Devices, Vol. 44, No. 3, March 1997, pp. 414-422; (10) G. O. Workman and J. G. Fossum, "A Comparative Analysis of the Dynamic Behavior of BTG/SOI MOSFETs and Circuits with Distributed Body Resistance," IEEE Transactions on Electron Devices, Vol. 45, No. 10, October 1998 pp. 2138-2145; and (11) T.-S. Chao, et al., "High-voltage and High-temperature Applications of DTMOS with Reverse Schottky Barrier on Substrate Contacts," IEEE Electron Device Letters, Vol. 25, No. 2, February 2004, pp. 86-88.

As described herein, applications such as RF switch circuits, may use SOI MOSFETs operated with off-state bias voltages, for which accumulated charge may result. The SOI MOSFETs are defined herein as operating within the accumulated charge regime when the MOSFETs are biased in the off-state, and when carriers having opposite polarity to the channel carriers are present in the channel regions of the MOSFETs. In some embodiments, the SOI MOSFETs may operate within the accumulated charge regime when the MOSFETs are partially depleted yet still biased to operate in the off-state. Significant benefits in improving nonlinear effects on source-drain capacitance can be realized by removing or otherwise controlling the accumulated charge according to the present teachings. In contrast to the disclosed techniques, none of the cited prior art teach or suggest ACS methods and apparatuses that are uniquely useful for removing or controlling accumulated charge. Nor are they informed regarding problems caused by the accumulated charge such as nonlinear effects on the off-state source-drain capacitance C_{off}. Consequently, the prior art body contacts described in the references cited above differ greatly (in structure, function, operation and design) from the ACSs described with reference to FIGS. **3**A-**4**D.

In one example, the ACS **308** operates effectively to remove or otherwise control the accumulated charge from the SOI NMOSFET **300** using a high impedance connection to and throughout the body **312**. High impedance ACSs may be used because the accumulated charge **120** is primarily generated by phenomena (e.g., thermal generation) that take a relatively long period of time to produce significant accumulated charge. For example, a typical time period for producing non-negligible accumulated charge when the NMOSFET operates in the accumulated charge regime is approximately a few milliseconds or greater. Such relatively slow generation of accumulated charge corresponds to very low currents, typically less than 100 nA/mm of transistor width. Such low currents can be effectively conveyed even using very high impedance connections to the body. According to one example, the ACS **308** is implemented with a connection having a resistance of greater than 10^6 ohms. Consequently, the ACS **308** is capable of effectively removing or otherwise controlling the accumulated charge **120** even when implemented with a relatively high impedance connection, relative to the low impedance prior art body contacts.

In stark contrast, the prior art teachings of body contacts described in the references cited above require low impedance (high efficiency) access to the body regions of SOI MOSFETs for proper operation (see, e.g., references (3), (6), and (7) above). A principal reason for this requirement is that the prior art body contacts are primarily directed to reducing the adverse effects on SOI MOSFET functions caused by much faster and more effective electron-hole pair generation processes than occur when the FET is operated in the accumulated charge regime. For example, in some prior art MOSFETs not operated in the accumulated charge regime, electron-hole pair carriers are generated as a result of impact ionization. Impact ionization produces electron-hole pairs at a much faster rate than occurs when the FET is operated in the accumulated charge regime.

The relative rates for electron-hole pair generation by impact ionization versus the pair generation processes causing accumulated charge can be estimated from the roll-off frequencies for the two phenomena. For example, reference (3) cited above indicates roll-off frequencies for impact ionization effects in the range of 10^5 Hz. In contrast, a roll-off frequency for the accumulated charge effects has been observed to be in the range of 10^3 Hz or less, as indicated by recovery times for odd harmonics. These observations indicate that the ACS **308** can effectively control accumulated charge using an impedance that is at least 100 times larger than required of prior art body contacts used in controlling impact ionization charge, for example. Further, because impact ionization primarily occurs when the SOI MOSFET operates in an on-state, the effects of impact ionization can be amplified by on-state transistor operation. Low impedance body contacts to and throughout a body region is even more critical in these environments in order to control the effects of impact ionization under the on-state conditions.

In stark contrast, the ACS **308** of the present teachings removes or otherwise controls the accumulated charge only when the ACC SOI MOSFET operates in the accumulated

charge regime. By definition, the FET is in the off-state in this regime, so there is no requirement to remove impact ionization as amplified by an on-state FET. Therefore, a high impedance ACS **308** is perfectly adequate for removing the accumulated charge under these operating conditions. The prior art requirements for low impedance body connections results in numerous problems of implementation that are overcome by the present teachings, as described below in more detail.

In addition, the ACS **308** may be implemented with much lower source-to-drain parasitic capacitance as compared to the body contacts of the prior art. The above-described low impedance connection to the SOI MOSFET body required of the prior art body contacts necessitates proximity of the contacts to the entire body. This may require a plurality body contact "fingers" that contact the body at different locations along the body. The low impedance connection to the body also necessitates proximity of the prior art body contacts to the source and drain. Because of parasitic capacitances produced by such body contacts, the cited prior art references teach away from the use of such structures for many high frequency applications such as RF. In stark contrast, the ACS **308** of the present disclosure may be positioned a selected distance away from the source **304** and the drain **306**, and the ACS **308** may also be coupled to the body **312** at a first distal end of the body **312** (shown in FIGS. **3**A and **3**B). Arranged in this manner, the ACS **308** makes minimal contact (as compared to the prior art body contacts that may contact the body at many locations along the body) with the body **312**. This configuration of the ACS **308** with the MOSFET eliminates or greatly reduces the parasitic capacitances caused by a more proximate positioning of the ACS **308** relative to the source, drain, and body. Further, the ACS **308** may be implemented in SOI MOSFETs operated with a depleted channel. In general, the cited prior art references teach away from the use of body contacts for this environment (see, e.g., reference (3), cited above).

Further, because impact ionization hole currents are much larger (in the range of 5,000 nA per mm body width) than for accumulated charge generation (less than approximately 100 nA per mm body width), the prior art does not teach how to effectively implement very large body widths (i.e., much greater than approximately 10 μm). In contrast, the ACS **308** of the present disclosed device may be implemented in SOI MOSFETs having relatively large body widths. This provides improvements in on-state conductance and transconductance, insertion loss and fabrication costs, particularly for RF switch devices. According to the prior art teachings cited above, larger body widths adversely affect the efficient operation of body contacts because their impedances are necessarily thereby increased. Although the cited prior art suggests that a plurality of fingers may be used to contact the body at different locations, the plurality of fingers adversely affects parasitic source-to-drain capacitances, as described above.

For these reasons, and for the reasons described below in more detail, the present disclosure provides novel MOSFET devices, circuits and methods that overcome the limitations according to the prior art teachings as cited above.

FIG. **3**C is a cross-sectional perspective schematic of an ACC SOI NMOSFET **300'** adapted to control accumulated charge in accordance with the disclosed method and apparatus. In the example shown in FIG. **3**C, the ACC NMOSFET **300'** includes four terminals that provide electrical connection to the various FET component regions. In one embodiment, the terminals provide means for connecting external integrated circuit (IC) elements (such as metal leads, not shown) to the various FET component regions. Three of the terminals shown in FIG. **3**C are typically available in prior art FET devices. For example, as shown in FIG. **3**C, the ACC NMOSFET **300'** includes a gate terminal **302'** that provides electrical connection to the gate **302**. Similarly, the ACC NMOSFET **300'** includes source and drain terminals **304'**, **306'** that provide electrical connection to the source **304** and drain **306**, respectively. As is well known in the electronic design arts, the terminals are coupled to their respective FET component regions (i.e., gate, drain and source) via so-called "ohmic" (i.e., low resistance) contact regions. The manufacturing and structural details associated with the coupling of the various FET terminals to the FET component regions are well known in the art, and therefore are not described in more detail here.

As described above with reference to FIGS. **3**A and **3**B, the ACC NMOSFET **300'** is adapted to control accumulated charge when the NMOSFET operates in the accumulated charge regime. To this end, in the exemplary embodiment shown in FIG. **3**C, the ACC NMOSFET **300'** includes a fourth terminal that provides electrical connection to the body **312**, and thereby facilitates reduction (or other control) of the accumulated charge when the FET **300'** operates in the accumulated charge regime. More specifically, and referring again to FIG. **3**C, the ACC NMOSFET includes a "body" terminal, or Accumulated Charge Sink (ACS) terminal **308'**. The ACS terminal **308'** provides an electrical connection to the ACS **308** (not shown in FIG. **3**C, but shown in FIGS. **3**A and **3**B) and to the body **312**. Although the ACS terminal **308'** is shown in FIG. **3**C as being physically coupled to the body **312**, those skilled in the electronic design arts shall understand that this depiction is for illustrative purposes only. The direct coupling of the ACS terminal **308'** to the body **312** shown in FIG. **3**C illustrates the electrical connectivity (i.e., not the physical coupling) of the terminal **308'** with the body **312**. Similarly, the other terminals (i.e., terminals **302'**, **304'** and **306'**) are also shown in FIG. **3**C as being physically coupled to their respective FET component regions. These depictions are also for illustrative purposes only.

In most embodiments, as described above with reference to FIGS. **3**A-**3**B, and described further below with reference to FIGS. **3**D-**3**K, the ACS terminal **308'** provides the electrical connection to the body **312** via coupling to the ACS **308** via the electrical contact region **310**. However, the present disclosure also contemplates embodiments where the coupling of the ACS terminal **308'** is made directly to the body **312** (i.e., no intermediate regions exist between the ACS terminal **308'** and the body **312**).

In accordance with the disclosed method and apparatus, when the ACC NMOSFET **300'** is biased to operate in the accumulated charge regime (i.e., when the ACC NMOSFET **300'** is in the off-state, and there is an accumulated charge **120** of P polarity (i.e., holes) present in the channel region of the body **312**), the accumulated charge is removed or otherwise controlled via the ACS terminal **308'**. When accumulated charge **120** is present in the body **312**, the charge **312** can be removed or otherwise controlled by applying a bias voltage (V_b (for "body") or V_{ACS} (ACS bias voltage)) to the ACS terminal **308'**. In general, the ACS bias voltage V_{ACS} applied to the ACS terminal **308'** may be selected to be equal to or more negative than the lesser of the source bias voltage Vs and drain bias voltage Vd. More specifically, in some embodiments, the ACS terminal **308'** can be coupled to various accumulated charge sinking mechanisms that remove (or "sink") the accumulated charge when the FET operates in the accumulated charge regime.

Several exemplary accumulated charge sinking mechanisms and circuit configurations are described below with reference to FIGS. **4**A-**5**D.

Similar to the prior art NMOSFET **100** described above with reference to FIG. **1**, the ACC SOI NMOSFET **300'** of FIG. **3**C can be biased to operate in the accumulated charge regime by applying specific bias voltages to the various terminals **302'**, **304'**, and **306'**. In one exemplary embodiment, the source and drain bias voltages (Vs and Vd, respectively) are zero (i.e., the terminals **304'** and **306'** are connected to ground). In this example, if the gate bias voltage (Vg) applied to the gate terminal **302'** is sufficiently negative with respect to the source and drain bias voltages, and with respect to V_{th} (for example, if V_{th} is approximately zero, and if Vg is more negative than approximately −1 V), the ACC NMOSFET **300'** operates in the off-state. If the ACC NMOSFET **300'** continues to be biased in the off-state, the accumulated charge (holes) will accumulate in the body **312**. Advantageously, the accumulated charge can be removed from the body **312** via the ACS terminal **308'**. In some embodiments, as described below in more detail with reference to FIG. **4**B, the ACS terminal **308'** is coupled to the gate terminal **302'** (thereby ensuring that the same bias voltages are applied to both the gate (Vg) and the body (shown in FIG. **3**C as "Vb" or "V_{ACS}").

However, those skilled in the electronics design arts shall appreciate that a myriad of bias voltages can be applied to the four device terminals while still employing the techniques of the present disclosed method and apparatus. As long as the ACC SOI NMOSFET **300'** is biased to operate in the accumulated charge regime, the accumulated charge can be removed or otherwise controlled by applying a bias voltage V_{ACS} to the ACS terminal **308'**, and thereby remove the accumulated charge from the body **312**.

For example, in one embodiment wherein the ACC NMOSFET **300'** comprises a depletion mode device, V_{th} is negative by definition. In this embodiment if both the Vs and Vd bias voltages comprise zero volts (i.e., both terminals tied to circuit ground node), and a gate bias Vg applied to the gate terminal **302'** is sufficiently negative to V_{th} (for example, Vg is more negative than approximately −1 V relative to V_{th}), holes may accumulate under the gate oxide **110** thereby becoming the accumulated charge **120**. In this example, in order to remove the accumulated holes (i.e., the accumulated charge **120**) from the FET body **312**, the voltage V_{ACS} applied to the ACS **308** may be selected to be equal to or more negative than the lesser of Vs and Vd.

In other examples, the source and drain bias voltages, Vs and Vd, respectively, may comprise voltage other than zero volts. According to these embodiments, the gate bias voltage Vg must be sufficiently negative to both Vs and Vd (in order for Vg to be sufficiently negative to V_{th}, for example) in order to bias the NMOSFET in the off-state. As described above, if the NMOSFET is biased in the off-state for a sufficiently long time period (approximately 1-2 ms, for example) an accumulated charge will accumulate under the gate oxide. In these embodiments, as noted above, in order to remove the accumulated charge **120** from the body **312**, the ACS bias voltage V_{ACS} applied to the ACS terminal **308'** may be selected to be equal to or more negative than the lesser of Vs and Vd.

It should be noted that, in contrast to the examples described above, the prior art body contacts are implemented largely for purposes of mitigating the adverse effects caused by impact ionization. Consequently, the prior art body contacts are typically tied to the source of the MOSFET. In order to effectively control, reduce, or entirely remove the accumulated charge in an NMOSFET, V_{ACS} should, in the exemplary embodiments, be equal to or more negative than the lesser of Vs and Vd. Those skilled in the electronic device design arts shall appreciate that different Vs, Vd, Vg and V_{ACS} bias voltages may be used when the ACC MOSFET comprises a PMOSFET device. Because the prior art body contacts are typically tied to the source, this implementation cannot be effected using the prior art body contact approach.

FIG. **3**D is a simplified schematic diagram of a top view of an ACC SOI NMOSFET **300"** adapted to control accumulated charge **120** (FIG. **1**) in accordance with the present disclosure. FIG. **3**D shows the ACC NMOSFET **300"** without its gate contact **301**, gate **302**, and gate oxide being visible. The ACC NMOSFET **300"** of FIG. **3**D is very similar in design to the ACC NMOSFET **300** described above with reference to FIGS. **3**A and **3**B. For example, similar to the ACC NMOSFET **300**, the ACC NMOSFET **300"** includes a source **304** and drain **306** comprising N+ regions. The ACC NMOSFET **300"** also includes an accumulated charge sink (ACS) **308** comprising a P− region. As shown in FIG. **3**D, the P− region that comprises the ACS **308** abuts (i.e., is directly adjacent) the body **312**, which also comprises a P− region. Similar to the ACC NMOSFET **300**, the ACC NMOSFET **300"** includes an electrical contact region **310** that provides electrical connection to the ACS **308**. As noted above, in some embodiments, the electrical contact region **310** comprises a P+ region. In another embodiment, the electrical contact region **310** may comprise an N+ region (which thereby prevents positive current flow into the body **312** as noted above). As shown in FIG. **3**D, the electrical contact region **310** is formed in the ACC NMOSFET **300"** directly adjacent the ACS **308**. The ACC SOI NMOSFET **300"** functions to control accumulated charge similarly to the operation of the ACC NMOSFETs described above with reference to FIGS. **3**A-**3**C.

FIG. **3**E is a simplified schematic diagram of a top view of an ACC SOI NMOSFET **300'"** adapted to control accumulated charge in accordance with the present disclosure. The ACC NMOSFET **300'"** is very similar in design and function to the ACC NMOSFETs described above with reference to FIGS. **3**A-**3**D. FIG. **3**E shows a dashed cross-sectional view line A-A' taken along the approximate center of the NMOSFET **300"**. This cross-sectional view is used herein to describe structural and performance characteristics of some exemplary prior art MOSFETS and some embodiments of the ACC NMOSFET that may occur as a result of the fabrication processes. Details of this cross-sectional view A-A' are now described with reference to FIG. **3**F.

View line A-A' slices through the following component regions of the ACC NMOSFET **300'"**: the P+ electrical contact region **310**, the ACS **308** (shown in FIG. **3**E, but not shown in FIG. **3**F), a P+ overlap region **310'**, a gate oxide **110**, and a poly-silicon gate **302**. In some embodiments, during the fabrication process, when the region **310** is doped with p-type dopant material, proximate the P− body region, some additional P+ doping may be implanted (i.e., the p-type dopant material may overlap) into the P+ overlap region **310'** of the poly-silicon gate **302**. In some embodiments, such overlapping is performed intentionally to ensure that all of the gate oxide **110** is completely covered by the P+ region (i.e., to ensure that no gap exists on the edge of the oxide **110** between the gate **302** and the P+ region **310**). This, in turn, aids in providing a minimum impedance connection between the P+ region **310** and the body **312**.

Although the present teachings encompass such embodiments described above, those skilled in the electronic device

design and manufacturing arts shall recognize that such low-resistance connections are not required. Therefore, disadvantages associated with the embodiment shown in FIG. **3**H, as described below in more detail, can be overcome by using other embodiments described herein (for example, the embodiments **300** and **300""** described below with reference to FIGS. **3**G and **3**J, respectively), in which gaps are intentionally implemented between the P+ region **310** and the body **312**. In one exemplary embodiment, the P+ overlap region **310'** overlaps the oxide **110** by approximately 0.2-0.7 microns. Those skilled in the MOSFET design and manufacturing arts shall appreciate that other overlap region dimensions can be used in practicing the present disclosed method and apparatus. In some embodiments, as shown in FIG. **3**F, for example, the remaining area over the gate oxide **110** and over the P− body is doped with n-type dopant material (i.e., it comprises an N+ region).

Referring again to FIG. **3**F, owing to the presence of the P+ overlap region **310'** over the gate oxide **110**, over the body **312**, and proximate an edge **340** of the poly-silicon gate **302**, an increased threshold voltage region is created in the NMOSFET **300'"**. More specifically, due to the P+ doping (in the P+ overlap region **310'**) proximate the edge **340** of the gate **302** over the channel region of the body **312**, a region of increased threshold voltage is formed in that region of the MOSFET **300'"**. The effects of the region of increased threshold voltage are now described in more detail with reference to FIGS. **3**H and **3**I.

FIG. **3**I shows a plot **380** of inversion channel charge versus applied gate voltage for an ACC NMOSFET. The plot **380** shown in FIG. **3**I illustrates one effect of the above-described increased threshold voltage that can occur in prior art MOSFETs, and in some embodiments of the present ACC NMOSFETs due to certain manufacturing processes. As described in more detail below, the increased threshold voltage region, shown in FIG. **3**H and described in more detail below, also occurs in prior art MOSFET designs due to the proximity of body ties to the FET body. As described below in more detail with reference to FIG. **3**J, for example, the present disclosed method and apparatus can be used to reduce or eliminate the region of increased threshold voltage found in some prior art SOI MOSFET designs.

FIG. **3**H shows one embodiment of an ACC NMOSFET without its gate contact, gate, and gate oxide being visible. The MOSFET region of increased threshold voltage described above with reference to FIGS. **3**E and **3**F is shown in FIG. **3**H as occurring in the region encompassed by the ellipse **307**. As will be well understood by those skilled in the electronic design and manufacturing arts, for the reasons set forth above with reference to FIGS. **3**E and **3**F, due to the increased threshold voltage, the region **307** of the ACC MOSFET shown in FIG. **3**H effectively "turns on" after the rest of the ACC MOSFET channel region.

The increased threshold voltage can be reduced by reducing the size of the region **307**. Eliminating the region **307** altogether eliminates the threshold voltage increase. Because the threshold voltage increase can increase harmonic and intermodulation distortion of the "on" state MOSFET, eliminating this effect improves MOSFET performance. The increased threshold voltage also has the detrimental effect of increasing the MOSFET on-resistance (i.e., the resistance presented by the MOSFET when it is in the on-state (conducting state), which detrimentally impacts the MOSFET insertion loss.

In one exemplary embodiment, as shown, for example in the embodiments of the ACC NMOSFET **300** described above with reference to FIGS. **3**A and **3**B, and as described below in more detail with reference to the cross-sectional view of the ACC MOSFET **300** of FIG. **3**G, the detrimental effects associated with threshold voltage increase are mitigated or overcome by positioning the P+ region **310** a selected distance away from an edge of the poly-silicon gate **302**. This approach is shown both in the top view of the ACC MOSFET **300** of FIG. **3**A, and in the cross-sectional view of the ACC MOSFET **300** shown in FIG. **3**G. As shown in the cross-sectional view of the ACC MOSFET **300** of FIG. **3**G, the P+ region **310** does not extend all the way to the edge **340** of the poly-silicon gate **302**. This is in stark contrast to the embodiment **300'"** shown in FIG. **3**F, where the P+ region **310'** extends all the way to the gate edge **340**. By positioning the P+ region **310** a distance away from the gate edge **340** as shown in the embodiment **300** of FIG. **3**G, no P+ region is positioned proximate the poly-silicon gate **302** (i.e., there is no P+ region present in the poly-silicon gate **302**).

This configuration of the P+ region **310** eliminates or greatly reduces the problems associated with threshold voltage increase as described above. As described above with reference to FIGS. **3**A and **3**B, and with reference to the comparisons to the prior art body contact references, the relatively high impedance of the ACS **308** P− region (shown in FIG. **3**A) between the P+ region **310** and the gate **302** does not adversely affect the performance of the ACC NMOSFET **300**. As described above, the accumulated charge can be effectively removed even using a relatively high impedance ACS connection.

In another exemplary embodiment, as described below with reference to FIG. **3**J, the threshold voltage increase is removed by positioning the P+ region **310** (and the ACS **308**) a distance away from the body **312**. Because the electrical connectivity between the ACS **308** and the body **312** has relatively high impedance when the small region of P+ **310** is positioned a distance away from the body **312**, this approach is never taught or suggested by the body contact prior art references (which require low impedance contacts as described above). This improved embodiment is described next with reference to FIG. **3**J.

FIG. **3**J is a simplified top view schematic of another embodiment of an ACC SOI NMOSFET **300""** adapted to control accumulated charge and configured in a "T-gate" configuration. FIG. **3**J shows the ACC NMOSFET **300""** without its gate contact **301**, gate **302**, and gate oxide being visible. The gate (not shown in FIG. **3**J) and the body **312** are configured as "supporting" members of the "T-gate" configured ACC MOSFET **300""** (i.e., they comprise the "bottom" portion of the "T-shaped" FET). These "supporting" members "support" the "supported" member of the T-gate configured MOSFET **300"**, which comprises the ACS **308** as shown in FIG. **3**J (i.e., the ACS **308** comprises the "top" portion of the "T-shaped" FET). As shown in FIG. **3**J, the ACC NMOSFET **300""** includes a small P+ region **310** conjoined to an ACS **308**. As shown in FIG. **3**J, the P+ region **310** (and thus the ACS external electrical connection) is disposed a selected distance away from the body **312**. The total impedance of the electrical connection from the body **312**, through the ACS **308**, and to the P+ region **310** is increased by positioning the P+ region **310** a selected distance away from the body **312**. However, as described above, the present ACC NMOSFET **300""** works perfectly well to remove accumulated charge even using relatively high impedance ACS connections. For the reasons described above with reference to FIGS. **3**A and **3**B, due to the nature of the accumulated charge when the NMOSFET **300""** operates in the accumulated charge regime, the ACC

NMOSFET **300""** does not require low impedance ACS electrical connections in order to remove accumulated charge from the body **312**. Rather, an ACS connection of relatively large impedance may be used in practicing the present teachings, with corresponding improvements in NMOSFET performance as described above (e.g., reductions in parasitic capacitance as compared with prior art low impedance body contacts). However, in other embodiments, if desired, a low impedance ACS connection may be used to practice the disclosed method and apparatus for use in improving linearity characteristics of SOI MOSFETs.

Moreover, as described above with reference to FIG. **3**H, the embodiment of FIG. **3**J improves device performance owing to the fact that the small P+ region **310** is positioned a distance away from the body **312**. Because the small P+ region **310** is positioned a distance away from the body **312**, the threshold voltage increase is reduced or entirely eliminated, together with the consequent adverse performance effects described above.

FIG. **3**K is a simplified top view schematic of another embodiment of an ACC SOI NMOSFET **300"""** adapted to control accumulated charge and configured in an "H-gate" configuration. FIG. **3**K shows the ACC NMOSFET **300"""** without its gate contact **301**, gate **302**, and gate oxide being visible. With the exception of some structural differences described herein, the ACC NMOSFET **300"""** is very similar in design and function to the ACC NMOSFETs described above with reference to FIGS. **3**A-**3**D and **3**J. As shown in FIG. **3**K, the ACC NMOSFET **300"""** includes two ACSs, **308** and **308"**, disposed at opposite ends of the H-gate ACC NMOSFET **300"""**. P+ regions **310** and **310"** are formed to abut their respective ACSs, **308** and **308"**, and provide electrical contact thereto. In accordance with the disclosed method and apparatus, as described above, when the ACC NMOSFET **300"""** is biased to operate in the accumulated charge regime, the accumulated charge is removed or otherwise controlled via the two ACSs **308** and **308"**.

It shall be understood by those skilled in the electronic device design arts that although the illustrated embodiment shows the ACSs **308** and **308"** extending approximately the entire width of the ACC NMOSFET **300"""**, the ACSs **308** and **308"** may also comprise much narrower (or wider) regions, and still function perfectly well to remove or otherwise control the accumulated charge. Also, in some embodiments, it is not necessary that the impedance of the ACS **308** matches the impedance of the ACS **308"**. It will further be understood by the skilled person that the ACSs **308** and **308"** may comprise different sizes and configurations (i.e., rectangular, square, or any other convenient shape), and may also be positioned at various distances away from the body **312** (i.e., not necessarily the same distance away from the body **312**). As described above with reference to FIG. **3**J, when the ACS **308** is positioned a selected distance away from the body **312**, the problems associated with threshold voltage increase are reduced or eliminated.

Four-Terminal ACC MOSFET Devices—Simple Circuit Configurations

The SOI NMOSFET **300** of FIGS. **3**A and **3**B may be implemented as a four terminal device, as illustrated schematically in FIG. **4**A. As shown in the improved ACC SOI NMOSFET **300** of FIG. **4**A, a gate terminal **402** is electrically coupled to the gate contact **301** (e.g., FIG. **3**A) and is analogous to the gate terminal **302'** shown in FIG. **3**C. The gate contact **301** is electrically coupled to the gate **302** (e.g., FIGS. **3**A and **3**C). Similarly, a source terminal **404** is electrically coupled to the source **304** (e.g., FIGS. **3**A-**3**C) and is analogous to the source terminal **304'** of FIG. **3**C. Similarly, a drain terminal **406** is electrically coupled to the drain **306** (e.g., FIGS. **3**A-**3**C) and is analogous to the drain terminal **306'** of FIG. **3**C. Finally, the ACC NMOSFET **300** includes an ACS terminal **408** that is electrically coupled to the ACS **308** (e.g., see FIGS. **3**A-**3**B, and FIGS. **3**D, **3**J-**3**K) via the region **310**. Those skilled in the electronic design and manufacturing arts shall understand that the region **310** may be used in some embodiments to facilitate electrical coupling to the ACS **308** because, in some embodiments, it may be difficult to make a direct contact to a lightly doped region (i.e., the ACS **308**). The ACS terminal **408** is analogous to the ACS terminal **308'** shown in FIG. **3**C.

The ACC SOI NMOSFET **300** of FIG. **4**A may be operated using various techniques and implemented in various circuits in order to control accumulated charge present in the FET when it is operating in an accumulated charge regime. For example, in one exemplary embodiment as shown in FIG. **4**B, the gate and ACS terminals, **402** and **408**, respectively, are electrically coupled together. In one embodiment of the simplified circuit shown in FIG. **4**B, the source and drain bias voltages applied to the terminals **404** and **406**, respectively, may be zero. If the gate bias voltage (Vg) applied to the gate terminal **402** is sufficiently negative with respect to the source and drain bias voltages applied to the terminals **404** and **406**, and with respect to the threshold voltage V_{th}, (for example, if V_{th} is approximately zero, and if Vg is more negative than approximately −1 V) the ACC NMOSFET **300** operates in the accumulated charge regime. As described above with reference to FIG. **3**C, for example, when the MOSFET operates in this regime, accumulated charge (holes) may accumulate in the body of the NMOSFET **300**.

Advantageously, the accumulated charge can be removed via the ACS terminal **408** by connecting the ACS terminal **408** to the gate terminal **402** as shown. This configuration ensures that when the FET **300** is in the off-state, it is held in the correct bias region to effectively remove or otherwise control the accumulated charge. As shown in FIG. **4**B, connecting the ACS terminal **408** to the gate ensures that the same bias voltages are applied to both the gate (Vg) and the body (shown in FIG. **3**C as "Vb" or "V_{ACS}"). Because the bias voltage V_{ACS} is the same as the gate voltage Vg in this embodiment, the accumulated charge is no longer trapped below the gate oxide (by attraction to the gate bias Vg) because it is conveyed to the gate terminal **402** via the ACS terminal **408**. The accumulated charge is thereby removed from the body via the ACS terminal **408**.

In other exemplary embodiments, as described above with reference to FIG. **3**C, for example, Vs and Vd may comprise nonzero bias voltages. According to these examples, Vg must be sufficiently negative to both Vs and Vd in order for Vg to be sufficiently negative to V_{th} to turn the NMOSFET **300** off (i.e., operate the NMOSFET **300** in the off-state). When so biased, as described above, the NMOSFET **300** may enter the accumulated charge regime and thereby have accumulated charge present in the body. For this example, the voltage V_{ACS} may also be selected to be equal to Vg by connecting the ACS terminal **408** to the gate terminal **402**, thereby conveying the accumulated charge from the body of the ACC NMOSFET, as described above.

In another exemplary embodiment, as described above, the ACC NMOSFET **300** comprises a depletion mode device. In this embodiment, the threshold voltage, V_{th} is, by definition, less than zero. For Vs and Vd both at zero volts, when a gate bias Vg sufficiently negative to V_{th} is applied to the gate terminal **402** (for example, Vg more negative than approximately −1 V relative to V_{th}), holes may accumulate

under the gate oxide and thereby comprise an accumulated charge. For this example, the voltage V_{ACS} may also be selected to be equal to Vg by connecting the ACS terminal **408** to the gate terminal **402**, thereby conveying the accumulated charge from the ACC NMOSFET as described above.

In some embodiments of the improved ACC SOI NMOSFET **300**, such as that described above with reference to FIG. **4**B, when the FET is biased on, diodes formed at the edge of the device (such as described above with reference to the interface between the ACS **308** and the drain **304** (and the source **306**) as shown in FIG. **3**D) may become forward biased thereby allowing current to flow into the source and drain regions. In addition to wasting power, this may introduce nonlinearity into the NMOSFET. The nonlinearity results because the current that flows as a result of the forward biased interface diodes comprises nonlinear current. As Vgs and Vgd are reduced in that region of the device, the on resistance Ron at the edge of the device is increased. As is well known, and for the reasons set forth above, if the interface diodes formed at the edge of the device become forward biased, the device on-state characteristics are consequently dramatically adversely affected. Those skilled in the electronic device design arts shall understand that the configuration shown in FIG. **4**B limits application of a gate bias voltage Vgs to approximately 0.7 Volts. The simplified circuit shown in FIG. **4**C can be used to overcome these problems.

Another exemplary simplified circuit using the improved ACC SOI NMOSFET **300** is shown in FIG. **4**C. As shown in FIG. **4**C, in this embodiment, the ACS terminal **408** may be electrically coupled to a diode **410**, and the diode **410** may, in turn, be coupled to the gate terminal **402**. This embodiment may be used to prevent a positive current flow into the MOSFET body **312** caused by a positive Vg-to-Vs (or, equivalently, Vgs, where Vgs=Vg−Vs) bias voltage, as may occur, for example, when the SOI NMOSFET **300** is biased into an on-state condition.

As with the device shown in FIG. **4**B, when biased off, the ACS terminal voltage V_{ACS} comprises the gate voltage plus a voltage drop across the diode **410**. At very low ACS terminal current levels, the voltage drop across the diode **410** typically also is very low (e.g., <<500 mV, for example, for a typical threshold diode). The voltage drop across the diode **410** can be reduced to approximately zero by using other diodes, such as a 0Vf diode, for example. In one embodiment, reducing the voltage drop across the diode is achieved by increasing the diode **410** width. Additionally, maintaining the ACS-to-source or ACS-to-drain voltage (whichever bias voltage of the two bias voltages is lower) increasingly negative, also improves the linearity of the ACC MOSFET device **300**.

When the SOI NMOSFET **300** is biased in an on condition, the diode **410** is reverse-biased, thereby preventing the flow of positive current into the source and drain regions. The reverse-biased configuration reduces power consumption and improves linearity of the device. The circuit shown in FIG. **4**C therefore works well to remove accumulated charge from the ACC MOSFET body when the FET is in the off-state and is operated in the accumulated charge regime. It also permits almost any positive voltage to be applied to the gate voltage Vg. This, in turn, allows the ACC MOSFET to effectively remove accumulated charge when the device operates in the off-state, yet assume the characteristics of a floating body device when the device operates in the on-state.

With the exception of the diode **410** used to prevent the flow of positive current into the ACS terminal **408**, exemplary operation of the simplified circuit shown in FIG. **4**C is the same as the operation of the circuit described above with reference to FIG. **4**B.

In yet another embodiment, the ACS terminal **408** may be coupled to a control circuit **412** as illustrated in the simplified circuit of FIG. **4**D. The control circuit **412** may provide a selectable ACS bias voltage V_{ACS} that selectively controls the accumulated charge (i.e., the accumulated charge **120** described above with reference to FIG. **1**). As shown in FIG. **4**D, rather than having a local circuit provide the ACS bias voltage V_{ACS} (e.g., as derived from the gate voltage Vg), in some embodiments the ACS bias voltage V_{ACS} is produced by a separate source that is independent of the ACC MOSFET device **300**. In the case of a switch (as described below in more detail with reference to FIG. **4**E), the ACS bias voltage V_{ACS} should be driven from a source having a high output impedance. For example, such a high output impedance source can be obtained using a large series resistor in order to ensure that the RF voltage is divided across the MOSFET and that the ACS bias voltage V_{ACS} has Vds/2 "riding" on it, similarly to the gate voltage. This approach is described in more detail below with reference to FIG. **4**E.

It may be desirable to provide a negative ACS bias voltage V_{ACS} to the ACS terminal **408** when the SOI NMOSFET **300** is biased into an accumulated charge regime. In this exemplary embodiment, the control circuit **412** may prevent positive current flow into the ACS terminal **408** by selectively maintaining an ACS bias voltage V_{ACS} that is consistently negative with respect to both the source and drain bias voltages. In particular, the control circuit **412** may be used to apply an ACS bias voltage that is equal to or more negative than the lesser of Vs and Vd. By application of such an ACS bias voltage, the accumulated charge is thereby removed or otherwise controlled.

In the exemplary embodiment of the simplified circuit shown in FIG. **4**D, the source and drain bias voltages applied to the terminals **404** and **406**, respectively, may be zero. If the gate bias voltage (Vg) applied to the gate terminal **402** is sufficiently negative with respect to the source and drain bias voltages applied to the terminals **404** and **406**, and with respect to V_{th}, (for example, if V_{th} is approximately zero, and if Vg is more negative than approximately −1 V) the ACC NMOSFET **300** operates in the accumulated charge regime, and the accumulated charge (holes) may accumulate in the body of the ACC NMOSFET **300**. Advantageously, the accumulated charge can be removed via the ACS terminal **408** by connecting the ACS terminal **408** to the control circuit **412** as shown. In order to ensure that the accumulated charge is conveyed from the body of the ACC NMOSFET **300**, the ACS bias voltage V_{ACS} that is applied to the ACS terminal **408** should be equal to or more negative than the gate voltage and more negative than the lesser of Vs and Vd. Because the accumulated charge **120** is conveyed to the bias voltage V_{ACS} applied to the ACS terminal **408** by the control circuit **412**, the accumulated charge does not remain trapped under the gate oxide due to attraction to the gate bias voltage Vg.

In other embodiments, Vs and Vd may comprise bias voltages that are other than zero. According to these examples, Vg must be sufficiently negative to both Vs and Vd in order for Vg to be sufficiently negative to V_{th}, in order to bias the NMOSFET **300** in the off-state. This allows the accumulation of accumulated charge under the gate oxide. For this example, the ACS bias voltage V_{ACS} may be selected to be equal to or more negative than the lesser of Vs

and Vd by connecting the ACS terminal **408** to the control circuit **412** to provide selected ACS bias voltages, thereby conveying the accumulated charge from the ACC NMOSFET **300**.

In other embodiments, if the ACC NMOSFET **300** of FIG. **4**D comprises a depletion mode device, V_{th} is, by definition, less than zero. For Vs and Vd both at zero volts, when a gate bias Vg sufficiently negative to V_{th} is applied (for example, Vg more negative than approximately −1 V relative to V_{th}), holes may accumulate under the gate oxide. For this example, the ACS bias voltage V_{ACS} that is applied to the ACS terminal **408** may also be selected to be equal to or more negative than the lesser of Vs and Vd by connecting the ACS terminal **408** to the control circuit **412** and thereby provide the desired ACS bias voltages V_{ACS} that are necessary to remove the accumulated charge from the ACC NMOSFET **300**.

As described above, in one embodiment, instead of having the control circuit **412** provide a bias to the ACS terminal **408** as shown in FIG. **4**D, the ACS terminal **408** can be driven by a separate bias source circuit, as shown, for example, in the embodiment of FIG. **4**E. In one exemplary circuit implementation, as exemplified in the circuit of FIG. **4**E, in an RF switch circuit, the separate V_{ACS} source has a high output impedance element **403** which ensures that the RF voltage is divided across the ACC NMOSFET **300**, and which further ensures that the voltage applied to the ACS terminal **408** has Vds/2 applied thereon, similar to the voltage Vgs that is applied to the gate terminal **402**. In one exemplary embodiment, an inverter **405** is configured in series with the high output impedance element **403** and supplied by GND and $-V_{DD}$. In one exemplary embodiment, $-V_{DD}$ is readily derived from a convenient positive voltage supply. It could, however, comprise an even more negative voltage for improved linearity (i.e., it can be independent of the gate voltage).

In another embodiment, the circuit shown in FIG. **4**C can be modified to include a clamping circuit configured in series with an ACS terminal **408**. Such an exemplary embodiment is shown in FIG. **4**F. Under certain operating conditions, current that flows out of the ACC NMOSFET **300**, conveying the accumulated charge from the body of the ACC NMOSFET **300**, via the ACS terminal **408** is sufficiently high such that it causes problems in the biasing circuitry (i.e., under some conditions the ACS current is so high that the biasing circuitry cannot adequately sink the current flowing out of the body of the ACC NMOSFET **300**). As shown in the circuit of FIG. **4**F, one exemplary embodiment solves this problem by interrupting the flow of ACS current out of the body of the ACC NMOSFET **300**, and thereby returning the ACC NMOSFET **300** to a floating body condition.

In one exemplary circuit, as shown in FIG. **4**F, a depletion-mode FET **421** is configured in series between the ACS terminal **408** and a diode **410**. In this exemplary circuit, the depletion-mode FET **421** includes a gate terminal that is electrically connected to the FET's source terminal. In this configuration, the depletion-mode FET **421** functions to clip or limit the current that flows from the ACS terminal **408** when the ACC MOSFET operates in the accumulated charge regime. More specifically, the depletion-mode FET **421** enters saturation upon reaching a predefined threshold. The current leaving the body of the ACC MOSFET is thereby limited by the saturation current of the FET **421**. In some embodiments, the predefined saturation threshold may optionally be adjusted to change the point at which clamping occurs, such as by selecting a higher threshold voltage, which results in a lower maximum current and earlier clamping.

In some embodiments, such as for example in an RF switch circuit, the gate terminal **402** and the ACS terminal **408** follow Vds at half the rate (Vds/2) of Vds. At high Vds excursions, Vgs may approach the threshold voltage Vth, resulting in increased Ids leakage current. In some cases, such a leakage current exits the ACS terminal **408** and can overwhelm associated circuitry (e.g., a negative voltage generator). Hence, the circuit shown in FIG. **4**F solves or otherwise mitigates these problems. More specifically, by coupling the FET **421** in series between the ACS terminal **408** and the diode **410**, the current that exits the ACS terminal **408** is limited to the saturation current of the FET **421**.

In yet another exemplary embodiment, the simplified circuit shown in FIG. **4**C can be modified to include an AC shorting capacitor placed in parallel with the diode **410**. The simplified circuit of FIG. **4**G can be used to compensate for certain undesirable nonlinearities present in a full circuit application. In some embodiments, due to parasitics present in the MOSFET layout, nonlinearity characteristics existing in the diode **410** of FIG. **4**C may introduce undesirable nonlinearities in a full circuit implementation. As the diode is in place to provide DC bias conditions and is not intended to have any AC signals across it, it may be desirable in some embodiments to take steps to mitigate the effects of any AC signal present across the diode **410**.

As shown in the simplified circuit of FIG. **4**G, the circuit of FIG. **4**C has been modified to include an AC shorting capacitor **423** wherein the AC shorting capacitor **423** is configured in parallel across the diode **410**. The AC shorting capacitor **423** is placed in parallel with the diode **410** to ensure that nonlinearities of the diode **410** are not excited by an AC signal. In some exemplary circuits, such as in an RF switch, the AC shorting capacitor **423** does not impact the higher level full circuit, as the gate terminal **402** and the ACS terminal **408** typically have the same AC signal applied (i.e., AC equipotential).

In some circuit embodiments, body nodes of a multi-finger FET implementation may be connected to one another (using, for example, metal or silicon), overlapping the source fingers. On another side of the FET implementation, gate nodes may be are connected to one another (using, for example, metal or silicon) overlapping the drain fingers. As a result of this FET implementation, additional capacitance may result between the source and body (S-B), and further additional capacitance may result between the drain and gate (D-G). These additional capacitances may degrade the symmetry of the intrinsic device. Under AC excitation, this results in the gate terminal following the drain terminal more closely, and the body terminal following the source terminal more closely, which effectively creates an AC signal across the diode **410**, which can excite nonlinearities of the diode **410** as described above. Using the exemplary embodiment shown in FIG. **4**G, parasitic nonlinear excitation due to the overlapping fingers is mitigated.

Improved C_{off} Performance Characteristics of ACC MOSFETs Made in Accordance with the Present Disclosed Method and Apparatus

FIG. **4**H is a plot **460** of the off-state capacitance (C_{off}) versus an applied drain-to-source voltage of an SOI MOSFET when an AC signal is applied to the MOSFET (the plot **460** is relevant to an exemplary 1 mm wide MOSFET, though similar plots result using wider and narrower devices). In one embodiment, a gate voltage equals −2.5

Volts+Vd/2, and Vs equals 0. A first plot **462** shows the off-state capacitance C_{off} of a typical prior art NMOSFET operating within the accumulated charge regime and thereby having an accumulated charge as described above with reference to FIG. **1**. As shown in FIG. **4**H, the off-state capacitance C_{off} shown in plot **462** of the prior art FET is voltage-dependent (i.e., it is nonlinear) and peaks when Vd=0 Volts. A second plot **464** illustrates the off-state capacitance C_{off} of an improved ACC SOI MOSFET made in accordance with the present teachings, wherein the accumulated charge is conveyed from the ACC MOSFET, thereby reducing, controlling and/or eliminating the accumulated charge from the ACC MOSFET body. As shown in FIG. **4**H, the off-state capacitance C_{off} shown in plot **464** of the ACC SOI MOSFET is not voltage-dependent (i.e., it is linear).

As described above with reference to FIG. **2**A, by controlling, reducing or eliminating the accumulated charge, the impedance **212** of the NMOSFET body **312** (FIG. **3**C, and shown as the MOSFET body **114** in the electrical model of FIG. **2**A) is increased to a very large value. This increase in the impedance **212** of the MOSFET body reduces the contribution to C_{off} caused by the impedance of the junctions **218** and **220** (FIG. **2**A), thereby reducing the overall magnitude of C_{off} and the nonlinear effects associated with the impedances of the junctions **218** and **220**. Plot **464** illustrates how the present teachings advantageously reduce both the nonlinearity and overall magnitude of the off-state capacitance C_{off} of the MOSFET. The reduced nonlinearity and magnitude of the off-state capacitance C_{off} improves the performance of circuits using MOSFETs operating in an accumulated charge regime, such as RF switching circuits. Exemplary RF switching circuits implemented with the ACC MOSFETs described above with reference to FIGS. **4**A-**4**G are now described with reference to FIGS. **5**A-**5**D. Exemplary Improved Performance RF Switch Implementations Using ACC SOI MOSFETs in Accordance with the Present Teachings

FIG. **5**A shows a schematic diagram of a single pole, single throw (SPST) RF switch circuit **500** in accordance with prior art. The RF switch circuit **500** is one example of a general class of well-known RF switch circuits. Similar RF switch circuits are described in the following co-pending and commonly assigned U. S. Applications and Patent: Provisional Application No. 60/651,736, filed Feb. 9, 2005, entitled "UNPOWERED SWITCH AND BLEEDER CIRCUIT:" application Ser. No. 10/922,135, filed Aug. 18, 2004, pending, which is a continuation application of application Ser. No. 10/267,531, filed Oct. 8, 2002, which issued Oct. 12, 2004 as U.S. Pat. No. 6,804,502, entitled "SWITCH CIRCUIT AND METHOD OF SWITCHING RADIO FREQUENCY SIGNALS". Application Ser. No. 10/267,531, filed Oct. 8, 2002, which issued Oct. 12, 2004 as U.S. Pat. No. 6,804,502 claims the benefit of U.S. Provisional Application No. 60/328,353, filed Oct. 10, 2001. All of the above-cited applications and issued patent set forth above are hereby incorporated by reference herein as if set forth in full for their teachings on RF switch circuits including SOI MOSFET switch circuits.

Referring again to FIG. **5**A, a switching SOI NMOSFET **506** is adapted to receive an RF input signal "RFin" at an input terminal **502**. The switching SOI MOSFET **506** is electrically coupled to selectively couple the RFin input signal to an output terminal **504** (i.e., thereby convey an RF output signal Rfout at the output terminal **504**). In the exemplary embodiment, the switching SOI NMOSFET **506** is controlled by a first control signal C**1** that is conveyed by a control line **512** through a gate resistor **510** (optionally included for suppression of parasitic RF coupling). The control line **512** is electrically coupled to a control circuit **520**, which generates the first control signal C**1**.

Referring again to FIG. **5**A, a shunting SOI NMOSFET **508** is adapted to receive the RF input signal RFin at its drain terminal, and to selectively shunt the input signal RFin to ground via an optional load resistor **518**. The shunting SOI NMOSFET **508** is controlled by a second control signal C**1**x which is conveyed by a control line **516** through a gate resistor **514** (optionally included for suppression of parasitic RF coupling and for purposes of voltage division). The control line **516** is electrically coupled to the control circuit **520**, which generates the second control signal C**1**x.

The terms "switching" and "shunting", as pertains to the transistors shown in FIG. **5**A and also described below with reference to the RF switch circuits of FIGS. **5**B-**5**D, **6**, **8**, and **9**, are used interchangeably herein with the terms "switch" and "shunt", respectively. For example, the switching transistor **506** (and all of its analogous switching transistors described below in FIGS. **5**B-**5**D, **6**, **8**, and **9**) is also referred to herein as the "switch" transistor. Similarly, the shunting transistor **508** (and all of its analogous shunting transistors described below in FIGS. **5**B-**5**D, **6**, **8**, and **9**) is also referred to herein as the "shunt" transistor. The terms "switch" and "switching" (and similarly the terms "shunt" and "shunting"), when used to describe the RF switch circuit transistors, are used interchangeably herein. Further, as described below in more detail with reference to FIG. **6**, those skilled in the RF switching design and fabrication arts shall recognize that although the switch and shunt transistors are shown in FIGS. **5**A-**5**D and FIG. **9** as comprising a single MOSFET, it shall be understood that they may comprise transistor groupings comprising one or more MOSFET transistors.

It will also be appreciated by those skilled in RF switch circuits that all of the exemplary switch circuits may be used "bi-directionally," wherein the previously described input ports function as output ports, and vice versa. That is, although an exemplary RF switch may be described herein as having one or more input ports (or nodes) and one or more output ports (or nodes), this description is for convenience only, and it will be understood that output ports may, in some applications, be used to input signals, and input ports may, in some applications, be used to output signals. The RF switch circuits described with reference to FIGS. **2**B, **4**E, **5**A-**5**D, **6**, **8** and **9** are described herein as having "input" and "output" ports (or "nodes") that input and output RF signals, respectively. For example, as described below in more detail with reference to FIG. **9**, RF input node **905** and RF input node **907** are described below as inputting RF signals RF**1** and RF**2** respectively. RFC common port **903** is described below as providing an RF common output signal. Those skilled in the RF switch circuit design arts shall recognize that the RF switch is bidirectional, and that the previously described input ports function perfectly well as output ports, and vice versa. In the example of the RF switch of FIG. **9**, the RFC common port can be used to input an RF signal which is selectively output by the RF nodes **905** and **907**.

Referring again to FIG. **5**A, the first and second control signals, C**1** and C**1**x, respectively, are generated so that the switching SOI NMOSFET **506** operates in an on-state when the shunting SOI NMOSFET **508** operates in an off-state, and vice versa. These control signals provide the gate bias voltages Vg to the gate terminals of the NMOSFETs **506** and **508**. When either of the NMOSFETs **506** or **508** is biased to select the transistor off-state, the respective Vg must comprise a sufficiently large negative voltage so that the respective NMOSFET does not enter, or approach, an on-state due

to the time varying applied voltages of the RF input signal RFin. The maximum power of the RF input signal RFin is thereby limited by the maximum magnitude of the gate bias voltage Vg (or, more generally, the gate-to-source operating voltage, Vgs) that the SOI NMOSFETs **506** and **508** can reliably sustain. For RF switching circuits such as those exemplified herein, the magnitude of Vgs(max)=|Vg|+|Vds(max)/2|, where Vds=Vd−Vs, and Vds(max) comprises the maximum Vds due to the high-power input signal voltage levels associated with the RF input signal RFin.

Exemplary bias voltages for the switching and shunting SOI NMOSFETs **506** and **508**, respectively, may include the following: with V_{th} approximately zero volts, Vg, for the on-state, of +2.5 V, and Vg, for the off-state, of −2.5 V. For these bias voltages, the SOI NMOSFETs may eventually operate in an accumulated charge regime when placed into their off-states. In particular, and as described above with reference to FIG. **2**B, when the switching NMOSFET **506** is in the on-state, and the shunting NMOSFET **508** is biased in the off-state, the output signal RFout may become distorted by the nonlinear behavior of the off capacitance C_{off} of the shunting NMOSFET **508** caused by the accumulated charge. Advantageously, the improved ACC MOSFETs made in accordance with the present teachings can be used to improve circuit performance, especially as it is adversely affected by the accumulated charge.

FIG. **5**B is a schematic of an improved RF circuit **501** adapted for higher performance using the present accumulated charge reduction and control techniques. The switch circuit **501** differs from the prior art circuit **500** (FIG. **5**A) in that the shunting NMOSFET **508** is replaced by a shunting ACC NMOSFET **528** made in accordance with the present teachings. The shunting ACC NMOSFET **528** is analogous to the ACC NMOSFET described above with reference to FIGS. **4**A and **4**B. Similarly, the gate, source, drain and ACC terminals of the shunting ACC NMOSFET **528** are analogous to the respective terminals of the ACC NMOSFET **300**. With the exception of the improved switch performance afforded by the improved shunting ACC NMOSFET **528**, the operation of the RF switch circuit **501** is very similar to the operation of the RF switch circuit **500** described above with reference to FIG. **5**A.

Exemplary bias voltages for the switching NMOSFET **526** and the shunting ACC NMOSFET **528** may include: with V_{th} approximately zero, Vg, for the on-state, of +2.5 V, and Vg, for the off-state, of −2.5 V. For these bias voltages, the SOI NMOSFETs may operate in an accumulated charge regime when placed into the off-state. However, when the switching NMOSFET **526** is in the on-state and the shunting ACC NMOSFET **528** is in the off-state, the output signal RFout at the output terminal **505** will not be distorted by nonlinear behavior of the off-state capacitance C_{off} of the improved shunting ACC NMOSFET **528** due to the accumulated charge. When the shunting ACC NMOSFET **528** operates in the accumulated charge regime, the accumulated charge is removed via the ACS terminal **508'**. More specifically, because the gate terminal **502'** of the shunting ACC NMOSFET **528** is connected to the ACS terminal **508'**, the accumulated charge is removed or otherwise controlled as described above in reference to the simplified circuit of FIG. **4**B. The control of the accumulated charge improves performance of the switch **501** by improving the linearity of the off transistor, shunting ACC NMOSFET **528**, and thereby reducing the harmonic and intermodulation distortion of the RF output signal Rfout generated at the output terminal **505**.

FIG. **5**C is a schematic of another embodiment of an improved RF switch circuit **502** adapted for higher performance using the accumulated charge control techniques of the present disclosure. The switch circuit **502** differs from the prior art circuit **500** (FIG. **5**A) in that the NMOSFET **508** is replaced by an ACC NMOSFET **528** made in accordance with the present teachings. The ACC NMOSFET **528** is analogous to the ACC NMOSFET **300** described above with reference to FIGS. **4**A and **4**C. Similarly, the gate, source, drain and ACC terminals of the ACC NMOSFET **528** are analogous to the respective terminals of the ACC NMOSFETs **300** described above with reference to FIGS. **4**A and **4**C. With the exception of the improved switch performance afforded by the improved ACC NMOSFET **528**, the operation of the switch circuit **502** is very similar to the operations of the switch circuits **500** and **501** described above with reference to FIGS. **5**A and **5**B, respectively.

Exemplary bias voltages for the NMOSFET **526** and the ACC NMOSFET **528** may include the following: with V_{th} approximately zero volts, Vg, for the on-state, of +2.5 V, and Vg, for the off-state, of −2.5 V. For these bias voltages, the SOI NMOSFETs **526**, **528** may operate in an accumulated charge regime when placed into an off-state. However, when the NMOSFET **526** is in the on-state and the ACC NMOSFET **528** is in the off-state, the output signal RFout will not be distorted by nonlinear behavior of the off-state capacitance C_{off} of the ACC NMOSFET **528** due to the accumulated charge. Because the gate terminal **502'** of the ACC NMOSFET **528** is connected to the ACS terminal **508'** via a diode **509**, the accumulated charge is entirely removed, reduced or otherwise controlled, as described above with reference to FIG. **4**C. Similar to the improved switch **501** described above with reference to FIG. **5**B, control of the accumulated charge improves performance of the switch **502** by improving the linearity of the off transistor, **528**, and thereby reducing the harmonic and intermodulation distortion of the RF output signal Rfout output of the RF output terminal **505**. Connection of the diode **509** as shown may be desired in some embodiments for suppression of positive current flow into the ACC NMOSFET **528** when it is biased into an on-state, as described above with reference to FIG. **4**C.

FIG. **5**D is a schematic of another embodiment of an improved RF switch circuit **503** adapted for higher performance using the present accumulated charge control techniques. The switch circuit **503** differs from the prior art circuit **500** (FIG. **5**A) in that the NMOSFET **508** of FIG. **5**A is replaced by an ACC NMOSFET **528** made in accordance with the present teachings. The ACC NMOSFET **528** is analogous to the ACC NMOSFET described above with reference to FIGS. **4**A and **4**D. With the exception of the improved switch performance afforded by the improved ACC NMOSFET **528**, the operation of the switch circuit **503** is very similar to the operations of the switch circuits **500**, **501** and **502** described above with reference to FIGS. **5**A-**5**C, respectively.

Exemplary bias voltages for the NMOSFET **526** and the ACC NMOSFET **528** may include the following: with V_{th} approximately zero volts, Vg, for the on-state, of +2.5 V, and Vg, for the off-state, of −2.5 V. For these bias voltages, the SOI NMOSFETs **526**, **528** may operate in an accumulated charge regime when placed into the off-state. However, when the NMOSFET **526** is in the on-state and the ACC NMOSFET **528** is in the off-state, the output signal RFout produced at the output terminal **505** will not be distorted by the nonlinear behavior of the off-state capacitance C_{off} of the ACC NMOSFET **528** due to the accumulated charge. When the NMOSFET **528** operates in the accumulated charge regime, the accumulated charge is removed via the ACS

terminal **508'**. More specifically, because the ACS terminal **508'** of the ACC NMOSFET **528** is electrically coupled to the control circuit **520** via the control line **517** (i.e., controlled by the control signal "C**2**" as shown), the accumulated charge can be eliminated, reduced or otherwise controlled by applying selected bias voltages to the ACS terminal **508'** as described above with reference to FIG. **4**D. Those skilled in the arts of electronic circuit design shall understand that a wide variety of bias voltage signals can be applied to the ACS terminal for the purpose of reducing or otherwise controlling the accumulated charge. The specific bias voltages may be adapted for use in a particular application. The control of the accumulated charge improves performance of the switch **503** by improving the linearity of the off-state transistor, **528**, and thereby reducing the harmonic and intermodulation distortion of the RF output signal Rfout generated at the output terminal **505**.

In the circuits described above with respect to FIGS. **5**B-**5**D, the switching SOI MOSFETs **526** are shown and described as implemented using SOI MOSFETs of the prior art (i.e., they do not comprise ACC MOSFETs and therefore do not have an ACS terminal). Those skilled in the electronic device design arts shall understand and appreciate that in other embodiments of the disclosed method and apparatus, the prior art switching SOI MOSFETs **526** may be replaced, as desired or required, by ACC SOI MOSFETs made in accordance with the present disclosure. For example, in some embodiments of RF switches implemented using the ACC MOSFET of the present teachings, the RF switch comprises a single-pole double-throw RF switch. In this embodiment, the switching SOI MOSFETs (e.g., analogous to the switching SOI MOSFETs **526** described above with reference to FIGS. **5**B-**5**D) may comprise ACC SOI MOSFETs. Such an implementation prevents nonlinear behavior of the off-state switching SOI MOSFETs (which is turned off when it is not selected as an input "pole") from detrimentally affecting the output of the RF signal as switched through the selected "pole". Implementation of the RF switches using switching ACC MOSFETs reduces the magnitude, drift, and voltage dependency of the off capacitance C_{off} of the switching transistors. Consequently, and as described above in more detail, the switch performance characteristics, such as its isolation, insertion loss and drift characteristics, are also improved. This implementation is described in more detail below with reference to the RF switch circuit shown in FIG. **9**. Many other examples will be apparent to those skilled in the arts of electronic circuits.

For example, as set forth above, although the exemplary RF switches have been described as being implemented using ACC SOI NMOSFET devices, they can also be implemented using ACC SOI PMOSFET devices. Further, although single-pole single-throw, and single-pole double-throw RF switches have been described above as examples of RF switches implemented in accordance with the present teachings, the present application encompasses any variation of single-pole multi-throw, multi-pole single-throw, and multi-pole multi-throw RF switch configurations. Those skilled in the RF switch design and fabrication arts shall recognize and appreciate that the present teachings can be used in implementing any convenient RF switch configuration design.

Exemplary RF Switch Implementation Using Stacked Transistors

In the exemplary embodiments of RF switch circuits described above, the switch circuits are implemented using a single SOI NMOSFET (e.g., the single SOI NMOSFET **506** of FIG. **5**A, and the single SOI NMOSFET **526** of FIGS. **5**B-**5**D) that selectively couples or blocks (i.e., electrically opens the circuit connection) the RF input signal to the RF output. Similarly, in the exemplary embodiments described above with reference to FIGS. **5**A-**5**D, a single SOI NMOSFET (e.g., the single SOI NMOSFET **508** of FIG. **5**A, and ACC SOI NMOSFET **528** of FIGS. **5**B-**5**D) is used to shunt (FET in the on-state) or block (FET in the off-state) the RF input signal to ground. Commonly assigned U.S. Pat. No. 6,804,502, entitled "SWITCH CIRCUIT AND METHOD OF SWITCHING RADIO FREQUENCY SIGNALS", issued Oct. 12, 2004, describes RF switch circuits using SOI NMOSFETs implemented with stacked transistor groupings that selectively couple and block RF signals.

One example of how stacked NMOSFETs may be implemented in accordance with the teachings of the present disclosure is illustrated in FIG. **6**. An RF switch circuit **600** is analogous to the RF switch circuit **503** of FIG. **5**D, wherein the single SOI NMOSFET **526** is replaced by a stack of SOI NMOSFETs **602**, **604** and **606**. Similarly, the single ACC SOI NMOSFET **528** is replaced by a stack of ACC SOI NMOSFETs **620**, **622** and **624**. The control signal C**2** is provided to the ACS terminals of the ACC SOI NMOSFETs **620**, **622** and **624** via optional resistors **626**, **628**, and **630**, respectively. The resistors **626**, **628**, and **630** may optionally be included in order to suppress parasitic RF signals between the stacked ACC SOI NMOSFETs **620**, **622**, and **624**, respectively. The RF switch circuit **600** operates analogously to the operation of the RF switch circuit **503** described above with reference to FIG. **5**D.

Three stacked ACC SOI NMOSFETs are shown in each ACC NMOSFET stack in the exemplary stacked RF switch circuit **600** of FIG. **6**. A plurality of three ACC NMOSFETs is shown for illustrative purposes only, however, those skilled in the integrated circuit design arts will understand that an arbitrary plurality may be employed according to particular circuit requirements such as power handling performance, switching speed, etc. A smaller or larger plurality of stacked ACC NMOSFETs may be included in a stack to achieve a desired operating performance.

Other stacked RF switch circuits, adapted for accumulated charge control, analogous to the circuits described above with reference to FIGS. **5**B-**5**D, may also be employed. Implementations of such circuits shall be obvious from the teachings above to those skilled in the electronic device design arts, and therefore are not described further herein. Moreover, is shall be obvious to those skilled in the electronic device design arts that, although a symmetrically stacked (i.e., having an equal number of shunting and switching transistors) RF switch is shown in the stacked RF switch of FIG. **6**, the present inventive ACC method and apparatus is not so limited. The present teachings can be applied in implementing both symmetrically and asymmetrically stacked (having an unequal number of shunting and switching transistors) RF switches. The designer will readily understand how to use the ACC MOSFETs of the present disclosure in implementing asymmetrical, as well as symmetrical, RF switch circuits.

Exemplary Method of Operation

FIG. **7** illustrates an exemplary method **700** of improving the linearity of an SOI MOSFET having an accumulated charge sink (ACS) in accordance with the present disclosure. The method **700** begins at a STEP **702**, whereat an ACC SOI MOSFET having an ACS terminal is configured to operate in a circuit. The ACS terminal may be operatively coupled to the gate of the SOI MOSFET (as described above with reference to FIGS. **4**B, **4**C, **5**B and **5**C), or to a control circuit (as described above with reference to FIGS. **4**D and **5**D). In

other embodiments, the ACS terminal may be operatively coupled to any convenient accumulated charge sinking mechanism, circuit, or device as is convenient to the circuit or system designer. The method then proceeds to a step **704**.

At the STEP **704**, the ACC SOI MOSFET is controlled, at least part of the time, so that it operates in an accumulated charge regime. In most embodiments, as described above, the ACC MOSFET is operated in the accumulated charge regime by applying bias voltages that place the FET in an off-state condition. In one exemplary embodiment, the ACC SOI MOSFET comprises an ACC SOI NMOSFET that is configured as part of a shunting circuit of an RF switch. According to this exemplary embodiment, the SOI NMOSFET may be operated in an accumulated charge regime after the shunting circuit is placed into an off-state by applying a negative bias voltage to the gate terminal of the ACC NMOSFET.

The method then proceeds to a STEP **706**, whereat the accumulated charge that has accumulated in the channel region of the ACC MOSFET is removed or otherwise controlled via the ACS terminal. In this embodiment, the accumulated charge is conveyed to another circuit terminal and is thereby reduced or otherwise controlled. One such exemplary circuit terminal that can be used to convey the accumulated charge from the MOSFET body comprises a gate terminal of the ACC MOSFET (see, e.g., the description above with reference to FIGS. **4**B, **4**C, **5**B and **5**C). Another exemplary circuit terminal that can be used to remove or otherwise control the accumulated charge comprises the terminal of a control circuit (see, e.g., FIGS. **4**D and **5**D). As described in more detail above, removing or otherwise controlling the accumulated charge in the ACC MOSFET body improves the linearity of the off-state ACC MOSFET, which reduces the harmonic distortion and IMD of signals affected by the ACC MOSFET, and which, in turn, improves circuit and system performance. In RF switch circuits, improvements (in both linearity and magnitude) are made to the off capacitance of shunting ACC MOSFET devices, which, in turn, improves the performance of the RF switch circuits. In addition to other switch performance characteristics, the harmonic and intermodulation distortions of the RF switch are reduced using the ACC method and apparatus of the present teachings.

FIGS. **8** and **9** show schematics of additional exemplary embodiments of RF switching circuits made in accordance with the disclosed method and apparatus for use in improving linearity of MOSFETs having an ACS. As described in more detail below with reference to FIGS. **8** and **9**, in some exemplary embodiments of RF switch circuits made in accordance with the present disclosure, it may be desirable to include drain-to-source resistors, Rds, and thereby improve some switch performance characteristics when the switch is used in a particular application. These exemplary RF switch circuits are now described in more detail.

Exemplary RF Switch Implementations Using Stacked Transistors Having Source to Drain Resistors

FIG. **8** shows one exemplary embodiment of an RF switch circuit **800** made in accordance with the present disclosure. As shown in FIG. **8**, some embodiments of RF switches made in accordance with the present disclosure may include drain-to-source (R_{ds}) resistors electrically connected to the respective sources and drains of the ACC MOSFETs. For example, the exemplary switch **800** of FIG. **8** includes drain-to-source R_{ds} resistors **802**, **804**, and **806** electrically connected to the respective sources and drains of the shunting ACC SOI NMOSFETs **620**, **622**, and **624**, respectively. Motivation for use of the drain-to-source R_{ds} resistors is now described.

As shall be appreciated by skilled persons from the present teachings, removal of the accumulated charge via the ACS terminal causes current to flow from the body of the ACC SOI MOSFET. For example, when a hole current flows from the body of an ACC SOI MOSFET via the ACS, an equal electron current flows to the FET source and/or drain. For some circuits (e.g., the RF switch circuit of FIG. **8**), the sources and/or drains of the ACC SOI NMOSFETs are connected to other SOI NMOSFETs. Because off-state SOI NMOSFETs have a very high impedance (e.g., in the range of 1 Gohm for a 1 mm wide SOI NMOSFET), even a very small drain-to-source current (e.g., in the range of 1 nA) can result in an unacceptably large drain-to-source voltage Vds across the ACC SOI NMOSFET in satisfaction of Kirchhoff's well known current and voltage laws. In some embodiments, such as that shown in the RF switch circuits of FIGS. **8** and **9**, such resultant very large drain-to-source voltages Vds undesirably impacts reliability and linearity of the ACC SOI NMOSFET. The drain-to-source resistors R_{ds} provide a path between the ACC FET drain and source whereby currents associated with controlling the accumulated charge may be conducted away from the sources and drains of ACC SOI NMOSFETs when implemented in series with high impedance elements such as other ACC SOI NMOSFETs.

Exemplary operating voltages for the NMOSFETs **602-606** of FIG. **8**, and the ACC NMOSFETs **620-624**, may include the following: V_{th} approximately zero volts, Vg, for the on-state, of +2.5 V, and Vg, for the off-state, of −2.5 V. In an exemplary embodiment, the ACC SOI NMOSFET **622** of FIG. **8** may have a width of 1 mm, and an electron-hole pair generation rate for accumulated charge producing a current of 10 pA/μm for operation in the accumulated charge regime. For the electron current supplied equally by the source and drain, and an impedance of the ACC SOI NMOSFETs **620** and **622** on the order of 1 Gohm, then an unacceptable bias of −5 V would result on the source and drain of the ACC SOI NMOSFET **622** without the presence of R_{ds} resistors **802** and **806**. This bias voltage would also be applied to the interior nodes of the ACC SOI NMOSFETs **620** and **624**.

Even currents smaller than the exemplary currents may produce adverse affects on the operation of the RF switching circuit **800** by reducing Vgs and/or Vgd of the ACC SOI MOSFETs **620-624** in the off-state, thereby reducing the power handling capability and reliability of the circuit by increasing leakage (e.g., when either Vgs or Vgd approaches V_{th}), by increasing hot-carrier damage caused by excess leakage, etc. Linearity of the MOSFETs is also degraded by reducing Vgs and/or Vgd when either value approaches V_{th}.

Exemplary values for the R_{ds} resistors **802** to **806** may be selected in some embodiments by selecting a value approximately equal to the resistance of the gate resistors **632-636** divided by the number of ACC SOI NMOSFETs in the stack (in the exemplary embodiment, there are three ACC FETs in the stack). More generally, the value of the R_{ds} resistors may be equal to the gate resistor value divided by the number of ACC SOI NMOSFETs in the stack. In one example, a stack of eight ACC SOI NMOSFETs may have gate resistors of 80 kohm and R_{ds} resistors of 10 kohm.

In some embodiments, the R_{ds} resistors may be selected so that they do not adversely affect switch performance characteristics, such as, for example, the insertion loss of the switch **800** due to the off-state ACC SOI NMOSFETs. For

example, for a net shunt resistance greater than 10 kohm, the insertion loss is increased by less than 0.02 dB.

In other embodiments, the R_{ds} resistors may be implemented in circuits comprising a single ACC SOI MOSFET (as contrasted with the stacked shunting configuration exemplified in FIG. **8** by the shunting ACC FETs **620**, **622** and **624**). For example, such circuits may be desirable if there are other high-impedance elements configured in series with an ACC SOI MOSFET that may cause a significant bias voltage to be applied to the source or drain as a result of the current flow created when removing or otherwise controlling accumulated charge. One exemplary embodiment of such a circuit is shown in FIG. **9**.

FIG. **9** shows an exemplary single-pole double-throw (SPDT) RF switch circuit **900** made in accordance with the present teachings. As shown in FIG. **9**, a DC blocking capacitor **904** is connected to a first RF input node **905** that receives a first RF input signal RF**1**. Similarly, a DC blocking capacitor **906** is connected to a second RF input node **907** that receives a second RF input signal RF**2**. Further, a DC blocking capacitor **902** is electrically connected to an RF common output node **903** that provides an RF common output signal (RFC) selectively conveyed to the node RFC **903** by the switch circuit **900** from either the first RF input node **905** or the second RF input node **907** (i.e., RFC either outputs RF**1** or RF**2**, depending upon the operation of the switch as controlled by the control signals C**1** and C**1**x described below in more detail).

A first control signal C**1** is provided to control the operating states of the ACC SOI NMOSFETs **526** and **528'** (i.e., C**1** selectively operates the FETs in the on-state or the off-state). Similarly, a second control signal C**1**x is provided to control the operating states of the ACC SOI NMOSFETs **528** and **526'**. As is well known, and as described for example in the above incorporated commonly assigned U.S. Pat. No. **6,804,502**, the control signals C**1** and C**1**x are generated so that the ACC SOI NMOSFETs **526** and **528'** are in an on-state when the ACC SOI NMOSFETs **528** and **526'** are in an off-state, and vice versa. This configuration allows the RF switch circuit **900** to selectively convey either the signal RF**1** or RF**2** to the RF common output node **903**.

A first ACS control signal C**2** is configured to control the operation of the ACS terminals of the SOI NMOSFETs **526** and **528'**. A second ACS control signal C**2**x is configured to control the ACS terminals of the ACC SOI NMOSFETs **528** and **526'**. The first and second ACS control signals, C**2** and C**2**x, respectively, are selected so that the ACSs of the associated and respective NMOSFETs are appropriately biased in order to eliminate, reduce, or otherwise control their accumulated charge when the ACC SOI NMOSFETs operate in an accumulated charge regime.

As shown in the RF switch circuit **900** of FIG. **9**, in some embodiments, an R_{ds} resistor **908** is electrically connected between the source and drain of the switching ACC NMOSFET **526**. Similarly, in some embodiments, an R_{ds} resistor **910** is electrically connected between the source and drain of the switching ACC NMOSFET **526'**. According to this example, the circuit **900** is operated so that either the shunting ACC NMOSFET **528** or the shunting ACC NMOSFET **528'** operate in an on-state at any time (i.e., at least one of the input signals RF**1** at the node **905** or RF**2** at the node **907** is always conveyed to the RFC node **903**), thereby providing a low-impedance path to ground for the node **905** or **907**, respectively. Consequently, either the R_{ds} resistor **908** or the R_{ds} resistor **910** provides a low-impedance path to ground from the RF common node **903**, thereby preventing voltage bias problems caused as a result of ACC current flow into the nodes **903**, **905** and **907** that might otherwise be caused when using the DC blocking capacitors **902**, **904** and **906**.

Additional Exemplary Benefits Afforded by the ACC MOSFETs of the Present Disclosure

As described above, presence of the accumulated charge in the bodies of the SOI MOSFETs can adversely affect the drain-to-source breakdown voltage (BVDSS) performance characteristics of the floating body MOSFETs. This also has the undesirable effect of worsening the linearity of off-state MOSFETs when used in certain circuits such as RF switching circuits. For example, consider the shunting SOI NMOSFET **528** shown in FIG. **9**. Further consider the case wherein the shunting NMOSFET **528** is implemented with a prior art SOI NMOSFET, rather than with the ACC NMOSFET made in accordance with the present teachings. Assume that the RF transmission line uses a 50-ohm system. With small signal inputs, and when the NMOSFET **528** operates in an off-state, the prior art off-state shunting NMOSFET **528** may introduce harmonic distortion and/or intermodulation distortion in the presence of multiple RF signals This will also introduce a noticeable loss of signal power.

When sufficiently large signals are input that cause the NMOSFET **528** to enter a BVDSS regime, some of the RF current is clipped, or redirected through the NMOSFET **528** to ground, resulting in a loss of signal power. This current "clipping" causes compression behavior that can be shown, for instance, in a RF switch "Pout vs. Pin" plot. This is frequently characterized by P1 dB, wherein the insertion loss is increased by 1.0 dB over the small-signal insertion loss. This is an obvious indication of nonlinearity of the switch. In accordance with the present disclosed method and apparatus, removing, reducing or otherwise controlling the accumulated charge increases the BVDSS point. Increases to the BVDSS point of the NMOSFET **528** commensurately increases the large-signal power handling of the switch. As an example, for a switch, doubling the BVDSS voltage of the ACC NMOSFET increases the P1 dB point by 6 dB. This is a significant accomplishment as compared with the prior art RF switch designs.

In addition, as described above in more detail, presence of the accumulated charge in SOI MOSFET body adversely impacts the magnitude of Coff and also takes time to form when the FET is switched from an on-state to an off-state. In terms of switch performance, the nonlinearity of C_{off} adversely impacts the overall switch linearity performance (as described above), and the magnitude of C_{off} adversely affects the small-signal performance parameters such as insertion loss, insertion phase (or delay), and isolation. By reducing the magnitude of C_{off} using the present disclosed method and apparatus, the switch (implemented with ACC MOSFETs) has reduced insertion loss due to lowered parasitic capacitance, reduced insertion phase (or delay), again due to lowered parasitic capacitance, and increased isolation due to less capacitive feedthrough.

The ACC MOSFET also improves the drift characteristic of SOI MOSFETs as pertains to the drift of the small-signal parameters over a period of time. As the SOI MOSFET takes some time to accumulate the accumulated charge when the switch is off, the C_{off} capacitance is initially fairly small. However, over a period of time while operated in the accumulated charge regime, the off-state capacitance C_{off} increases toward a final value. The time it takes for the NMOSFET to reach a full accumulated charge state depends on the electron-hole pair (EHP) generation mechanism. Typically, this time period is on the order of approximately hundreds of milliseconds for thermal EHP generation at

room temperature, for example. During this charge-up time period, the insertion loss and insertion phase increase. Also, during this time period, the isolation decreases. As is well known, these are undesirable phenomena in standard SOI MOSFET devices. These problems are alleviated or otherwise mitigated using the ACC NMOSFETs and related circuits described above.

In addition to the above-described benefits afforded by the disclosed ACC MOSFET method and apparatus, the disclosed techniques also allow the implementation of SOI MOSFETs having improved temperature performance, improved sensitivity to Vdd variations, and improved sensitivity to process variations. Other improvements to the prior art SOI MOSFETs afforded by the present disclosed method and apparatus will be understood and appreciated by those skilled in the electronic device design and manufacturing arts.

Exemplary Fabrication Methods

In one embodiment of the present disclosure, the exemplary RF switches described above may be implemented using a fully insulating substrate semiconductor-on-insulator (SOI) technology. Also, as noted above, in addition to the commonly used silicon-based systems, some embodiments of the present disclosure may be implemented using silicon-germanium (SiGe), wherein the SiGe is used equivalently in place of silicon.

In some exemplary embodiments, the MOSFET transistors of the present disclosure may be implemented using "Ultra-Thin-Silicon (UTSi)" (also referred to herein as "ultrathin silicon-on-sapphire") technology. In accordance with UTSi manufacturing methods, the transistors used to implement the inventive methods disclosed herein are formed in an extremely thin layer of silicon in an insulating sapphire wafer. The fully insulating sapphire substrate enhances the performance characteristics of the inventive RF circuits by reducing the deleterious substrate coupling effects associated with non-insulating and partially insulating substrates. For example, insertion loss improvements may be realized by lowering the transistor on-state resistances and by reducing parasitic substrate conductance and capacitance. In addition, switch isolation is improved using the fully insulating substrates provided by UTSi technology. Owing to the fully insulating nature of silicon-on-sapphire technology, the parasitic capacitance between the nodes of the RF switches is greatly reduced as compared with bulk CMOS and other traditional integrated circuit manufacturing technologies.

Examples of and methods for making silicon-on-sapphire devices that can be implemented in the MOSFETs and circuits described herein, are described in U.S. Pat. No. 5,416,043 ("Minimum charge FET fabricated on an ultrathin silicon on sapphire wafer"); U.S. Pat. No. 5,492,857 ("High-frequency wireless communication system on a single ultrathin silicon on sapphire chip"); U.S. Pat. No. 5,572,040 ("High-frequency wireless communication system on a single ultrathin silicon on sapphire chip"); U.S. Pat. No. 5,596,205 ("High-frequency wireless communication system on a single ultrathin silicon on sapphire chip"); U.S. Pat. No. 5,600,169 ("Minimum charge FET fabricated on an ultrathin silicon on sapphire wafer"); U.S. Pat. No. 5,663,570 ("High-frequency wireless communication system on a single ultrathin silicon on sapphire chip"); U.S. Pat. No. 5,861,336 ("High-frequency wireless communication system on a single ultrathin silicon on sapphire chip"); U.S. Pat. No. 5,863,823 ("Self-aligned edge control in silicon on insulator"); U.S. Pat. No. 5,883,396 ("High-frequency wireless communication system on a single ultrathin silicon on sapphire chip"); U.S. Pat. No. 5,895,957 ("Minimum charge FET fabricated on an ultrathin silicon on sapphire wafer"); U.S. Pat. No. 5,920,233 ("Phase locked loop including a sampling circuit for reducing spurious side bands"); U.S. Pat. No. 5,930,638 ("Method of making a low parasitic resistor on ultrathin silicon on insulator"); U.S. Pat. No. 5,973,363 ("CMOS circuitry with shortened P-channel length on ultrathin silicon on insulator"); U.S. Pat. No. 5,973,382 ("Capacitor on ultrathin semiconductor on insulator"); and U.S. Pat. No. 6,057,555 ("High-frequency wireless communication system on a single ultrathin silicon on sapphire chip"). All of these referenced patents are incorporated herein in their entirety for their teachings on ultrathin silicon-on-sapphire integrated circuit design and fabrication.

Similarly to other bulk and SOI CMOS processes, an SOS enhancement mode NMOSFET, suitable for some embodiments of the present disclosure, may, in some embodiments, be fabricated with a p-type implant into the channel region with n-type source and drain regions, and may have a threshold voltage of approximately +500 mV. The threshold voltage is directly related to the p-type doping level, with higher doping resulting in higher thresholds. Similarly, the SOS enhancement mode PMOSFET may, in some exemplary embodiments, be implemented with an n-type channel region and p-type source and drain regions. Again, the doping level defines the threshold voltage with higher doping resulting in a more negative threshold.

In some exemplary embodiments, an SOS depletion-mode NMOSFET, suitable for some embodiments of the present disclosure, may be fabricated by applying the p-type channel-implant mask to the n-type transistor, resulting in a structure that has n-type channel, source, and drain regions and a negative threshold voltage of approximately −500 mV. Similarly, in some exemplary embodiments, a suitable depletion-mode PMOSFET may be implemented by applying the n-type channel-implant mask to the p-type transistor, resulting in a structure that has p-type channel, source, and drain regions and a positive threshold voltage of approximately +500 mV.

As noted in the background section above, the present ACC MOSFET apparatus can also be implemented using any convenient semiconductor-on-insulator technology, included, but not limited to, silicon-on-insulator, silicon-on-sapphire, and silicon-on-bonded wafer technology. One such silicon-on-bonded wafer technique uses "direct silicon bonded" (DSB) substrates. Direct silicon bond (DSB) substrates are fabricated by bonding and electrically attaching a film of single-crystal silicon of differing crystal orientation onto a base substrate. Such implementations are available from the Silicon Genesis Corporation headquartered in San Jose, Calif. As described at the Silicon Genesis Corporation website (publicly available at "www.sigen.com"), silicon-on-bonded wafer techniques include the so-called Nano-Cleave™ bonding process which can be performed at room temperature. Using this process, SOI wafers can be formed with materials having substantially different thermal expansion coefficients, such as in the manufacture of Germanium-on-Insulator wafers (GeOI). Exemplary patents describing silicon-on-bonded wafer implementations are as follows: U.S. Pat. No. 7,056,808, issued Jun. 6, 2006 to Henley, et al.; U.S. Pat. No. 6,969,668, issued Nov. 29, 2005 to Kang, et al.; U.S. Pat. No. 6,908,832, issued Jun. 21, 2005 to Farrens et al.; U.S. Pat. No. 6,632,724, issued Oct. 14, 2003 to Henley, et al. and U.S. Pat. No. 6,790,747, issued Sep. 14, 2004 to Henley, et al. All of the above-cited patents are

incorporated by reference herein for their teachings on techniques and methods of fabricating silicon devices on bonded wafers.

A reference relating to the fabrication of enhancement-mode and depletion-mode transistors in SOS is "CMOS/SOS/LSI Switching Regulator Control Device," Orndorff, R. and Butcher, D., Solid-State Circuits Conference, Digest of Technical Papers, 1978 IEEE International, Volume XXI, pp. 234-235, February 1978. The "Orndorff" reference is hereby incorporated in its entirety herein for its techniques on the fabrication of enhancement-mode and depletion-mode SOS transistors.

EXEMPLARY RESULTS—APPENDIX A

Exemplary results that can be obtained using the disclosed method and apparatus for use in improving the linearity of MOSFETs are described in the attached Appendix A, entitled "Exemplary Performance Results of an SP6T Switch Implemented with ACC MOSFETs". The contents of Appendix A are hereby incorporated by reference herein in its entirety. The results shown in detail in Appendix A are now briefly described. As noted in the attached Appendix A, the measured results are provided for a single pole, six throw (SP6T) RF switch. Those skilled in the art of RF switch circuit design shall understand that the results can be extended to any practical RF switch configuration, and therefore are not limited to the exemplary SP6T switch for which results are shown.

Slides 2-7 of Appendix A show harmonic performance versus Input Power for prior art devices and for ACC MOSFET devices made in accordance with the present disclosed method and apparatus. Switch circuits implemented with the ACC MOSFET of the disclosed method and apparatus have a third harmonic response that rises at a 3:1 slope (cube of the input) versus input power on the log scale. Those skilled in the electronic device design arts shall appreciate that no input-power dependent dynamic biasing occurs with the improved RF switch designs made in accordance with the present disclosure. In contrast, prior art floating body FET harmonics disadvantageously do not follow a 3:1 slope. This is disadvantageous for small-signal third-order distortions such as IM3.

As shown in the attached Appendix A, at a GSM maximum input power of +35 dBm, the 3fo is improved by 14 dB. This is shown in detail in slide number 3 of the attached Appendix A. Improvements in third order harmonic distortion is also applicable to all odd order responses, such as, for example, 5^{th} order responses, 7^{th} order responses, etc.

Similar to 3fo, the second order response of the improved ACC MOSFET-implemented RF switch follows a 2:1 slope (square of the input) whereas the prior art RF switch does not. This results in improved 2fo and IM2 performance at low input power, and roughly the same performance at +35 dBm.

Slide numbers 6 and 7 of the attached Appendix A treat the performance under non 50-ohm loads. In this case, the load represents a 5:1 mismatch wherein the load impedance can be of any convenient value that results in a reflection coefficient magnitude of ⅔. In the case of SOI MOSFETs, reflection coefficients that result in higher voltages cause the most severe problems. At 5:1 VSWR, the voltage can be 1.667× higher. Those skilled in the art may view this similarly by sweeping the input power up to higher voltages which equate to the mismatch conditions.

The slides provided in Appendix A illustrate that the improved RF switch, implemented with ACC MOSFETs made in accordance with the present disclosed method and apparatus, has improved large voltage handling capabilities as compared to the prior art RF switch implementations. As shown in the slides, the harmonics are approximately 20 dB at the worst mismatch phase angle. Transient harmonics are also shown. Those skilled in the art shall observe that the standard SP6T switch 3fo overshoots by several dB before reaching a final value. The improved SP6T switch made in accordance with the present disclosed method and apparatus does not exhibit such a time-dependency.

Slide number 8 of the Appendix A shows insertion loss performance results achieved using the improved SP6T RF switch of the present teachings. It can be observed that the improved SP6T switch has slightly improved insertion loss (IL) performance characteristics. Slide number 9 of Appendix A shows that isolation is also slightly improved using the present improved SP6T RF switch.

Slide number 10 of the Appendix A shows IM3 performance which is a metric of the slightly nonlinear behavior of the RF switch. The IM3 performance is shown versus phase again due to a load mismatch in the system under test. As can be observed by reviewing Slide number 10 of the Appendix A, the performance of the improved SP6T RF switch is improved by 27 dB.

Finally, Slide number 11 of the Appendix A is a summary table which also includes IM2 data. Slide number 11 shows almost 20 dB improvement for a low frequency blocker and 11 dB for a high frequency blocker. In one exemplary application wherein the SP6T may be used, all IM products must fall below −105 dBm. The improved SP6T switch is the only RF switch manufactured at the time of filing the present application meeting this requirement.

A number of embodiments of the present inventive concept have been described. Nevertheless, it will be understood that various modifications may be made without departing from the scope of the inventive teachings. For example, it should be understood that the functions described as being part of one module may in general be performed equivalently in another module. Also, as described above, all of the RF switch circuits can be used in bi-directionally, with output ports used to input signals, and vice versa. Furthermore, the present inventive teachings can be used in the implementation of any circuit that will benefit from the removal of accumulated charge from MOSFET bodies. The present teachings will also find utility in circuits wherein off-state transistors must withstand relatively high voltages. Other exemplary circuits include DC-to-DC converter circuits, power amplifiers, and similar electronic circuits.

Accordingly, it is to be understood that the concepts described herein are not to be limited by the specific illustrated embodiments, but only by the scope of the appended claims.

What is claimed is:

1. A Radio Frequency (RF) switching method comprising the steps of:

providing an RF input port;

configuring the RF input port to receive an RF signal;

providing an RF output port;

providing a switch transistor grouping having a first node and second node;

coupling the first node of the switch transistor grouping to the RF input port;

coupling the second node of the switch transistor grouping to the RF output port;

providing a shunt transistor grouping having a first node and a second node, the shunt transistor grouping com-

prising one or more accumulated charge control N-type MOSFETs (ACC N-MOSFET) wherein each of the one or more ACC-NMOSFETs comprises:

a gate, drain, source and a gate oxide layer, where the gate oxide layer is positioned between the gate and a body; and

an accumulated charge sink (ACS) region connected to the body;

coupling the first node of the shunt transistor grouping to the RF input port;

coupling the second node of the **[**switch**]** *shunt* transistor grouping to ground;

in a first state:

(a) enabling the switch transistor grouping and disabling the shunt transistor grouping thereby passing the RF input signal from the RF input port to the RF output port;

(b) biasing each of the one or more **[**ACC-MOSFETs**]** *ACC N-MOSFETs* to operate in an accumulated charge regime;

(c) for each of the one or more ACC N-MOSFETs: applying a bias voltage, to the ACS region to control or to remove accumulated charge from the body via the ACS region, wherein the bias voltage is negative with respect to ground, the drain and the source;

in a second state:

(d) enabling the shunt transistor grouping and disabling the switch transistor grouping, thereby isolating the RF input port from the RF output port.

2. The RF switching method of claim **1** used in an RF switching circuit.

3. The RF switching method of claim **2**, wherein the RF switching circuit is implemented inside a cellular communication device.

4. The RF switching method of claim **3**, wherein the cellular communication device is a GSM cell phone.

5. The RF switching method of claim **3**, wherein the cellular communication device is used in a cellular communication system where the harmonics are at a level below −30 dBm.

6. The RF switching method of claim **2**, wherein steps (b)-(c) are for improving linearity, harmonic and intermodulation suppression, and power consumption performance characteristics of the RF switching circuit.

7. The RF switching method of claim **1**, further comprising the step of fabricating the one or more ACC N-MOSFETs on direct silicon bond substrates by bonding and electrically attaching a film of single-crystal silicon onto a base insulating substrate or on an insulating layer on a base silicon substrate.

8. The RF switching method of claim **1**, wherein all the steps are implemented on a single die.

[9. The RF switching method of claim **1**, wherein all the steps are implemented on a single die.**]**

10. The RF switching method of claim **1**, further comprising the step of connecting drain-to-source resistors to the one or more ACC N-MOSFET; the drain-to-source resistors providing a conduction path between corresponding one or more ACC-N-MOSFETs' drains and sources.

11. The RF switching method of claim **10**, further comprising the step of coupling a gate resistor to each gate of each of the one or more ACC N-MOSFETs.

12. A Radio Frequency (RF) switching method comprising the steps of:

providing a first RF port;

configuring the first RF port to receive or output a first RF signal;

providing a second RF port;

configuring the second RF port to receive or output a second RF signal;

providing an RF common port;

providing a first switch transistor grouping having a first node and a second node, the first switch transistor grouping comprising a first one or more accumulated charge control N-type MOSFETs (ACC N-MOSFETs), wherein each of the first one or more ACC-NMOSFETs comprises:

a first gate, first drain, first source and a first gate oxide layer positioned between the first gate and a first body; and

a first accumulated charge sink (ACS) region connected to the first body;

coupling the first node of the first switch transistor grouping to the first RF port;

coupling the second node of the first switch transistor grouping to the RF common port;

providing a second switch transistor grouping having a first node and a second node, the second switch transistor grouping comprising a second one or more ACC N-MOSFETs, wherein each of the second one or more ACC N-MOSFETs comprises:

a second gate, second drain, second source and a second gate oxide layer positioned between the second gate and a second body; and

a second accumulated charge sink (ACS) region connected to the second body;

coupling the first node of the second switch transistor grouping to the second RF port;

coupling the second node of the second switch transistor grouping to the RF common port;

in a first state:

(a) enabling the first switch transistor grouping and disabling the second switch transistor grouping, thereby electrically coupling the first RF port with the RF common port and isolating the second RF port from the RF common port;

(b) biasing each of the second one or more ACC N-MOSFETs to operate in an accumulated charge regime;

(c) for each of the second one or more ACC N-MOSFETs: applying a second bias voltage, to the second ACS region to control or to remove accumulated charge from the second body via the second ACS region, wherein the second bias voltage is negative with respect to ground, the second drain and the second source;

in a second state:

(d) enabling the second switch transistor grouping and disabling the first switch transistor grouping thereby electrically coupling the second RF port with the RF common port and isolating the first RF port from the RF common port;

(e) biasing each of the first one or more ACC N-MOSFETs to operate in an accumulated charge regime;

(f) for each of the first one or more ACC N-MOSFETs: applying a first bias voltage, to the first ACS region to control or to remove accumulated charge from the first body via the first ACS region, wherein the first bias voltage is negative with respect to ground, the first drain and the first source.

13. The RF switching method of claim **12** used in an RF switching circuit.

14. The RF switching method of claim 13, wherein the RF switching circuit is implemented inside a cellular communication device.

15. The RF switching method of claim 14, wherein the cellular communication device is a GSM cell phone.

16. The RF switching method of claim 14, wherein the cellular communication device is used in a cellular communication system.

17. The RF switching method of claim 12, wherein steps (b)-(c) and (e)-(f) are for improving linearity, harmonic and intermodulation suppression, and power consumption performance characteristics of the RF switching circuit.

18. The RF switching method of claim 12, further comprising the step of fabricating the first and the second one or more ACC N-MOSFETs on direct silicon bond substrates by bonding and electrically attaching a film of single-crystal silicon onto a base insulating substrate or on an insulating layer on a base silicon substrate.

* * * * *